



Vaasan yliopisto
UNIVERSITY OF VAASA

Boris YONDJIN NGAMY

Grid-Code Certification by Simulation for Grid- Forming Connected Inverters

School of Technology and Innovation
Master of Science in Technology
Master's Programme in Electrical Engineering

Vaasa 2026

UNIVERSITY OF VAASA**School of Technology**

Author:	Boris YONDJIN NGAMY		
Title of the thesis:	Grid-Code Certification by Simulation for Grid-Forming Connected Inverters: Grid-Code Certification by Simulation for Grid-Forming Connected Inverters		
Degree:	Master of Science in Technology		
Degree Programme:	Master's Programme in Electrical Engineering		
Supervisor:	Mustafa Alrayah Hassan Ibraheem		
Year:	2026	Pages:	172

ABSTRACT:

The increasing penetration of inverter-based resources is transforming modern power systems and creating new challenges for grid-code compliance. Unlike synchronous machines, these resources do not inherently provide voltage formation, inertia or frequency support. This thesis investigates how simulation-based evidence can support the verification of grid-forming inverter behaviour according to selected requirements of the VDE FNN guideline *Technical Requirements for Grid-Forming (GFM) Capabilities Including Provision of Inertia*.

The study focuses on two requirements: voltage-source behaviour and Primary Control Based on Network Security (PCNB). The GFM model developed by Professor Lingling Fan is used as the EMT (Electromagnetic Transient) simulation test object in MATLAB/Simulink. The thesis also develops AGIS, the Automatic GFM Inverter Simulator, to automate selected VDE FNN virtual island network tests, extract active power, reactive power, voltage and frequency, calculate deviations and generate structured validation reports.

The results show that AGIS can distinguish between baseline and tuned simulation scenarios and provide repeatable evidence for the selected verification procedures. For voltage-source behaviour, the analysis focuses on post-islanding voltage recovery, while for PCNB it links frequency deviation to active-power response. Overall, the thesis demonstrates that automated EMT-based simulation can support structured and traceable grid-code verification for grid-forming inverter models, while recognising that hardware-based validation remains necessary for future work.

KEYWORDS: grid-forming inverter, inverter-based resources, EMT simulation, VDE FNN guideline, PCNB, voltage-source behaviour, MATLAB/Simulink, AGIS, grid-code certification.

Acknowledgements

I would like to express my sincere gratitude to my thesis supervisor, Assistant Professor Mustafa Alrayah Hassan Ibraheem, for his guidance, support and valuable feedback throughout the development of this thesis. His advice helped me refine the technical direction of the work and improve the quality of the research.

I am also deeply grateful to Professor Hannu Laaksonen, SMACCs Coordinator at the University of Vaasa, for his support during my academic mobility and for his contribution to the organisation and coordination of the programme. His commitment to the Smart Cities and Communities programme has greatly supported my academic experience at the University of Vaasa.

I would also like to thank the University of Vaasa, the SMACCs programme and all the lecturers and staff who contributed to my academic development during this master's programme. Their teaching, guidance and support provided the foundation for the work presented in this thesis.

Finally, I would like to thank my family and friends for their continuous encouragement, patience and support throughout my studies. Their motivation and confidence in me have been a constant source of strength during this journey.

Contents

1	Introduction	11
1.1	Background and context	11
1.2	Research problem and motivation	12
1.3	Aim and research questions	13
1.4	Scope, methodological approach and limitations	14
1.5	Structure of the thesis	16
2	Literature and Standard Reviews	18
2.1	IBR dynamic behaviour, control, and grid-forming taxonomy	18
2.2	Simulation and validation methods for compliance and certification	22
2.3	Standards and regulatory review	24
3	Grid Code Requirements and Assessment Criteria	30
3.1	From the European Grid-Code Framework to the VDE FNN Guideline	30
3.2	Technical Requirements for Grid-Forming Units	32
3.2.1	Voltage Source Behaviour	32
3.2.2	Primary Control Based on Network Security (PCNB)	34
3.3	EMT Validation and Verification Methodology	35
3.3.1	EMT Model Validation Requirements	35
3.3.2	Virtual Island Network	36
3.3.3	Measurement Quantities	37
3.4	Assessment Criteria and Test Scenarios	38
3.4.1	Operating Points Defined by the Guideline	38
3.4.2	Assessment of Voltage Source Behaviour	42
3.4.3	Assessment of PCNB Behaviour	43
3.4.4	Compliance Evaluation Metrics	44
3.4.5	Test Scenarios Implemented in this Thesis	44
4	Modelling Framework and Validation Strategy	46
4.1	EMT-based modelling framework	46
4.2	Power architecture of the GFM testbed	50

4.3	Control logic of the GFM model	52
4.3.1	Reference-frame transformation	53
4.3.2	Power-frequency droop loop	53
4.3.3	Reactive power-voltage droop loop	54
4.3.4	Outer voltage control	55
4.3.5	Inner current control	56
5	Certification by Simulation	59
5.1	Automatic GFM Inverter Simulator	59
5.2	Scenario One: Non-compliance baseline simulation	64
5.2.1	Non-compliant Test 1.1: ($Q = 0$)	65
5.2.2	Non-compliant Test 1.2: maximum inductive reactive power	65
5.2.3	Non-compliant Test 1.3: maximum capacitive reactive power	66
5.3	Scenario Two: Compliant tuned simulation	67
5.3.1	Compliant Test 1.1: ($Q = 0$)	68
5.3.2	Compliant Test 1.2: maximum inductive reactive power	69
5.3.3	Compliant Test 1.3: maximum capacitive reactive power	70
6	Results Interpretation	72
6.1	Interpretation of voltage-source behaviour measurements	72
6.1.1	Measurement 1.1: neutral reactive-power operation	74
6.1.2	Measurement 1.2: maximum inductive reactive-power operation	75
6.1.3	Measurement 1.3: maximum capacitive reactive-power operation	76
6.1.4	Link between voltage-source EMT validation and physical requirement	77
6.2	Interpretation of PCNB behaviour measurements	78
6.2.1	Measurement 1.1: PCNB behaviour at ($Q = 0$)	80
6.2.2	Measurement 1.2: PCNB behaviour at maximum inductive reactive power	81
6.2.3	Measurement 1.3: PCNB behaviour at maximum capacitive reactive power	82
6.2.4	Link between PCNB EMT validation and physical requirement	83
7	Conclusion and Future Work	85

References	90
Appendices	93
Appendix 1. General workflow of the AGIS automation framework	93
Appendix 2. Scenario One - Voltage source behaviour - Test 1.1 plots	94
Appendix 3. Scenario One - Instantaneous phase voltages and currents - Test 1.1 plot	95
Appendix 4. Scenario One - PCNB behaviour - Test 1.1 plot	96
Appendix 5. Scenario One - Voltage source behaviour - Test 1.2 plot	97
Appendix 6. Scenario One - Instantaneous phase voltages and currents - Test 1.2 plot	98
Appendix 7. Scenario One - PCNB behaviour - Test 1.2 - active power and frequency plot	99
Appendix 8. Scenario One - Voltage source behaviour - Test 1.3 plot	100
Appendix 9. Scenario One - Instantaneous phase voltages and currents - Test 1.3 plot	101
Appendix 10. Scenario One - PCNB behaviour - Test 1.3 plot	102
Appendix 11. Scenario Two - Voltage source behaviour - Test 1.1 plots	103
Appendix 12. Scenario Two - Instantaneous phase voltages and currents - Test 1.1 plot	104
Appendix 13. Scenario Two - PCNB behaviour - Test 1.1 plot	105
Appendix 14. Scenario Two - Voltage source behaviour - Test 1.2 plot	106
Appendix 15. Scenario Two - Instantaneous phase voltages and currents - Test 1.2 plot	107
Appendix 17. Scenario Two - Voltage source behaviour - Test 1.3 plot	109
Appendix 18. Scenario Two - Instantaneous phase voltages and currents - Test 1.3 plot	110
Appendix 20. main_run_all_tests	112
Appendix 21. data	119
Appendix 22. define_FNN_test	125
Appendix 23. run_single_test	127

Appendix 24. extract_metrics	130
Appendix 25. fnn_evaluate_compliance	133
Appendix 26. generate_report	139
Appendix 27. generate_fnn_report	140

Figures

Figure 1: Flow Chart of relationship between regulations, modelling methods and certification logic	28
Figure 2: Powergui Simulink block	47
Figure 3: GFM Simulink testbed	49
Figure 4: Power – frequency droop loop	54
Figure 5: Reactive power – voltage droop loop	55
Figure 6: Outer voltage control loop	56
Figure 7: Inner Current control loop	57
Figure 8: Simulink Control logic of the GFM model	58
Figure 9: AGIS architecture	62

Tables

Table 1: - Measurements in the virtual island network for the verification of inherent stability, voltage source behaviour and PCNB for units which provide negative inertia	38
Table 2: AGIS functional modules	62
Table 3: Baseline parameters for non-compliance scenario	64
Table 4: Tuned parameters for the compliant scenario	68
Table 5: Voltage-source behaviour measurements for Test 1.1	74
Table 6: Deviations for Test 1.1	74
Table 7: Voltage-source behaviour measurements for Test 1.2	75
Table 8: Deviations for Test 1.2	75
Table 9: Voltage-source behaviour measurements for Test 1.3	76
Table 10: Deviations for Test 1.3	77
Table 11: PCNB measurements for Test 1.1	80
Table 12: PCNB deviations for Test 1.1	80
Table 13: PCNB measurements for Test 1.2	81

Table 14: PCNB deviations for Test1.2	81
Table 15: PCNB measurements for Test 1.3	82
Table 16: PCNB deviations for Test 1.3	83

Abbreviations

Abbreviation	Full name
AC	Alternating Current
AGIS	Automatic GFM Inverter Simulator
CCU	Controllable Consumption Unit
C-HIL	Controller-Hardware-in-the-Loop
DC	Direct Current
DER	Distributed Energy Resource
dVOC	Dispatchable Virtual Oscillator Control
EMT	Electromagnetic Transient
ENTSO-E	European Network of Transmission System Operators for Electricity
EU	European Union
FNN	Forum Network Technology/Network Operation
FRT	Fault Ride Through
FSM	Frequency Sensitive Mode
GFM	Grid-Forming
GFL	Grid-Following
HIL	Hardware-in-the-Loop
HVDC	High-Voltage Direct Current
IBR	Inverter-Based Resource
IEEE	Institute of Electrical and Electronics Engineers
IOP	Initial Operating Point
LFSM-O	Limited Frequency Sensitive Mode – Overfrequency
LFSM-U	Limited Frequency Sensitive Mode – Underfrequency
LV	Low Voltage
MATLAB	Matrix Laboratory
MPP	Maximum Power Point
MV	Medium Voltage
NC RfG	Network Code on Requirements for Generators
NCP	Network Connection Point
NERC	North American Electric Reliability Corporation

Abbreviation	Full name
NREL	National Renewable Energy Laboratory
OEM	Original Equipment Manufacturer
OVRT	Overvoltage Ride Through
PCC	Point of Common Coupling
PCNB	Primary Control Based on Network Security
PGM	Power-Generating Module
PGU	Power-Generating Unit
PGSU	Power-Generating and Storage Unit
PHIL	Power-Hardware-in-the-Loop
PI	Proportional-Integral
PLL	Phase-Locked Loop
PWM	Pulse-Width Modulation
RMS	Root Mean Square
RoCoF	Rate of Change of Frequency
SCR	Short-Circuit Ratio
SFS	Finnish Standards Association
SiL	Software-in-the-Loop
SMACCS	Smart Cities and Communities
TCR	Technical Connection Rule
THD	Total Harmonic Distortion
UVRT	Undervoltage Ride Through
VDE	Association for Electrical, Electronic and Information Technologies
VSC	Voltage Source Converter
VSM	Virtual Synchronous Machine

1 Introduction

1.1 Background and context

European power systems are being reshaped by decarbonisation, electrification and the rapid growth of inverter-based resources (IBRs), including wind power plants, photovoltaic generation and battery-connected systems. As a larger share of generation is connected through power-electronic interfaces rather than directly through synchronous machines, conventional assumptions concerning inertia, short-circuit strength, fault response and voltage formation no longer hold in the same way. Consequently, the central technical question is no longer only how to connect more converter-based generation, but how to ensure that increasingly inverter-dominated systems remain stable, controllable and compliant with evolving grid-code requirements (European Commission, 2016; IRENA, 2022, pp. 10–11).

In the European context, this discussion is anchored first in Commission Regulation (EU) 2016/631, the Network Code on Requirements for Generators (NC RfG), and then in the national and regional implementation rules that operationalise it. ENTSO-E presents the NC RfG as a harmonised framework for generator connection across Europe, while the code itself recognises both compliance testing and compliance simulation. This is a crucial point for IBRs, because it means that simulation evidence is already embedded in the regulatory architecture; the practical challenge is therefore to determine what kind of modelling, validation and interpretation can be considered sufficiently credible for compliance assessment in real projects (ENTSO-E, n.d.; European Commission, 2016).

Within this broader transition, GFM control has emerged as a strategically important capability for IBRs. NERC defines GFM control as control whose primary objective is to maintain an internal voltage phasor that is constant or nearly constant in the sub-transient to transient time frame, thereby enabling the inverter-based resource to respond immediately to external system changes. This differs fundamentally from grid-following

control, whose fast-time-scale objective is current regulation rather than voltage formation. Recent literature also shows that, because GFM behaviour changes fault response, voltage support, synchronisation and interoperability, the question of compliance can no longer be separated from the question of dynamic control behaviour itself (NERC, 2023a; Ghimire et al., 2025, pp. 2–6).

At the same time, GFM technology is not developing in a single application niche. Lin et al. (2020, pp. 44–47) argue that implementation is likely to proceed in stages, from microgrids and island systems to weak sections of larger grids and, ultimately, wider bulk-system deployment. This staged trajectory makes simulation-based validation especially important. It can support early controller development and prototyping, enable systematic exploration of operating points and disturbance severities, produce evidence before large-scale field deployment, and help build the technical confidence needed for broader adoption across current and emerging implementation areas of GFM technology (Ghimire et al., 2025, pp. 9–11; Lin et al., 2020, pp. 44–47; NERC, 2023b, pp. v–x).

1.2 Research problem and motivation

Despite this progress, a substantial gap remains between high-level grid-code expectations and a robust compliance methodology for GFM-capable IBRs. Recent reviews show that transmission system operators, standards bodies and technical organisations refer to overlapping but not identical sets of GFM functionalities, and that the resulting requirements are often formulated with varying degrees of specificity. Ghimire et al. (2025, pp. 2–6) show that specialised performance and testing requirements are needed for novel IBRs and that many GFM capabilities still have to be interpreted across differing control concepts, equipment constraints and use cases. In parallel, the NREL roadmap argues that the field still needs clearer definitions, requirement specifications, functional specifications and validation processes for grid-forming technology (Ghimire et al., 2025, pp. 2–6; Lin et al., 2020, p. 44).

For this reason, the central problem addressed in this thesis is not simply whether a GFM-capable IBR can fulfil selected technical functions, but how simulation-based evidence can be organised to demonstrate grid-code compliance in a manner that is transparent, repeatable and useful for interconnection and certification practice. This problem is reinforced by the fact that conventional positive-sequence studies are not always sufficient for inverter-dominated systems. NERC states that electromagnetic transient (EMT) studies are becoming increasingly necessary as IBR penetration rises, particularly for low system strength, control interactions, stability assessment, ride-through behaviour, short-circuit studies and the benchmarking of RMS models. IEEE 2800 and IEEE 2800.2 reinforce the same movement by linking technical performance requirements to plant-level conformity assessment procedures, including modelling and verification methods for demonstrating conformance (IEEE, 2022; IEEE, 2026; NERC, 2023b, pp. v–x).

Accordingly, this introduction foregrounds the relationship between IBRs and grid-code compliance at a pan-European level, using the NC RfG and its implementation environment as the primary regulatory frame. After this chapter, however, the thesis narrows the detailed operational analysis to the VDE FNN guideline. That choice is methodologically justified because recent literature identifies VDE FNN as one of the European sources that has translated general GFM expectations into explicit validation scenarios, including phase and magnitude steps, RoCoF response, harmonic behaviour, islanding and short-circuit-ratio variation (Ghimire et al., 2025, p. 4).

1.3 Aim and research questions

The aim of this thesis is to develop a compliance-oriented framework for assessing how simulation-based evidence can demonstrate conformity of GFM-capable IBRs with grid-code requirements. The emphasis is placed on methodology rather than on the optimisation of one specific converter design. More precisely, the thesis seeks to connect regulatory requirements to simulation scenarios, performance indicators, evidence criteria

and validation steps that can support credible compliance assessment for present and future applications of GFM technology (ENTSO-E, n.d.; IEEE, 2026; Lin et al., 2020, p. 44). The main research question of the thesis is therefore the following: How can simulation-based evidence demonstrate compliance of inverter-based resources with grid-code requirements for grid-forming operation? To answer this question, the thesis addresses four supporting issues. First, it examines which GFM-relevant requirements can be extracted from the European grid-code framework and its national implementation context. Second, it considers how those requirements can be translated into simulation scenarios, assessment criteria and compliance indicators. Third, it evaluates how EMT modelling, complemented by controller-hardware-in-the-loop validation, can strengthen the credibility of the evidence produced. Fourth, it identifies the practical limits of simulation-based validation in relation to plant behaviour, parameter uncertainty and real-world implementation constraints (ENTSO-E, n.d.; Ghimire et al., 2025, pp. 9–10; NERC, 2023b, pp. v–x).

By framing the study in this way, the thesis also addresses a broader issue that is central to current GFM development, namely how simulation-based validation contributes not only to formal compliance assessment, but also to controller development, model benchmarking, pre-deployment risk reduction and the staged roll-out of GFM technology across microgrids, islanded systems, weak-grid applications and future bulk-system operation. Simulation is therefore treated here not merely as a numerical tool, but as an evidence-generating mechanism within a wider compliance process (Ghimire et al., 2025, pp. 9–11; Lin et al., 2020, pp. 44–47; NERC, 2023b, pp. v–vii).

1.4 Scope, methodological approach and limitations

The scope of this thesis is limited to the simulation-based assessment of selected grid-forming requirements for inverter-based resources. The work does not aim to redesign European grid codes, develop a new grid-forming controller, or provide a complete certification procedure for all grid-forming functionalities. Instead, it focuses on a defined subset of the VDE FNN guideline: voltage-source behaviour and Primary Control Based

on Network Security (PCNB). These two requirements were selected because they directly represent the ability of a grid-forming unit to establish voltage and contribute to active-power/frequency stability during virtual island operation.

Methodologically, the thesis follows an EMT-based simulation approach. The implemented study uses the GFM grid-forming inverter model developed by Professor Lingling Fan as the test object. This choice is consistent with the objective of the thesis, because the focus is not on controller design but on how an existing grid-forming inverter model can be subjected to structured grid-code verification tests. The simulation model is implemented in MATLAB/Simulink and evaluated through automated test execution, measurement extraction, deviation calculation and report generation. The automation framework developed in this thesis, AGIS, is used to execute the selected VDE FNN operating points and produce repeatable verification outputs.

Controller-hardware-in-the-loop (C-HIL) is considered in this thesis as a possible future validation layer, but it is not implemented as part of the main experimental work. The implemented work is therefore limited to offline EMT-based simulation. This distinction is important because C-HIL would require a real-time simulator and external controller hardware, whereas the present thesis evaluates the complete plant and controller model within the MATLAB/Simulink environment. Nevertheless, C-HIL remains relevant as a future extension because it could strengthen the traceability between the simulated controller behaviour and an actual hardware controller implementation.

The main limitations of the thesis are related to model fidelity, parameter assumptions and the absence of physical hardware validation. Since the work is based on a simulation model, the results demonstrate the behaviour of the selected EMT model under the implemented test conditions; they do not by themselves prove the compliance of a physical commercial inverter. Furthermore, only Measurements 1.1 to 1.3 of the VDE FNN virtual island network procedure are implemented, and the study is restricted to the selected voltage-source and PCNB requirements. Other requirements of the guideline, such as

detailed inertia procurement tests, harmonic behaviour, damping above 10 Hz, network-parallel operation capability and full hardware-based certification, remain outside the scope of this thesis.

1.5 Structure of the thesis

Following this introduction, Chapter 2 reviews the technical and regulatory foundations of inverter-based resources, grid-forming control and simulation-based compliance assessment. It introduces the distinction between grid-following and grid-forming behaviour, reviews the main grid-forming control families and discusses the role of RMS simulation, EMT simulation and hardware-in-the-loop methods in modern inverter-based resource validation.

Chapter 3 narrows the broad regulatory context to the VDE FNN guideline, which is used as the operational verification framework of the thesis. The chapter extracts the requirements relevant to the implemented work, especially voltage-source behaviour and PCNB, and explains the corresponding operating points, assessment quantities and deviation criteria used in the virtual island network tests.

Chapter 4 presents the modelling framework and validation strategy. It introduces the GFM model used as the simulation test object, describes the power architecture of the Simulink testbed and explains the control logic, including the power-frequency droop loop, reactive power-voltage droop loop, outer voltage control and inner current control. The chapter also clarifies the role of offline EMT simulation and positions C-HIL as a possible future validation stage rather than as an implemented experimental setup.

Chapter 5 presents the simulation implementation. It describes the Automatic GFM Inverter Simulator (AGIS), the MATLAB-based automation framework developed to execute the selected VDE FNN tests, extract measurements and generate structured validation reports. The chapter then presents the two simulation scenarios used in the thesis:

a baseline scenario expected to reveal non-compliant behaviour and a tuned scenario expected to satisfy the implemented criteria.

Chapter 6 interprets the simulation results. Rather than simply repeating the pass/fail outcomes, it explains how the measured quantities should be understood in relation to the physical requirements of the VDE FNN guideline. The chapter first interprets the voltage-source behaviour measurements and then analyses the PCNB measurements, showing how the deviation calculations connect the EMT validation procedure to the underlying physical behaviour of a grid-forming unit.

The final chapter concludes the thesis by summarising the main findings, the contribution of the AGIS framework, the limitations of the simulation-based approach and recommendations for future work, including extension toward real-time C-HIL validation and broader coverage of VDE FNN verification requirements.).

2 Literature and Standard Reviews

2.1 IBR dynamic behaviour, control, and grid-forming taxonomy

The starting point for the literature review is the recognition that inverter-based resources are not merely smaller or cleaner substitutes for synchronous generation. Their AC-side behaviour is created through power-electronic conversion and digital control, so their system contribution is more explicitly “designed” than that of conventional machines. NREL’s roadmap emphasises that future power systems will be hybrid systems containing both synchronous and inverter-based resources, and that the control behaviour of the latter is central to stability, protection, fault ride-through and model validity. Ghimire et al. similarly note that rapid growth of IBRs reduces inertia and short-circuit power and can intensify voltage, frequency and synchronisation challenges, which is precisely why grid-forming functionality has moved from niche microgrid practice to the centre of present grid-code discussions (Lin et al., 2020; Ghimire et al., 2025).

The literature consistently distinguishes between **grid-following** and **grid-forming** control. In NREL’s formulation, the grid-following controller contains a phase-locked loop that estimates the terminal-voltage angle and a current-control loop that regulates injected AC current. Under this arrangement, the inverter behaves as a current source or PQ source whose operation depends on an externally established voltage waveform. NREL therefore describes grid-following behaviour as dependent on having a well-defined terminal voltage to which the PLL can latch, while Ghimire et al. characterise the same logic as synchronising to the grid and injecting constant power via controlled current. By contrast, grid-forming controllers do not rely on an external voltage source or PLL in the same way; instead, they define internal voltage and frequency and present voltage-source-like behaviour on the AC side (Lin et al., 2020; Ghimire et al., 2025).

Within grid-forming control, NREL identifies three broad control families that remain the most useful organising taxonomy for thesis writing: **droop control**, **virtual synchronous machines**, and **virtual oscillator control**. That classification is analytically useful because it separates controllers according to the fundamental mechanism by which synchronisation and power sharing emerge, while also showing that they share common steady-state droop-like properties. NREL explicitly states that droop control, VSMs and virtual oscillators all aim at grid-forming behaviour and can be compared through their steady-state P - ω and Q - V properties, even though their short-timescale implementations differ (Lin et al., 2020).

Droop-based grid-forming control remains the most mature and historically rooted family. NREL describes droop control as the most well-established grid-forming method, originally proposed in the early 1990s, and emphasises that its defining feature is a linear trade-off between frequency and voltage, on the one hand, and real and reactive power, on the other. This produces two system-level consequences that remain highly relevant for compliance studies: network-wide synchronisation and programmable power sharing. At the same time, the same NREL review notes that droop loops normally rely on low-pass or notch filtering of measured signals, so their dynamic performance depends strongly on the tuning trade-off between response speed, harmonic rejection and stability. For a thesis focused on certification, this means that droop control is attractive because its structure is comparatively interpretable against grid-code functions, but it also means that parameter settings, filter bandwidths and output-impedance shaping must be considered part of the compliance evidence rather than implementation detail (Lin et al., 2020).

Virtual synchronous machine control is best understood as an attempt to embed a synchronous-machine model, or at least a reduced swing-equation analogue, in the inverter controls. NREL notes that VSM implementations range from simplified virtual-inertia forms to more detailed machine-like models including damping and flux-linkage terms, and that these parameters can be tuned much more freely than in an actual rotating

machine. The attraction of VSMs in standards and certification discourse is that they map comparatively naturally onto legacy power-system concepts such as inertia, damping and synchronising torque. The complication is that “machine likeness” is not itself a compliance requirement; the thesis must therefore avoid assuming that a more synchronous-looking controller is automatically more grid-code compliant. In a certification context, the relevant issue is whether the chosen VSM implementation achieves the required measurable behaviours—phase-jump response, reactive support, ride-through, damping and system-strength support—within hardware and current limits (Lin et al., 2020; NERC, 2023a).

Virtual oscillator control, including **dispatchable virtual oscillator control**, is the most nonlinear of the three families and often offers some of the strongest theoretical grounding for decentralised synchronisation. NREL explains that virtual-oscillator methods emulate nonlinear oscillator circuits and, despite appearing structurally different from droop or VSM control, can still exhibit $Q-V$ and $P-\omega$ droop laws in steady state. The original dVOC work by Seo et al. then adds an explicitly dispatchable formulation and reports experimental validation of dynamic synchronisation, black-start operation, transient voltage regulation, load sharing and programmable droop characteristics. For the thesis writing, the main analytical point is that dVOC expands the literature beyond “droop versus VSM” and shows that grid-forming is more usefully treated as a behavioural class than as a single architecture. However, because dVOC is still less common in utility-scale conformity practice than droop- or VSM-based formulations, it is often more useful in a literature review as a conceptual benchmark than as the default basis for clause-by-clause compliance mapping (Lin et al., 2020; Seo et al., 2018).

The control literature also points to an important qualification that matters for certification: **current limiting, fault behaviour, interoperability and energy headroom are not secondary implementation details but defining features of grid-forming practicality.** NERC’s grid-forming white paper stresses that grid-forming resources must maintain stabilising characteristics while respecting current limits and that key functions include

phase-jump performance, system-strength support, fault current behaviour, seamless transition and negative-sequence behaviour. Ghimire et al. reach a similar conclusion by showing that some candidate GFM functionalities are best treated as mandatory, some as optional and some as advanced because they imply very different requirements for hardware, energy buffering or operating conditions. A literature review written for a compliance-oriented thesis should therefore avoid presenting GFM as a binary capability. It is better to describe it as a layered performance envelope whose credible assessment depends on the disturbance class, the time scale and the available validation evidence (NERC, 2023a; Ghimire et al., 2025).

A second layer of the taxonomy concerns **functional definitions**, not control families. NERC defines grid-forming control for bulk-power-system-connected IBRs as control whose primary objective is to maintain an internal voltage phasor that is constant or nearly constant in the sub-transient to transient time frame, thereby enabling immediate response to external disturbances. Ghimire et al. show why such behavioural definitions are valuable: they can cut across hardware families and align better with grid-code thinking than merely naming controller topologies. The same review also proposes a useful requirement taxonomy in which mandatory GFM capabilities cover core voltage-source behaviour, synchronising active power, damping active power, inertial contribution, voltage support, fault ride-through capability and robustness to SCR and RoCoF changes; optional capabilities include functions that can also be achieved by other converter controls, such as harmonic sinking or imbalance mitigation; and advanced capabilities include black start, large-system autonomous operation and some islanding and auto-resynchronisation functions. This taxonomy is especially helpful for a master's thesis because it gives a principled way to separate what must be modelled and tested now from what can be acknowledged as future work or context-dependent extension (NERC, 2023a; Ghimire et al., 2025).

2.2 Simulation and validation methods for compliance and certification

The methodological literature is clear that **no single simulation or testing method is sufficient across all IBR compliance questions**. Instead, the evidence chain must be matched to the type of requirement under study. NERC's EMT guideline is particularly explicit on this point: as IBR penetration increases, EMT studies are becoming increasingly necessary for low-system-strength networks, control interactions, small- and large-disturbance stability, black start, protection misoperation, power-quality issues and IEEE 2800 verification. At the same time, the same guideline states that positive-sequence RMS models remain relevant, especially when benchmarked against verified EMT models, because large-area planning and broader screening cannot practically be carried out using EMT alone (NERC, 2023b).

RMS simulation therefore retains a legitimate role, but that role is bounded. It is well suited to slower electromechanical phenomena, broader scenario screening, set-point studies, large-system contingency sweeps and preliminary interpretation of active-power and reactive-power functions that do not depend critically on sub-cycle converter dynamics. However, NERC explicitly notes that higher trust is placed in higher-fidelity models and recommends that positive-sequence dynamic models be benchmarked against verified EMT models. For a thesis concerned with grid-forming compliance, this means RMS models can support a chapter on wide-area context or preliminary scenario design, but they should not be treated as sufficient evidence for fast voltage-source behaviour, current-limiting effects, negative-sequence response, rapid phase-jump performance or protection-relevant transients (NERC, 2023b).

EMT simulation is the central modelling method for certification-oriented GFM assessment because it is the most suitable environment for representing fast inner-loop controls, current limits, asymmetrical faults, unbalanced conditions, harmonic content and control interactions in weak grids. NERC states that EMT models are generally regarded as the highest-fidelity models used in stability studies and that industry increasingly needs high-quality, validated and facility-specific EMT models. NERC's grid-forming white

paper goes further and argues that verification of GFM functionality requires accurate and detailed EMT models provided and certified directly by OEMs, together with validation reports against laboratory, field or HIL evidence. For a compliance thesis, EMT is therefore not just “one possible simulation platform”; it is the main environment in which the claimed evidence becomes regulatorily credible (NERC, 2023a; NERC, 2023b).

Hardware-in-the-loop methods occupy an intermediate position between pure simulation and full-power testing. Ghimire et al. describe simulation-based tests as the starting point for GFM capability assessment and then place HiL and SiL as more advanced stages used for prototyping, verification and the use of real control code. NERC likewise treats HIL results as a valid part of the model-validation chain and recommends that OEM-provided validated models be supported by validation test reports against laboratory, field or HIL tests. For a master’s thesis, this is important because it justifies a proportionate methodology: the thesis does not need to claim that HIL replaces all certification testing, but it can argue—credibly and with support from the literature—that HIL strengthens the traceability between controller implementation and EMT evidence (NERC, 2023a; Ghimire et al., 2025).

Within that broader HIL category, **controller-hardware-in-the-loop** is the most plausible validation layer for the present thesis because it keeps the power stage and network in real-time simulation while executing actual control logic on embedded or industrial hardware. Although the standards documents cited here more often use the broader term “HIL” than the narrower term “CHIL”, their logic strongly supports a CHIL-oriented thesis design: model credibility improves when real code is exercised against a detailed real-time plant model, yet the cost, safety burden and laboratory complexity remain much lower than for PHIL or full-scale testing. This is an interpretive conclusion drawn from the evidence chain proposed by NERC and Ghimire et al., and it aligns with the thesis scope assumed in the prior discussion.

Power-hardware-in-the-loop is the stronger but more demanding extension of the same logic. Ghimire et al. describe PHIL test benches with grid emulators and real-time simulations capable of emulating phase jumps, voltage steps, RoCoF, harmonic behaviour and dynamic impedance effects. NERC also cites PHIL experience from the HECO Maui system and notes that such tests helped quantify the amount of grid-forming inverter capability needed for stability in a realistic transmission setting. In a certification workflow, PHIL is particularly valuable when the research question extends from “Is the controller credible?” to “Does the integrated hardware-control package behave credibly under realistic grid emulation?” The practical drawback, of course, is that PHIL introduces additional cost, interface complexity and stability considerations, which is why it is often more appropriate as a follow-on method than as the core of a master’s thesis (NERC, 2023a; Ghimire et al., 2025).

Taken together, the methodological literature supports a certification-oriented evidence hierarchy: **RMS** for system-wide screening and context; **EMT** for main dynamic compliance claims; **CHIL/HIL** for implementation-aware validation of controller behaviour; and **PHIL or targeted laboratory/site tests** for the highest-confidence claims, especially where plant integration or hardware constraints are decisive. That hierarchy also mirrors the logic of recent conformity-assessment developments, especially IEEE 2800.2 and NERC’s emphasis on validated OEM models and equipment-specific evidence.

2.3 Standards and regulatory review

The standards landscape relevant to this thesis is best understood as a stack rather than a single rulebook. At the European level, the legal basis is **Commission Regulation (EU) 2016/631**, the Network Code on Requirements for Generators. ENTSO-E presents this code as the harmonised framework for generator connection across Europe and explicitly organises implementation work, guidance documents and monitoring around it. The ENTSO-E page also shows that the code covers different categories of generating modules and power park modules and includes specific chapters for offshore power park modules, which is significant because it confirms that a pan-European compliance

methodology must be able to handle both general and application-specific requirements (ENTSO-E, n.d.; European Commission, 2016).

From the perspective of simulation-based certification, the most important part of NC RfG is not only the list of plant capabilities but the fact that the regulation explicitly includes both **compliance testing** and **compliance simulation**. Article 42 concerns common provisions for compliance testing, while Article 43 concerns common provisions on compliance simulation. Article 43 states that the purpose of simulation is to demonstrate fulfilment of the regulation's requirements and also allows the relevant system operator to request additional or alternative simulations where the supplied evidence is insufficient. For type C and D power park modules, the later articles then make the evidentiary logic even clearer: several compliance simulations are deemed successful only if the simulation model has been validated against relevant compliance tests and the requirement itself is demonstrated. This is a crucial point for the thesis because it shows that the conceptual bridge between simulation and certification is already embedded in European law; the unresolved issue is the quality, scope and standardisation of the evidence process (European Commission, 2016).

A second strand of the standards review concerns the broader evolution of grid codes. IRENA argues that grid codes should be technology-neutral as far as possible and should evolve as system needs evolve. It also links this evolution explicitly to decentralisation, digitalisation and electrification, and notes that high-VRE systems increasingly require full frequency and voltage control capabilities, grid-forming capability, black-start support and broader controllability envelopes. This perspective is valuable for thesis writing because it frames grid-code evolution as a governance problem as well as a technical one: requirements must be specified in functional, testable terms without prematurely locking the industry into one implementation path (IRENA, 2022).

At the distribution level, **IEEE 1547-2018** remains a key reference because it defines technical specifications and testing for the interconnection and interoperability of distributed energy resources with electric power systems. The IEEE standards page states that it

covers response to abnormal conditions, power quality, islanding, interoperability and test specifications for design, installation, commissioning and periodic tests, with applicability across DER technologies connected at typical distribution voltages. For the present thesis, IEEE 1547 matters less as the final compliance target than as a useful comparator: it demonstrates how interconnection standards can tie functional requirements directly to testing and verification logic, even when the resource fleet is diverse (IEEE, 2018).

At the transmission and sub-transmission level, **IEEE 2800-2022** is much closer to the themes of this thesis. IEEE states that the standard establishes uniform technical minimum requirements for interconnection, capability and lifetime performance of IBRs connected to transmission and sub-transmission systems, including voltage and frequency ride-through, active and reactive power control, dynamic active power support, dynamic voltage support, power quality, negative-sequence current injection and protection. It also applies to isolated IBRs interconnected through VSC-HVDC facilities, which is relevant to offshore and HVDC-linked plant concepts. In analytical terms, IEEE 2800 is important because it moves well beyond basic interconnection and into the dynamic-performance regime that certification-oriented EMT studies must address (IEEE, 2022).

The recent approval of **IEEE 2800.2-2026** significantly strengthens the certification relevance of the standards stack. IEEE describes 2800.2 as a recommended practice for conformity-assessment procedures to verify plant-level conformity with IEEE 2800. Crucially, it complements the 2800 framework with specifications for equipment, conditions, tests, modelling methods and other conformity-assessment procedures needed to demonstrate conformance. This is perhaps the most directly relevant standards development for a thesis on simulation-based evidence because it formalises the notion that compliance is not just about raw performance but about the adequacy of the models, methods and verification steps used to prove that performance (IEEE, 2026).

The **VDE FNN guideline** is especially important as the bridge between the pan-European framework and the practical test philosophy to be used later in the thesis. The official VDE FNN publication page identifies the document *Technical Requirements for Grid-Forming Capabilities Including Provision of Inertia* as a technical basis for the verification of grid-forming units and for participation in future market-based procurement of inertia services. The guideline extends beyond general grid-code expectations by defining explicit technical requirements and verification procedures for voltage-source behaviour, continuous voltage control, start-up time constant behaviour, inertia provision, and frequency-control functions associated with Primary Control Based on Network Security (PCNB). In parallel, Ghimire et al. provide one of the clearest high-level reviews of the role of VDE FNN within the broader GFM landscape, emphasising that the guideline does not prescribe a single control implementation but instead establishes a structured validation framework based on representative disturbance scenarios and measurable performance criteria. These include voltage phase-angle and magnitude variations, frequency disturbances, harmonic and negative-sequence behaviour, network-strength variations, and assessments of stable operation under demanding system conditions. For this thesis, the VDE FNN guideline therefore serves as a particularly valuable operational framework for translating high-level grid-code expectations into concrete simulation-based compliance assessments, while NC RfG remains the broader regulatory foundation (VDE FNN, 2025; Ghimire et al., 2025).

Finally, two NERC documents are particularly relevant even though they are not binding European codes. The 2023 NERC white paper on grid-forming functional specifications provides one of the clearest behavioural definitions of GFM and identifies core functions such as autonomous near-instantaneous voltage and frequency support, phase-jump performance, system-strength support, standalone capability and appropriate fault behaviour. The 2023 NERC EMT guideline then translates the broader IBR challenge into modelling expectations, calling for validated, facility-specific EMT models and systematic benchmarking of positive-sequence models. Together, these documents are valuable not because they define the thesis's legal compliance target, but because they articulate the

technical evidence expectations that any serious simulation-based certification workflow must eventually meet (NERC, 2023a; NERC, 2023b).

The relationship between regulations, modelling methods and certification logic can be summarised as follows.

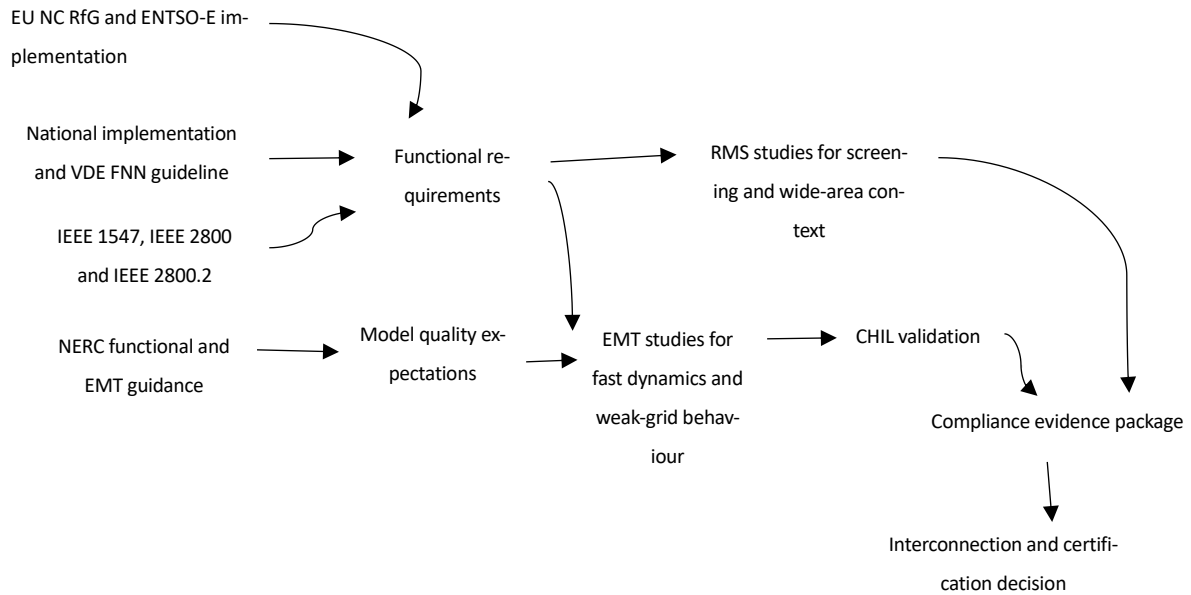


Figure 1: Flow Chart of relationship between regulations, modelling methods and certification logic

This diagram reflects the central conclusion of the standards review: modern IBR compliance is not moving towards a single universal test, but towards a structured evidence package in which legal requirements, performance specifications, modelling methods and validation steps must be explicitly linked. In this thesis, the NC RfG, ENTSO-E implementation framework, IEEE standards, IRENA guidance and NERC documents are reviewed to establish the wider regulatory and technical context for inverter-based resource compliance. However, these documents are not all used as direct assessment frameworks in the simulation part of the thesis. Instead, they provide the background for understanding why detailed grid-forming verification is necessary, why EMT modelling is required, and why simulation-based evidence must be traceable and repeatable. The operational verification framework used in the remainder of the thesis is the VDE

FNN guideline, because it provides explicit grid-forming requirements, virtual island network test conditions, EMT model validation expectations and measurable assessment criteria for voltage-source behaviour and Primary Control Based on Network Security. Therefore, Chapter 3 narrows the broader standards review to the VDE FNN guideline and extracts only the requirements, operating points and assessment criteria that are implemented in the simulation framework developed in this thesis.

3 Grid Code Requirements and Assessment Criteria

3.1 From the European Grid-Code Framework to the VDE FNN Guideline

The ongoing energy transition is fundamentally changing the structure and operation of power systems worldwide. The increasing penetration of inverter-based resources (IBRs), including wind turbines, photovoltaic systems and battery energy storage systems, is progressively replacing conventional synchronous generation. While this transition contributes significantly to decarbonisation objectives, it also introduces new technical challenges related to frequency stability, voltage control, inertia provision and system strength. Unlike synchronous generators, inverter-based resources are connected to the grid through power electronic converters and therefore do not inherently provide the electromechanical characteristics upon which traditional power system operation has historically relied.

At the European level, the regulatory framework governing the connection of generation facilities is established by Commission Regulation (EU) 2016/631, commonly referred to as the Network Code on Requirements for Generators (NC RfG). The NC RfG defines harmonised technical requirements for generation facilities connected to transmission and distribution networks across Europe. In addition to establishing common connection requirements, the regulation recognises both compliance testing and compliance simulation as acceptable methods for demonstrating conformity. Consequently, simulation-based assessment has become an increasingly important tool for evaluating the behaviour of inverter-based resources before commissioning and certification.

Despite providing the legal foundation for generator compliance, the NC RfG remains technology-neutral and does not define detailed technical requirements for grid-forming operation. As converter-based generation continues to replace synchronous machines, additional technical specifications have become necessary to define the expected behaviour of grid-forming units and to establish objective verification procedures. Several

organisations have therefore developed supplementary guidelines addressing the technical requirements of grid-forming technologies.

Among these initiatives, the VDE FNN Guideline Technical Requirements for Grid-Forming Capabilities Including Provision of Inertia (Version 2.0, October 2025) represents one of the most comprehensive frameworks currently available for the certification of grid-forming units. The guideline specifies the required functionalities, dynamic performance characteristics and verification procedures for grid-forming power-generating units, storage systems and controllable consumption units. Furthermore, it provides explicit requirements for electromagnetic transient (EMT) simulation models, making it particularly relevant for simulation-based certification methodologies.

The VDE FNN guideline identifies several key functionalities that a grid-forming unit must provide, including voltage source behaviour, inertia provision, frequency control, damping capability, current limitation and network stability support. However, considering the objectives and scope of this thesis, the analysis focuses on two fundamental requirements that form the basis of grid-forming operation:

- Voltage source behaviour;
- Primary Control Based on Network Security (PCNB).

These requirements were selected because they constitute the fundamental mechanisms through which a grid-forming inverter establishes and maintains voltage and frequency within an electrical network. Moreover, both functionalities are associated with explicit verification procedures and assessment criteria defined by the guideline, enabling their implementation within an automated simulation-based certification framework.

Consequently, this chapter narrows the broad European regulatory context introduced in Chapter 1 to the specific requirements and verification procedures defined by the VDE FNN guideline. The chapter first examines the technical requirements associated with voltage source behaviour and PCNB operation before presenting the corresponding EMT validation requirements, assessment criteria and test scenarios used throughout this thesis.

3.2 Technical Requirements for Grid-Forming Units

3.2.1 Voltage Source Behaviour

According to Section 4.2.1.1 of the VDE FNN guideline, a grid-forming unit shall behave as a controllable voltage source at the network connection point. Unlike grid-following converters, which synchronise to an externally imposed voltage waveform, grid-forming converters actively establish and regulate network voltage and frequency through an internal voltage source.

From a physical perspective, this requirement means that the converter must generate a positive-sequence voltage whose magnitude and phase angle are controlled independently of the surrounding network conditions. As a result, the converter becomes capable of maintaining voltage and frequency even in weak-grid or islanded operating conditions.

The guideline represents this behaviour using an equivalent voltage-source model connected to the network through an impedance. Under normal operating conditions, the active and reactive power exchange between the internal voltage source and the external network can be approximated using the following relationships.

The active power exchange is described by:

$$i_{P1,PGU} = \frac{p_{1,PGU}}{u_{1,PGU}} \approx -\frac{u_1}{x_{w,1}} \sin(\delta_1) \quad (3.1)$$

Similarly, the reactive power exchange is described by:

$$i_{Q1,PGU} = \frac{q_{1,PGU}}{u_{1,PGU}} \approx \frac{1}{x_{w,1}} (u_{1,PGU} - u_1 \cos(\delta_1)) \quad (3.2)$$

The angular difference between the terminal voltage and the internal voltage source is defined as:

$$\delta_1 = \varphi_{u_{1,PGU}} - \varphi_{u_1} \quad (3.3)$$

Where:

δ_1 is the angular difference between the positive sequence voltage at the terminals and the positive sequence voltage of the internal voltage source of the PGU

$\phi_{1,PGU}$ is the voltage angle of the positive sequence voltage at the terminals of the grid-forming unit

Φ_{u1} is the inertia-induced voltage angle of the positive sequence voltage of the internal voltage source of the grid-forming unit

$p_{1,PGU}$ is the positive sequence active power output/input of the grid-forming unit at its terminals

$q_{1,PGU}$ is the positive sequence reactive power output/input of the grid-forming unit at its terminals

$r_{w,1}$ is the active resistance of the positive sequence effective impedance $z_{w,1}$ of the grid-forming unit

$x_{w,1}$ is the inductive reactance of the positive sequence effective impedance $z_{w,1}$ of the grid-forming unit

u_1 is the magnitude of the positive sequence voltage of the internal voltage source of the PGU

$u_{1,PGU}$ is the magnitude of the positive sequence voltage at the terminals of the grid-forming unit

Interpretation

Equations (3.1) – (3.3) are extremely important because they describe the physical principle underlying grid-forming operation (VDE FNN, 2025, Section 4.2.1.1).

The active power transferred between the converter and the network depends primarily on the voltage-angle difference (δ_1). Consequently, active power can be controlled by modifying the phase angle of the internal voltage source.

Conversely, reactive power depends mainly on the voltage-magnitude difference between the internal voltage source and the network voltage. Therefore, reactive power can be regulated by adjusting the voltage magnitude generated by the converter.

This behaviour closely resembles the power-angle characteristics of synchronous generators and explains why grid-forming converters are often described as virtual synchronous machines. Unlike grid-following converters, which directly regulate output current, grid-forming converters regulate voltage and allow power exchange to emerge naturally from network interactions.

Continuous Voltage Control

To maintain stable network operation, the VDE FNN guideline further requires continuous voltage control. The voltage controller must continuously regulate the voltage magnitude at the network connection point while maintaining stable interaction with surrounding equipment.

The objective of continuous voltage control is to:

- maintain voltage within acceptable operating limits;
- support reactive power balancing;
- improve system stability;
- contribute to fault recovery following disturbances.

Furthermore, the guideline requires sufficient damping of voltage oscillations to avoid unstable behaviour during transient events.

3.2.2 Primary Control Based on Network Security (PCNB)

Definition

Primary Control Based on Network Security (PCNB) constitutes the second major requirement addressed in this thesis. According to Section 4.2.2.2 of the VDE FNN guideline, PCNB represents the primary frequency-control functionality that supports network stability outside the normal frequency deadband.

The objective of PCNB is to restore active power balance following disturbances and maintain frequency stability during both synchronous and islanded operation.

The guideline distinguishes between:

- unlimited PCNB operating range;
- limited PCNB operating range.

The unlimited operating range corresponds to the active-power region where the unit can provide frequency support without significant technological restrictions. Within this range, the converter must demonstrate stable frequency control behaviour and maintain a stable operating point following power imbalances.

Droop Characteristics

The active power response of the PCNB controller is characterised by the droop coefficient:

$$s = \left| \frac{\Delta f / f_n}{\Delta P / P_{ref}} \right| \quad (3.4)$$

Interpretation

The droop coefficient establishes the relationship between frequency deviations and active-power response.

When frequency decreases below its nominal value, the converter increases active power output. Conversely, when frequency rises above nominal, the converter reduces active power output.

Therefore, the droop controller acts as a proportional frequency stabiliser that continuously adjusts active power to restore power balance.

3.3 EMT Validation and Verification Methodology

3.3.1 EMT Model Validation Requirements

The increasing penetration of inverter-based resources has highlighted the limitations of traditional positive-sequence RMS models for assessing converter-dominated power systems. While RMS models remain suitable for many steady-state and electromechanical studies, they often fail to accurately represent the fast control dynamics, switching behaviour and electromagnetic interactions that characterise modern power electronic converters. Consequently, the VDE FNN guideline explicitly recognises electromagnetic transient (EMT) simulations as a necessary tool for the verification of grid-forming units. The objective of EMT model validation is to ensure that the simulation model accurately reproduces the behaviour of the physical equipment under both steady-state and transient operating conditions. According to Section 5.5.3 of the guideline, the EMT model shall represent all relevant control loops, dynamic interactions and protection functions that influence compliance-related behaviour. The model must therefore reproduce the

active power, reactive power, voltage and frequency responses associated with the required grid-forming functionalities.

The validation philosophy adopted by the guideline follows a certification-oriented approach. Rather than using simulations solely as a design tool, the validation of the EMT model can be used as part of the compliance evidence submitted during the certification procedures. Consequently, the model must accurately reproduce the physical behaviour of the grid-forming unit under the operating conditions defined by the verification procedures.

Within the scope of this thesis, the EMT model is implemented in MATLAB/Simulink using the GFM grid-forming inverter model developed by Lingling Fan. The model includes:

- A three-phase voltage source inverter;
- Inner current control loops;
- Outer voltage control loops;
- Active and reactive power control loops;
- Virtual inertia implementation;
- Droop-based frequency regulation;
- Current limitation mechanisms.

The model is subsequently subjected to the verification procedures defined by the VDE FNN guideline. Therefore, the compliance assessment presented in this thesis is performed entirely through a model subjected to the FNN verification procedure; however, hardware-based model validation remains outside the scope of this thesis.

3.3.2 Virtual Island Network

The primary verification environment specified by the VDE FNN guideline for grid-forming Type 2 units is the virtual island network.

The guideline defines a virtual island network as an operating condition in which the grid-forming unit becomes solely responsible for establishing and maintaining network voltage and frequency while supplying a residual load. Unlike conventional island operation, no explicit islanding signal is provided to the converter. Instead, the converter

must autonomously maintain stable operation following the transition from synchronous operation to islanded operation.

From a certification perspective, the virtual island network represents the most demanding operating condition because the grid-forming unit can no longer rely on an external voltage or frequency reference. Consequently, the converter must independently:

- establish network frequency;
- establish network voltage;
- maintain active-power balance;
- maintain reactive-power balance;
- ensure stable operation following disturbances.

The VDE FNN guideline uses this operating condition to verify three fundamental properties:

1. Inherent stability;
2. Voltage source behaviour;
3. Primary Control Based on Network Security (PCNB).

For the verification procedures considered in this thesis, the transition to virtual island operation is achieved through the disconnection of the external grid at a predefined instant. Following this event, the converter must maintain stable operation while supplying the residual load connected within the islanded system.

3.3.3 Measurement Quantities

The guideline specifies that the following electrical quantities shall be recorded during the verification process:

- Active power (P);
- Reactive power (Q);
- RMS voltage magnitude (V);
- Frequency (f);

In addition to these fundamental quantities, the guideline recommends recording instantaneous phase voltages and currents to evaluate transient behaviour immediately

before and after islanding. These signals form the basis of all subsequent compliance assessments.

3.4 Assessment Criteria and Test Scenarios

3.4.1 Operating Points Defined by the Guideline

The operating points used in this thesis are derived from Section 5.5.4.3 of the VDE FNN guideline, which defines the measurements to be performed in the virtual island network for grid-forming units providing negative inertia. The purpose of these measurements is to verify inherent stability, voltage-source behaviour and PCNB under defined active-power, reactive-power and residual-load conditions. The test begins from a steady-state operating point in parallel network operation. Then, the virtual island network is created by opening the network interconnecting circuit breaker, so that the grid-forming unit exclusively supplies the adjustable residual load. The operating condition must be maintained until a stable operating point is reached, for at least 50 s (VDE FNN, 2025, Section 5.5.4.3).

Table 3 of the VDE FNN guideline defines the measurement conditions for the virtual island network. The table is reproduced below in Table 1 because it provides the technical basis for the operating points implemented in this thesis.

Table 1: - Measurements in the virtual island network for the verification of inherent stability, voltage source behaviour and PCNB for units which provide negative inertia

Measurement		Initial power of the grid-forming unit		Residual load	
		P_{mom} (% P_{Emax})	Q / P_{Emax} (-)	P_{residual} (-)	$\frac{Q_{\text{rest}}}{P_{\text{Emax}}}$ (-)
Behaviour as a voltage source (large signal) and PCNB in the procured direction of inertia power	1.1	$\geq (P_{\text{residual}} + 23 \% P_{\text{Emax}}^{\text{e}})$	0.0	45 % P_{Emax} to 65 % P_{Emax} alternatively - 45 % P_{Emax} to - 65 % P_{Emax} when measuring 1.4	0.0
	1.2		max. ind.		
	1.3		max. cap.		
	1.4 ^{a)}	$P_{\text{Emax}} + P_{\text{residual}}$	0.0		
Small-signal behaviour in the non-procured direction of inertia	2.1 ^{b)-d)}	85 % – 95 % P_{residual}	0.0		

- a) Check load step with active power reversal only for units that operate both as load and generation (e.g. storage).
- b) Suitable throttled operation and sufficient primary energy supply are required for this test.
- c) If lower values are permitted in accordance with Table 10 Appendix B.I. regarding the power amplitude, these may be applied.
- d) Not applicable if the inertia is procured in both positive and negative directions.
- e) This corresponds to at least half of the power response to a phase angle step of 45% $P_{E_{max}}$ in the (negative) procured direction in accordance with the requirements. This is a compromise to enable the tests to be performed in practice with reasonable effort.

Where: P_{mom} = initial power output of the grid-forming unit

$P_{residual}$ = load that remains in the island network after disconnection

$P_{E_{max}}$ = maximum production capacity of the unit.

The first important condition in Table 1 is the residual-load range. For Measurements 1.1 to 1.3, the residual active load in the virtual island network shall be between (45%) and (65%) of ($P_{E_{max}}$). In this thesis, the selected residual-load target is

$$P_{residual} = 0.50 pu$$

This value is equivalent to (50% $P_{E_{max}}$) when ($P_{E_{max}}=1.0 pu$). Therefore, it lies inside the admissible range required by Table 1:

$$0.45 pu \leq P_{residual} \leq 0.65 pu \quad (3.5)$$

The second important condition is the required initial active power of the grid-forming unit before islanding. For Measurements 1.1 to 1.3, Table 1 requires the initial active power at the moment of islanding to satisfy

$$P_{mom} \geq P_{residual} + 0.23P_{E_{max}} \quad (3.6)$$

where (P_{mom}) is the active power of the grid-forming unit immediately before the transition to virtual island operation, ($P_{residual}$) is the residual active load in the virtual island network, and ($P_{E_{max}}$) is the maximum active power of the unit. With the values used in this thesis,

$$P_{residual} = 0.50 pu$$

$$P_{E_{max}} = 1.0 pu$$

the minimum required initial active power becomes

$$P_{mom} \geq 0.50 + 0.23 = 0.73 pu \quad (3.7)$$

The simulations are initialised around (0.75 pu). The selected value provides a small margin above the minimum requirement while remaining close to the operating condition prescribed by Table 1. Therefore, in the AGIS implementation, the pre-islanding active-power condition is interpreted as

$$P_{mom} \approx 0.75 \text{ pu}$$

$$P_{mom} \geq 0.73 \text{ pu}$$

The three measurements implemented in this thesis are therefore not arbitrary operating points. They are the three Table 1 measurements used to assess voltage-source behaviour and PCNB in the procured direction of inertia power under different reactive-power conditions. Measurement 1.1 is performed at approximately zero reactive power, Measurement 1.2 is performed at maximum inductive reactive power, and Measurement 1.3 is performed at maximum capacitive reactive power.

- **Test 1.1: Nominal Active-Power Operation**

$$P_{mom} = 0.75 \text{ pu}$$

$$Q \approx 0 \text{ pu}$$

P_{mom} = initial power output of the grid-forming unit

This operating point evaluates the converter under predominantly active-power loading conditions and serves as the reference case for assessing voltage source behaviour.

- **Test 1.2: Inductive Reactive-Power Operation**

$$Q = -0.33 \text{ pu}$$

$$P_{mom} = 0.75 \text{ pu}$$

This operating point evaluates the converter while supplying inductive reactive power. The objective is to determine whether stable voltage source behaviour can be maintained under lagging power-factor conditions.

- **Test 1.3: Capacitive Reactive-Power Operation**

$$P_{mom} = 0.75 \text{ pu}$$

$$Q = +0.33 \text{ pu}$$

This operating point evaluates the converter while supplying capacitive reactive power. The objective is to verify voltage source behaviour under leading power-factor conditions. Collectively, these three operating points allow the verification procedure to assess the converter across a representative range of operating conditions.

The VDE FNN guideline defines Measurement 1.2 and Measurement 1.3 as operation at maximum inductive and maximum capacitive reactive power, respectively. However, the FNN table does not explicitly assign a numerical value to these two limits. Therefore, the value used in this thesis is taken from the default reactive-power capability defined in SFS-EN 50549-2:2019. In Section 4.7.2.2, the standard states that, at nominal voltage, the default reactive-power requirement is up to 33% of the design active power (P_D) in both over-excited and under-excited operation when the active power is above 20% of (P_D). Since the simulated unit is operated at approximately 0.75 pu active power before islanding, it is clearly above the 20% threshold. (VDE FNN, 2025, section 5.5.4.3; SFS-EN 50549-2, 2019, Section 4.7.2.2).

This thesis limits the implemented verification to Measurements 1.1, 1.2 and 1.3. Measurement 1.4 is not implemented because it corresponds to a load step with active-power reversal and is only applicable to units that operate both as generation and load, such as storage systems. The GFM model used in this thesis is treated as a generating inverter model and is not operated in active-power absorption mode. Measurement 2.1 is also outside the implemented scope because it concerns small-signal behaviour in the non-procured direction of inertia, while this thesis focuses on voltage-source behaviour and PCNB in the procured direction of inertia power.

Therefore, Measurements 1.1 to 1.3 provide the complete operating-point basis for the simulations carried out in this thesis. They ensure that the residual-load condition lies within the required (45%) to (65% $P_{E_{max}}$) range, that the initial active-power condition satisfies ($P_{\{mom\}}P_{\{residual\}}+0.23P_{\{E_{max}\}}$), and that the grid-forming inverter is tested under zero, inductive and capacitive reactive-power conditions. These conditions

establish the foundation for the voltage-source and PCNB assessments presented in the following sections.

3.4.2 Assessment of Voltage Source Behaviour

The verification of voltage source behaviour is performed according to Section 5.5.4.4.1 of the guideline.

For each operating point, the following quantities are evaluated:

$$P_{init}, P_{min}, P_{max}, P_{ss}$$

where:

P_{init} = initial active power before islanding,

P_{min} = minimum transient active power at islanding,

P_{max} = maximum transient active power at islanding,

P_{ss} = final steady-state active power.

Similarly,

- $Q_{init}, Q_{min}, Q_{max}, Q_{ss}$
- $V_{init}, V_{min}, V_{max}, V_{ss}$
- $f_{init}, f_{min}, f_{max}, f_{ss}$

are extracted for reactive power, voltage magnitude and frequency respectively.

The primary objective is to verify that the converter successfully transitions from synchronous operation to virtual island operation while maintaining stable voltage and frequency.

For the voltage-source behaviour validation, the VDE FNN guideline (section 5.5.3.6.2.2.3) states that the steady-state terminal voltage of the EMT simulation model after transition into island network operation may deviate from the corresponding measured steady-state value by a maximum of $\pm 3\%$, relative to the nominal voltage. Since no physical hardware measurement is available in this thesis, the pre-islanding steady-state voltage of the simulated test is used as the reference value for comparison. The tolerance width is nevertheless calculated on the nominal per-unit voltage base. Therefore, the voltage-source criterion implemented is expressed as:

$$V_{init} - 0.03V_{nom} \leq V_{ss} \leq V_{init} + 0.03V_{nom} \quad (3.8)$$

where (V_{nom}) is the nominal voltage base. Since the simulation uses per-unit voltage with ($V_{nom} = 1.0 pu$), the tolerance band becomes

$$|V_{ss} - V_{init}| \leq 0.03V_{init} \quad (3.9)$$

This formulation preserves the intent of the guideline while adapting the comparison to the simulation-only scope of the thesis (VDE FNN, 2025, sections 5.5.4.4.1 and 5.5.3.6.2.2.3).

3.4.3 Assessment of PCNB Behaviour

The verification of PCNB behaviour follows Section 5.5.4.4.2 of the guideline.

Unlike voltage source verification, which focuses primarily on stability, the PCNB verification evaluates the accuracy of active-power and frequency regulation.

The measured quantities are compared against the corresponding operating-point references before and after islanding.

The active-power deviation is determined as

$$\Delta P = P_{meas} - P_{init} \quad (3.10)$$

where:

P_{meas} = measured active power ($P_{min}/P_{max}/P_{ss}$).

Similarly, the frequency deviation is determined as

$$\Delta f = f_{meas} - f_{init} \quad (3.11)$$

Where:

f_{meas} = measured frequency ($f_{min}/f_{max}/f_{ss}$).

According to the guideline (section 5.5.3.6.2.2.5), the measured (init/ss) values must remain within the prescribed tolerance limits of $\pm 5\%$, acceptance criterion specified for PCNB verification.

Consequently,

$$0.95P_{set} \leq P_{ss/init} \leq 1.05P_{set} \quad (3.12)$$

$$0.95f_{set} \leq f_{ss/init} \leq 1.05f_{set} \quad (3.13)$$

where:

f_{set} = reference frequency,

P_{set} = reference active power.

must be satisfied for successful compliance.

In practical terms, these requirements ensure that the converter can maintain both power balance and frequency stability before and following islanding. (VDE FNN, 2025, sections 5.5.4.4.2 and 5.5.3.6.2.2.5)

3.4.4 Compliance Evaluation Metrics

To automate the certification process, we developed a program in this thesis that extracts four key metrics from every simulation:

1. Initial steady-state value;
2. Minimum transient value;
3. Maximum transient value;
4. Final steady-state value.

These metrics are automatically extracted for:

- Active power;
- Reactive power;
- Voltage magnitude;
- Frequency.

The extracted values are then compared against the acceptance criteria defined by the VDE FNN guideline, allowing automatic identification of compliant and non-compliant behaviour.

3.4.5 Test Scenarios Implemented in this Thesis

To demonstrate the operation of the certification framework, two categories of simulations are performed.

- ***Non-Compliant Scenario***

The non-compliant scenario represents the baseline implementation of the grid-forming controller using default parameter settings.

These parameters intentionally produce deviations from one or more guideline requirements. The objective is to verify that the automated certification framework correctly identifies the non-compliant behaviour and reports the corresponding violations.

- ***Compliant Scenario***

The compliant scenario represents the optimised implementation of the controller. Controller gains, inertia settings and voltage-control parameters are adjusted until the converter satisfies the acceptance criteria associated with both voltage source behaviour and PCNB behaviour.

The resulting configuration is then subjected to the same verification procedures used for the non-compliant case.

By comparing the outcomes of both scenarios, the proposed framework demonstrates its ability to automatically distinguish compliant and non-compliant behaviour while generating reproducible certification evidence.

The requirements, operating conditions and assessment criteria established in this chapter provide the foundation for the simulation model and automated verification framework developed in the follow

4 Modelling Framework and Validation Strategy

The previous chapter defined the VDE FNN requirements and assessment criteria used in this thesis. This chapter presents the modelling framework used to implement these requirements in an electromagnetic transient (EMT) simulation environment. The purpose of the chapter is not to develop a new grid-forming control strategy, but to establish a reliable simulation and validation framework through which the selected FNN tests can be executed, measured and evaluated.

The model used in this thesis is based on the GFM model developed by Professor Lingling Fan. This choice is justified by the scope of the thesis, which focuses on grid-code certification by simulation rather than on the detailed design of a new converter controller. The GFM model is suitable for this purpose because it provides a complete EMT testbed with a voltage-source converter, filter, transformer, grid interface, residual load and a multi-loop grid-forming controller. It also implements the key characteristics required for this thesis: voltage support, power-based synchronisation and droop-based frequency response (Fan & Miao, 2024, Ch. 6).

4.1 EMT-based modelling framework

EMT simulation was selected because grid-forming inverter behaviour depends on fast electromagnetic and control dynamics. In phasor-based simulation, steady-state voltage and current quantities are represented mainly as magnitudes and phase angles. This is useful for large-scale electromechanical studies, but it does not directly show instantaneous three-phase waveforms. In EMT simulation, by contrast, the simulated currents and voltages are instantaneous time-domain signals, similar to what would be observed with an oscilloscope. This makes EMT simulation more appropriate for analysing inverter control, voltage-source behaviour, islanding transitions and short-duration dynamic responses (Fan & Miao, 2024, Ch. 2).

The modelling framework was implemented in MATLAB/Simulink using the Simscape Specialized Power Systems environment. The model is solved using a discrete simulation step of

$$T_s = 50 \times 10^{-6} \text{ s} \quad (4.1)$$

where:

T_s = simulation sampling time.

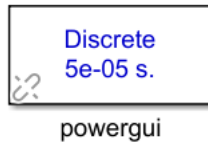


Figure 2: Powergui Simulink block

A small simulation step is necessary because the testbed contains power-electronic switching, inner current-control loops and fast voltage-control dynamics. In practical terms, this means that the solver updates the electrical states every 50 μs , which allows the model to capture the fast converter response during islanding and power disturbances.

The general power architecture of the model is composed of the following elements:

- a DC voltage source and DC-link capacitor;
- a three-phase voltage source converter (VSC);
- a coupling filter between the converter and the PCC bus;
- a PCC measurement bus;
- a shunt capacitor filter;
- a 500 kW residual load;
- a 400 V / 13.2 kV step-up transformer;
- an external grid represented by a three-phase programmable voltage source;
- breakers and measurement blocks used to create grid-connected and islanded operating conditions.

The model therefore reproduces the main physical path of a converter-interfaced resource connected to a medium-voltage grid. The DC source supplies the inverter, the VSC converts the DC energy into three-phase AC voltage, the filter attenuates high-frequency components, and the transformer connects the low-voltage converter side to the medium-voltage grid. The residual load is placed at the PCC side so that, after islanding, the

grid-forming inverter must supply the local demand and establish the island voltage and frequency.

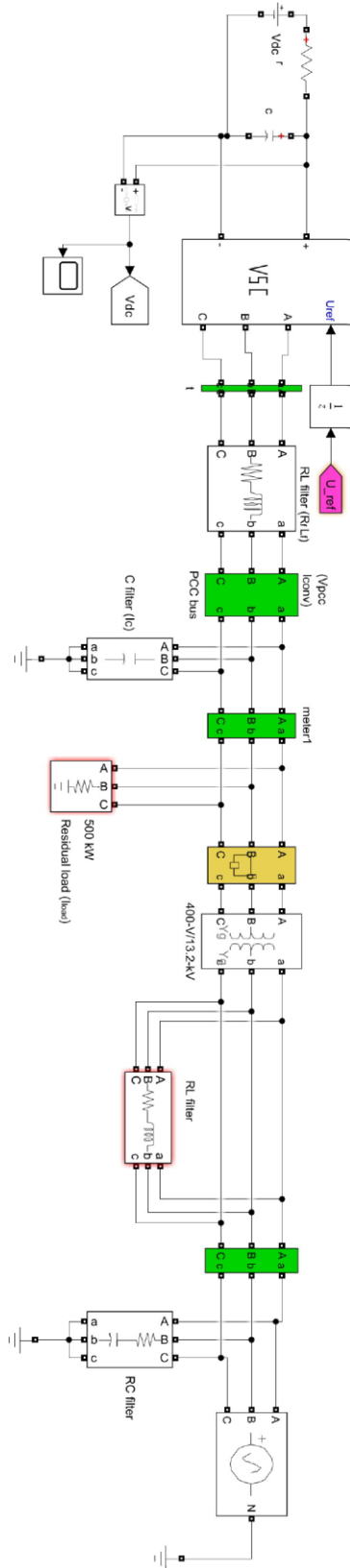


Figure 3: GFM Simulink testbed

The per-unit system is used to scale electrical quantities and simplify the comparison between operating points. The base apparent power is

$$S_b = 1 \times 10^6 \text{ VA} \quad (4.2)$$

where:

S_b = base apparent power.

The base impedance on the low-voltage side is calculated as

$$Z_{b,LV} = \frac{V_{b,LV}^2}{S_b} \quad (4.3)$$

where:

$V_{b,LV}$ = low-base voltage.

Similarly, the base impedance on the medium-voltage side is

$$Z_{b,MV} = \frac{V_{b,MV}^2}{S_b} \quad (4.4)$$

where:

$V_{b,MV}$ = medium-base voltage.

The use of per-unit values is important because the FNN tests are expressed in terms of relative active power, reactive power, voltage and frequency deviations. It also allows the same model to be interpreted independently of the absolute rating of the physical equipment.

4.2 Power architecture of the GFM testbed

The power circuit begins with a DC source feeding the voltage-source converter through a DC-link capacitor. The DC-link provides the energy buffer required by the inverter and stabilises the DC voltage during transient changes in power flow. The inverter then generates three-phase AC voltages according to the reference signals produced by the GFM controller.

The instantaneous three-phase converter voltage can be represented as

$$\mathbf{v}_{abc} = \begin{bmatrix} v_a \\ v_b \\ v_c \end{bmatrix} \quad (4.5)$$

The corresponding three-phase current vector is

$$\mathbf{i}_{abc} = \begin{bmatrix} i_a \\ i_b \\ i_c \end{bmatrix} \quad (4.6)$$

The output of the voltage-source converter is connected to the PCC through a passive filtering and network interface. In the implemented Simulink model, this interface includes a passive C–RL–RC filtering structure. The converter is first connected to the PCC through a series $R_f L_f$ coupling branch, while a shunt capacitor C_f is connected at the PCC bus. Additional resistive, inductive and capacitive elements on the grid side represent the downstream network/load interface. Therefore, the converter is not connected directly to the network; instead, its voltage is applied through a filtered interface that limits current variations, attenuates high-frequency components and defines the electrical coupling between the inverter and the virtual island network.

The voltage relation across the series ($R_f L_f$) coupling branch can be written as:

$$\mathbf{v}_{conv} = \mathbf{v}_{pcc} + R_f \mathbf{i}_{conv} + L_f \frac{d\mathbf{i}_{conv}}{dt} \quad (4.7)$$

Where:

\mathbf{v}_{conv} = converter-side voltage vector,

\mathbf{v}_{pcc} = PCC voltage vector,

R_f = filter resistance,

L_f = filter inductance,

\mathbf{i}_{conv} = converter current vector.

The shunt capacitor current at the PCC is expressed as

$$\mathbf{i}_C = C_f \frac{d\mathbf{v}_{pcc}}{dt} \quad (4.8)$$

where:

\mathbf{i}_C = current flowing through the PCC shunt capacitor,

C_f = shunt filter capacitance.

Applying Kirchhoff's current law at the PCC gives

$$\mathbf{i}_f = \mathbf{i}_{conv} + \mathbf{i}_{load} + \mathbf{i}_C \quad (4.9)$$

where:

\mathbf{i}_f = series filter current,

\mathbf{i}_{load} = current absorbed by the residual load.

These equations show that Equation (4.7) does not represent the complete output network of the converter. It only describes the voltage drop across the series ($R_f L_f$) branch. The complete PCC behaviour depends also on the shunt capacitor current, the residual load, the transformer and the grid-side impedance. This distinction is important because the voltage-source behaviour observed during islanding is influenced not only by the inverter controller but also by the passive network connected at the PCC.

The active and reactive power are calculated from the measured three-phase voltage and current. In the synchronous (dq) frame, they can be expressed as

$$P = \frac{3}{2}(v_d i_d + v_q i_q) \quad (4.10)$$

$$Q = \frac{3}{2}(v_q i_d - v_d i_q) \quad (4.11)$$

These quantities are essential because the FNN assessment criteria are based on the evolution of active power, reactive power, voltage and frequency before and after the transition to virtual island operation.

4.3 Control logic of the GFM model

The GFM controller is a multi-loop grid-forming control structure. According to Fan and Miao (2024, Ch. 6), multi-loop GFM control can be understood as a development from grid-following control, where the converter still uses inner current control but the synchronisation mechanism is modified. In the GFM case, the key idea is to apply a power-synchronisation method while making minimal changes to the rest of the converter control structure. Professor Fan (2024) describes this design as replacing the PLL by a P–f droop controller to generate the synchronising angle, while active power is controlled through the same P–f droop mechanism.

This modelling choice is suitable for the thesis because the objective is not to compare different GFM strategies, but to use an existing and technically credible GFM controller

as a test object for simulation-based certification.

4.3.1 Reference-frame transformation

The measured three-phase voltages and currents are transformed into a rotating (dq) reference frame. This is necessary because sinusoidal three-phase quantities become approximately constant quantities in the synchronous reference frame, which simplifies the design of PI controllers.

The Park transformation used for the conversion can be written as

$$\begin{bmatrix} f_d \\ f_q \end{bmatrix} = \frac{2}{3} \begin{bmatrix} \cos \theta & \cos \left(\theta - \frac{2\pi}{3} \right) & \cos \left(\theta + \frac{2\pi}{3} \right) \\ -\sin \theta & -\sin \left(\theta - \frac{2\pi}{3} \right) & -\sin \left(\theta + \frac{2\pi}{3} \right) \end{bmatrix} \begin{bmatrix} f_a \\ f_b \\ f_c \end{bmatrix} \quad (4.12)$$

In a grid-following inverter, the angle θ is usually obtained from a phase-locked loop (PLL). In the GFM controller, the angle is instead generated from the active-power droop loop. This is the central grid-forming modification of the model.

4.3.2 Power-frequency droop loop

The frequency dynamics of the GFM model are based on active-power droop. The measured active power is compared with the active-power reference, and the difference is used to modify the angular frequency of the internal voltage source.

The power-frequency relationship can be represented as

$$\omega = \omega_0 + K_p (P_{ref} - P) \quad (4.13)$$

Where:

ω = angular frequency generated by the grid-forming controller,

ω_0 = nominal angular frequency,

K_p = active-power droop gain,

P_{ref} = active-power reference,

P = measured active power

The synchronising angle is then obtained by integrating the angular frequency:

$$\theta(t) = \int \omega(t) dt \quad (4.14)$$

Where :

$\theta(t)$ = synchronising angle used by the converter control,

$\omega(t)$ = instantaneous angular frequency.

In simple terms, if the measured active power differs from its reference, the controller changes the internal frequency. This changes the angle of the converter voltage and therefore modifies the active power exchange with the grid. This is why the method is called power-based synchronisation. It replaces the external voltage-tracking behaviour of a PLL with an internal power-frequency relationship.

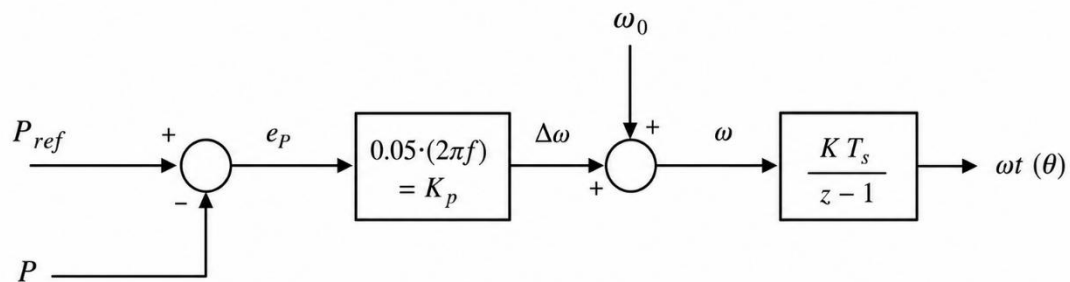


Figure 4: Power – frequency droop loop

4.3.3 Reactive power-voltage droop loop

Voltage support is provided through the reactive power-voltage droop loop. The reactive power is compared with the reactive power reference, and the resulting error modifies the voltage magnitude reference.

The reactive power-voltage droop can be written as

$$V_{ref} = V_0 + K_Q(Q_{ref} - Q) \quad (4.15)$$

Where:

V_{ref} = voltage magnitude reference,

V_0 = nominal voltage magnitude,

K_Q = reactive power-voltage droop gain,

Q_{ref} = reactive power reference,

Q = measured reactive power.

This loop gives the inverter the ability to support voltage through reactive power regulation. In simple terms, if the reactive power deviates from the desired value, the voltage reference is adjusted so that the converter changes its reactive current contribution.

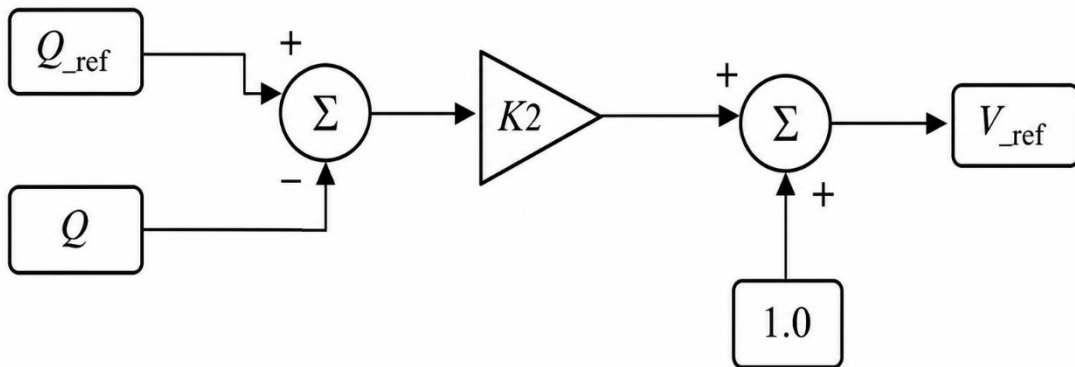


Figure 5: Reactive power – voltage droop loop

4.3.4 Outer voltage control

The outer voltage control regulates the direct- and quadrature-axis voltages. In the implemented GFM model, the (d)-axis voltage is compared with the voltage reference and the (q)-axis voltage is regulated towards zero. The general PI-control structure can be expressed as

$$i_{d,ref} = K_{pv}(V_{ref} - v_d) + K_{iv} \int (V_{ref} - v_d) dt \quad (4.16)$$

$$i_{q,ref} = K_{pvq}(0-v_q) + K_{ivq} \int (0-v_q)dt \quad (4.17)$$

Where:

$i_{d,ref}, i_{q,ref}$ = reference currents for the inner current controller in the (dq) frame,

K_{pv}, K_{iv} = proportional and integral gains of the (d)-axis voltage controller,

K_{pvq}, K_{ivq} = proportional and integral gains of the (q)-axis voltage controller,

v_d, v_q = measured PCC voltage components in the (dq) frame.

The purpose of the outer voltage controller is to transform voltage-regulation objectives into current references. These current references are then passed to the inner current controller.

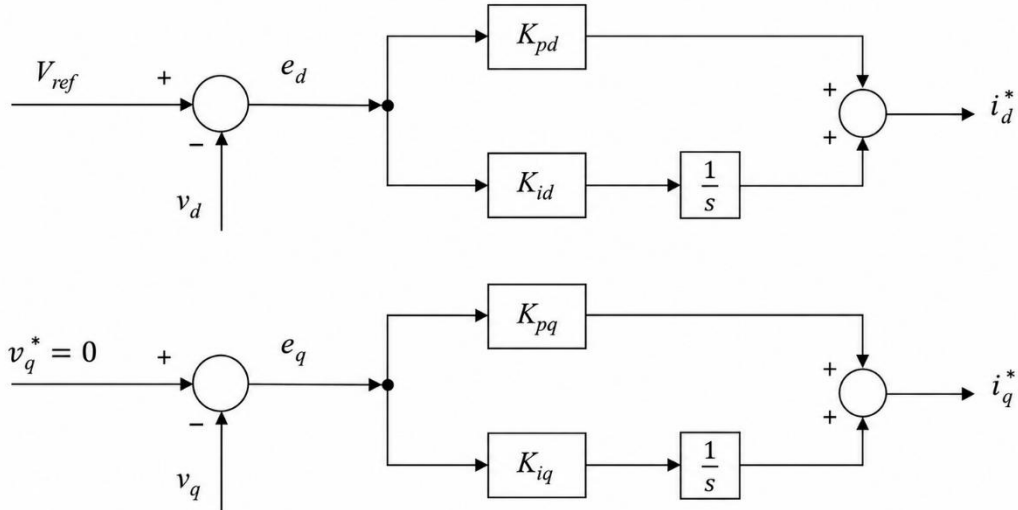


Figure 6: Outer voltage control loop

4.3.5 Inner current control

The inner current loop regulates the converter currents and produces the voltage references that are sent to the converter modulation stage. The current-control equations can be represented as

$$v_{d,ref} = K_{pi}(i_{d,ref}-i_d) + K_{ii} \int (i_{d,ref}-i_d)dt + v_d - \omega L_f i_q \quad (4.18)$$

$$v_{q,ref} = K_{pi}(i_{q,ref} - i_q) + K_{ii} \int (i_{q,ref} - i_q) dt + v_q + \omega L_f i_d \quad (4.19)$$

The feedforward and cross-coupling terms improve the dynamic performance of the controller. In simple terms, the inner current loop ensures that the current injected by the converter follows the references produced by the voltage controller while limiting excessive current deviations.

The (dq)-axis voltage references are then transformed back into three-phase quantities and applied to the voltage-source converter. (Modeling and Stability Analysis of Inverter-Based Resources, chp 4, p89)

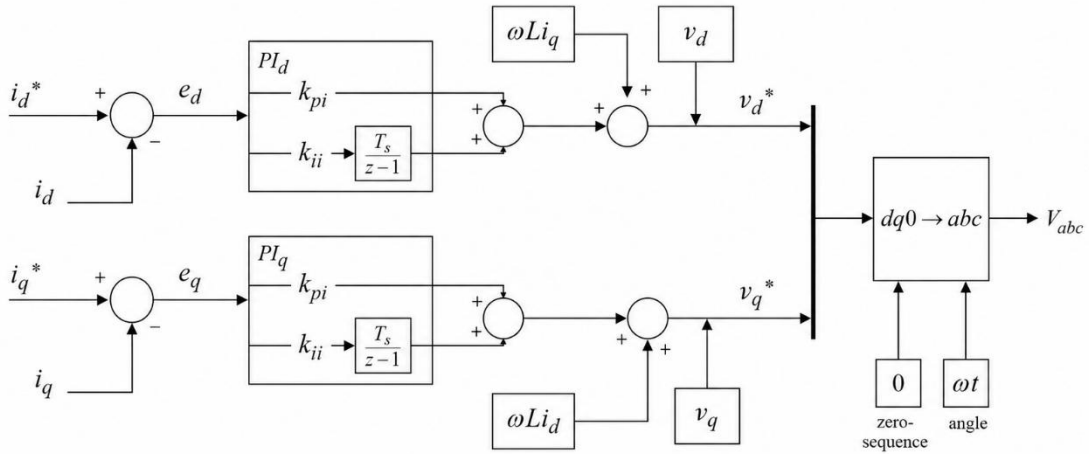


Figure 7: Inner Current control loop

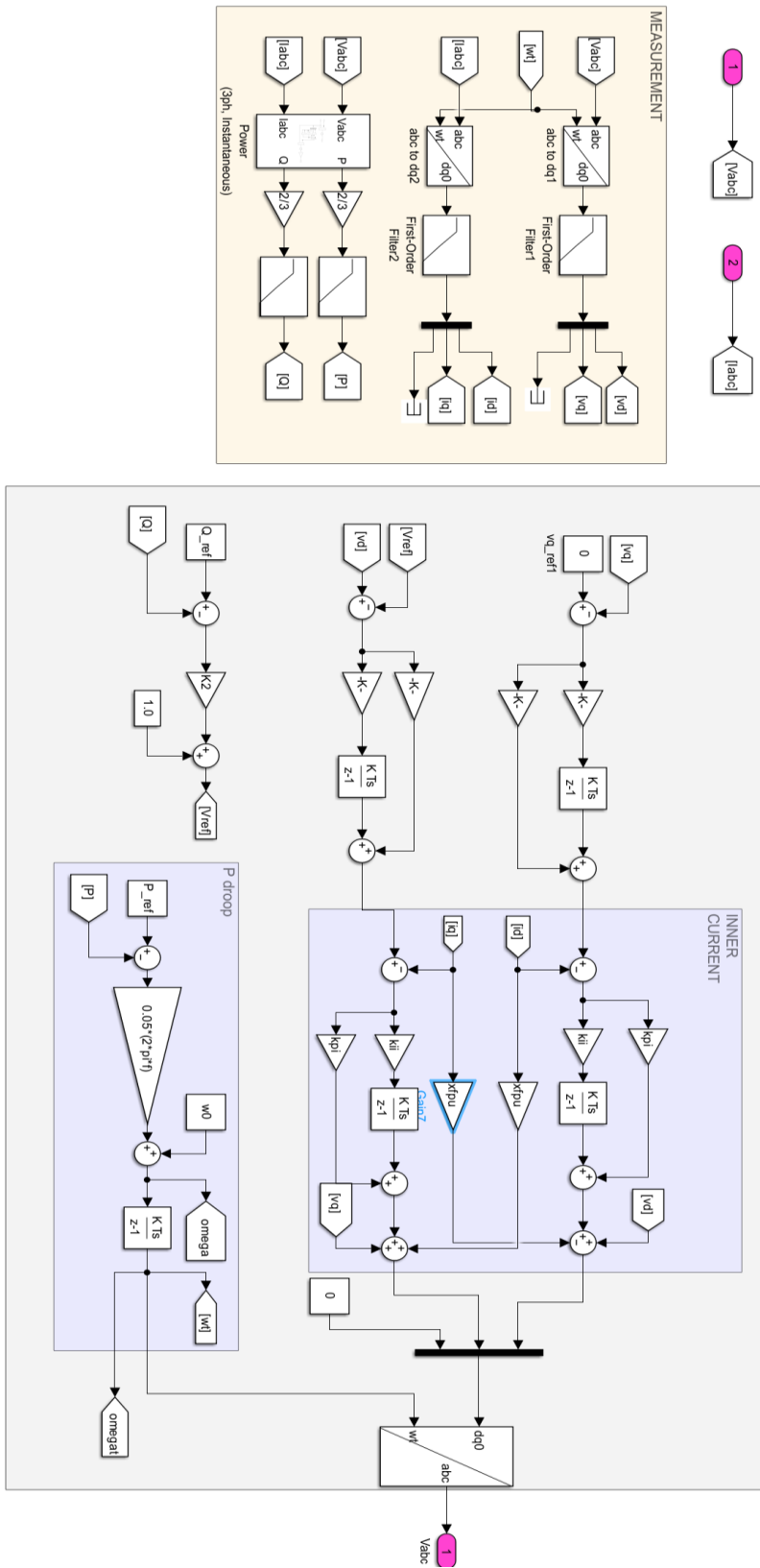


Figure 8: Simulink Control logic of the GFM model

5 Certification by Simulation

This chapter presents the simulation implementation used to verify the selected VDE FNN requirements for the grid-forming inverter model. The previous chapter introduced the modelling framework, the power architecture of the GFM model and the main control principles used in the EMT model. The present chapter focuses on the automated simulation process developed around this model. The objective is to show how the selected FNN operating points are executed, how the relevant quantities are extracted, and how the results are evaluated against the compliance criteria defined in Chapter 3. The simulation work was carried out using MATLAB/Simulink and automated through a programme developed during this thesis, named AGIS, which stands for Automatic GFM Inverter Simulator. AGIS was designed to reduce manual intervention during FNN verification tests. Instead of running each test manually, extracting the signals separately and preparing plots and compliance tables by hand, the programme allows the user to select a verification family, choose one or more FNN operating points, run the simulations and automatically generate a structured verification report.

5.1 Automatic GFM Inverter Simulator

AGIS is a MATLAB/Simulink-based automation framework developed to run the selected FNN verification tests on the grid-forming inverter model. The programme was built around the GFM model used in this thesis, but its structure was intentionally kept modular so that it can be adapted to other EMT models. The main function of the programme is to connect the simulation model, the selected test scenario, the FNN operating points, the extracted measurements and the final report into a single automated workflow.

The verification procedure begins with the selection of the test family. AGIS allows the user to run either voltage-source behaviour tests, PCNB behaviour tests, or both verification families together. In the final version used for this thesis, the combined option was selected to run all measurements 1.1, 1.2 and 1.3 from Table 1. The same simulation data are reused for both voltage-source and PCNB analyses when the same operating

point is selected. This avoids unnecessary repeated simulation runs and reduces the total execution time.

General workflow of the AGIS automation framework (Appendix 1)

The programme architecture can be divided into six functional layers: parameter definition, user selection, scenario configuration, simulation execution, signal extraction and report generation.

The first layer is the parameter definition layer. This is mainly handled by the data file, where the base values, model parameters, controller gains, initial active and reactive power references, residual-load factors and scenario-specific settings are defined. The parameters include the base power, base voltage, nominal frequency, residual load, active-power reference, reactive-power reference, voltage-control gains, Q–V droop gain and simulation time. In the current implementation, the base power is 1 MVA and the nominal frequency is 50 Hz. The islanding event is applied at 5 s and the total simulation stop time is 60 s. This simulation duration is selected so that the model reaches a pre-islanding steady state, experiences the transition to virtual island operation and then settles to a final steady-state condition.

The second layer is the user selection layer. This layer is implemented in the main control script of AGIS. The script prompts the user to select the verification scope. The user can select voltage-source behaviour, PCNB behaviour or all tests. A second selection determines whether a single operating point or all operating points must be executed. This structure makes the programme flexible, since the user can run a complete verification campaign or only repeat a specific failed test after parameter tuning.

The third layer is the scenario configuration layer. Two scenarios are implemented in the present thesis. Scenario One corresponds to the non-compliance baseline case. It uses the initial/default parameter configuration of the model before the tuning required to satisfy the FNN requirements. Scenario Two corresponds to the compliance case. It uses the tuned parameters selected after the behaviour of the model was analysed and adjusted. In the non-compliant case, the baseline configuration uses the initial controller

and load settings. In the compliant case, the tuning values are modified so that the initial active power, final residual-load response and voltage recovery remain within the selected compliance bands.

The fourth layer is the simulation execution layer. For each selected measurement, AGIS assigns the required initial operating point and residual-load condition to the Simulink model. The model is then executed once for the selected Table 1 operating point. During the simulation, the inverter initially operates in parallel with the external grid. At the islanding instant, the external network is disconnected and the grid-forming inverter must supply the residual load in the virtual island network. This follows the VDE FNN measurement logic, where the operating condition of the virtual island network is generated by opening the network interconnecting circuit breaker.

The fifth layer is the signal extraction layer. After each simulation, AGIS reads the logged output signals and extracts the quantities required by the selected verification family. For voltage-source behaviour, the programme extracts active power, reactive power, voltage magnitude and frequency. For PCNB behaviour, the programme extracts active power and frequency only. For each quantity, AGIS calculates the value before islanding, the maximum value after islanding, the minimum value after islanding and the final steady-state value. The deviation from the initial steady-state value is also calculated.

The final layer is the report generation layer. The report generator compiles the selected scenario, the test configuration, the extracted measurements, the compliance checks, the plots and the final verdict into an HTML report. The report includes a global compliance summary followed by detailed results for each measurement. It also includes the plot windows required for the presentation of voltage-source behaviour and PCNB behaviour. The generated report is therefore not only a simulation output but also a structured compliance document.

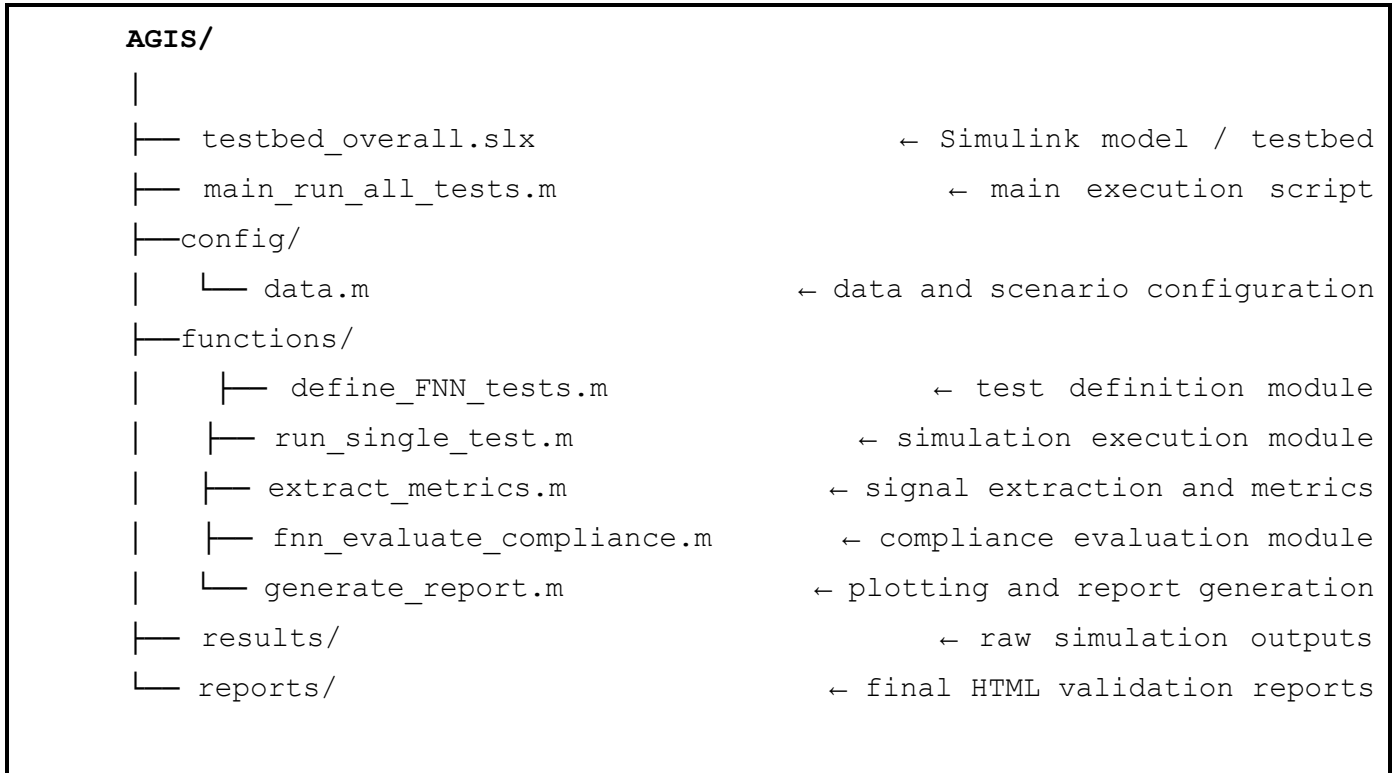
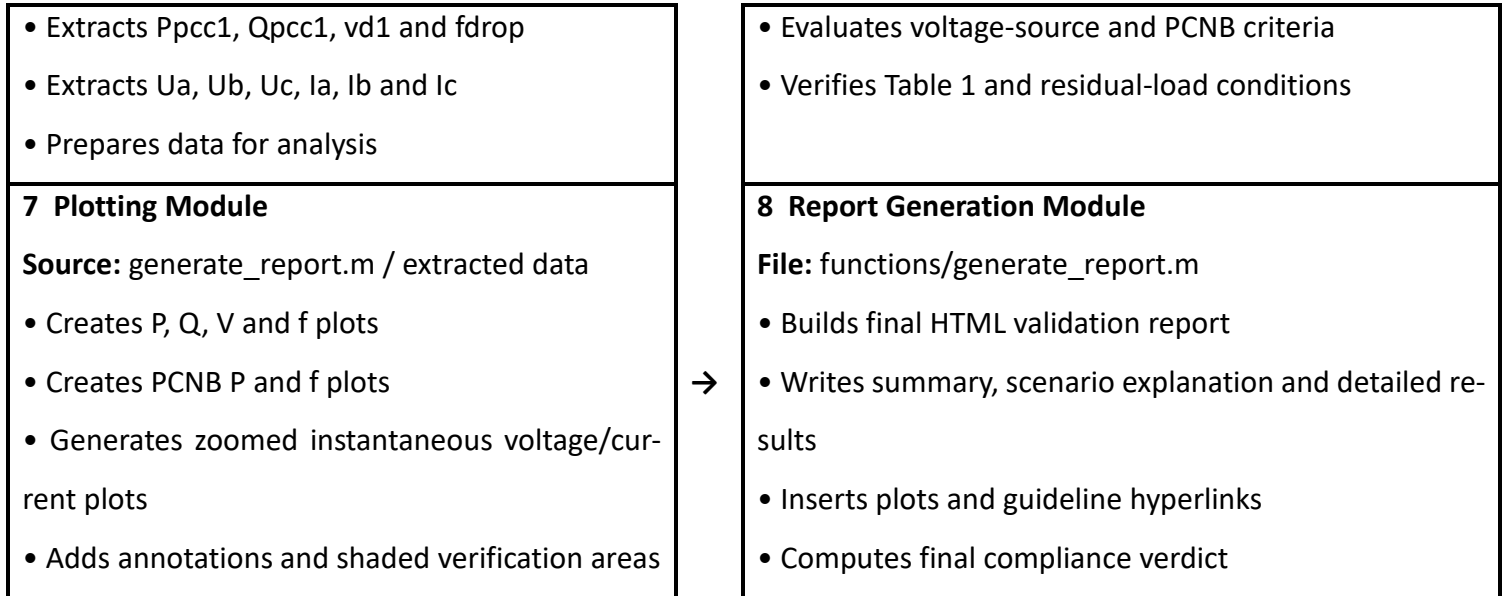


Figure 9: AGIS architecture

Table 2: AGIS functional modules

<p>1 Main Execution Module</p> <p>File: main_run_all_tests.m</p> <ul style="list-style-type: none"> • Displays AGIS introduction • Collects user scenario and test selections • Controls overall program flow • Launches required simulations 	→	<p>2 Data and Scenario Configuration Module</p> <p>File: config/data.m</p> <ul style="list-style-type: none"> • Defines base values and nominal frequency • Sets Pref, Qref, residual-load factors and controller gains • Manages non-compliance and compliance scenarios
<p>3 Test Definition Module</p> <p>File: functions/define_FNN_tests.m</p> <ul style="list-style-type: none"> • Defines Table 1 operating points • Includes 1.1, 1.2 and 1.3 • Excludes 1.4 and 2.1 	→	<p>4 Simulation Execution Module</p> <p>File: functions/run_single_test.m</p> <ul style="list-style-type: none"> • Applies selected operating point • Updates initial conditions and residual-load factor • Runs the Simulink model
<p>5 Signal Extraction Module</p> <p>File: functions/extract_metrics.m</p> <ul style="list-style-type: none"> • Reads logged outputs 	→	<p>6 Compliance Evaluation Module</p> <p>File: functions/fnn_evaluate_compliance.m</p> <ul style="list-style-type: none"> • Applies VDE FNN-based checks



All the MATLAB script files that composed AGIS are listed in Appendices (20 to 27). The codes of these scripts are not included directly in this chapter to preserve readability.

AGIS was developed for the GFM model used in this thesis, but it can be adapted to another grid-forming model. To do so, several modifications are required. First, the Simulink model name must be changed in the main execution script. Second, the logged signal names must be adapted so that AGIS can access the active power, reactive power, voltage, frequency, instantaneous voltages and instantaneous currents of the new model. Third, the path of the islanding breaker or the switching signal must be updated. Fourth, the base values and per-unit conversion factors must be modified according to the rating of the new model. Fifth, the residual-load block must be linked to the AGIS parameter file so that the programme can assign the correct Table 1 residual-load values automatically. Finally, if the new model uses a different sign convention for active or reactive power, the compliance logic must be adjusted accordingly.

This modular structure is important because the main objective of AGIS is not limited to the specific model used in this thesis. The same framework can support simulation-based verification of other grid-forming inverter models, provided that the model

exposes the required measurement signals and allows the operating points to be configured through MATLAB parameters.

5.2 Scenario One: Non-compliance baseline simulation

Scenario One corresponds to the baseline non-compliant configuration of the grid-forming inverter model. The purpose of this scenario is to demonstrate how the automated framework identifies deviations from the FNN criteria before the controller and load parameters are tuned. In the AGIS report, this scenario is identified as “Scenario One - Non-compliance baseline parameters”.

The non-compliant scenario uses the baseline parameter set shown in Table 3 below;

Table 3: Baseline parameters for non-compliance scenario

Parameter	Value
P_{ref}	0.75 pu
Q_{ref}	0 pu, -0.33 pu or +0.33 pu depending on the test
$P_{residual}$ target	0.50 pu
Simulink load factor P_{res}	0.50 pu
P_{Emax}	1.00 pu
f_{base}	50 Hz
K_2 Q-V droop gain	0.30
K_{Pv} voltage-loop gain	0.40
K_{iv} voltage-loop gain	40
Islanding instant	5 s
Simulation stop time	60 s

The simulator combines two verification families. The first is voltage-source behaviour, where (P), (Q), (V) and (f) are extracted. The second is PCNB behaviour, where (P) and (f) are extracted. The same simulations are reused for both analyses.

The overall compliance summary of Scenario One indicates that all six analyses fail the final verdict. The residual-load condition remains acceptable in all tests because the selected residual-load target lies within the required range. However, the initial active-

power condition fails because the measured pre-islanding active power is approximately 0.6839 pu, whereas the minimum required value is 0.7300 pu. Several main requirements also fail, especially in the inductive and capacitive reactive-power cases.

5.2.1 Non-compliant Test 1.1: ($Q = 0$)

Test 1.1 evaluates the inverter at approximately zero reactive power. This is the neutral reactive-power operating point of the Table 1 tests. The inverter is first operated in grid-connected mode and is then separated from the external network at 5 s.

For the voltage-source behaviour analysis, the measured active power before islanding is 0.68390 pu. The final active power settles at 0.46831 pu. The voltage remains close to its initial value, with a final voltage of 1.00689 pu. Therefore, the voltage-source voltage criterion is satisfied as showed in figure 10, but the overall test is considered non-compliant because the Table 1 (P_{mom}) entry condition is not satisfied.

Scenario One - Voltage source behaviour - Test 1.1 plots (Appendix 2)

Scenario One - Instantaneous phase voltages and currents - Test 1.1 plot (Appendix 3)

For the PCNB behaviour analysis, the same simulation data are evaluated using the (P) and (f) signals. The frequency remains within the $\pm 5\%$ static-value band around 50 Hz. However, the final active power is 0.46831 pu, which is slightly below the lower acceptable limit of 0.47500 pu around the 0.50 pu residual-load target. Consequently, the PCNB quantitative check fails. The failure of Test 1.1 therefore results from both the initial (P_{mom}) condition and the final active-power static-value requirement.

Scenario One – PCNB behaviour – Test 1.1 plot (Appendix 4)

5.2.2 Non-compliant Test 1.2: maximum inductive reactive power

Test 1.2 evaluates the inverter under maximum inductive reactive-power operation. In the sign convention used in this thesis, inductive operation is represented by negative reactive power. Therefore, the operating point is defined by

$$Q = -0.33 \text{ pu}$$

This value represents the maximum inductive reactive-power operating condition selected for the FNN Table 1 measurement.

For voltage-source behaviour, the initial active power is again 0.68390 pu, which does not satisfy the minimum (P_{mom}) requirement. The final voltage deviation is -0.08207 pu, while the allowed deviation is ± 0.03000 pu. The voltage-source behaviour criterion therefore fails. The final voltage settles at 0.90662 pu, which is significantly below the acceptable band defined around the pre-islanding voltage.

Scenario One – Voltage source behaviour – Test 1.2 plot (Appendix 5)

Scenario One – Instantaneous phase voltages and currents – Test 1.2 plot (Appendix 6)

For PCNB behaviour, the final active power settles at 0.38154 pu. This is far below the acceptable range of 0.47500 pu to 0.52500 pu around the 0.50 pu residual-load target. The final frequency remains inside the $\pm 5\%$ frequency band, but the active-power static-value requirement fails. The PCNB quantitative check is therefore non-compliant.

Scenario One – PCNB behaviour – Test 1.2 – active power and frequency plot (Appendix 7)

The result shows that the baseline controller is not able to maintain the required post-islanding active-power balance under maximum inductive reactive-power loading. The large voltage drop also indicates that the baseline Q–V droop and voltage-control configuration are not sufficient for this operating condition.

5.2.3 Non-compliant Test 1.3: maximum capacitive reactive power

Test 1.3 evaluates the inverter under maximum capacitive reactive-power operation. In the sign convention used in this thesis, capacitive operation is represented by positive reactive power. Therefore, the operating point is defined by

$$Q = +0.33 \text{ pu}$$

For voltage-source behaviour, the Table 1 (P_{mom}) condition again fails because the measured pre-islanding active power is below the required minimum. The final voltage deviation is +0.08614 pu, while the allowed deviation is ± 0.03000 pu. Therefore, the voltage-source behaviour criterion fails. This result indicates that the baseline configuration causes an excessive voltage rise in the capacitive reactive-power case.

Scenario One – Voltage source behaviour – Test 1.3 plot (Appendix 8)

Scenario One – Instantaneous phase voltages and currents – Test 1.3 plot (Appendix 9)

For PCNB behaviour, the active power increases transiently up to 1.07431 pu and finally settles at 0.56320 pu. The final active power is above the allowed upper limit of 0.52500 pu around the 0.50 pu target. Although the final frequency remains inside the $\pm 5\%$ frequency band, the final active-power condition fails. The PCNB quantitative check is therefore non-compliant.

Scenario One – PCNB behaviour – Test 1.3 plot (Appendix 10)

The non-compliant results demonstrate the usefulness of the automated framework. The scenario name alone does not determine the final verdict. Instead, the report-level verdict is calculated from the individual verification results. Since at least one requirement fails in every measurement, Scenario One is classified as non-compliant.

5.3 Scenario Two: Compliant tuned simulation

Scenario Two corresponds to the tuned compliant configuration of the grid-forming inverter model. The purpose of this scenario is to verify that the model can satisfy the selected FNN criteria after the controller and load parameters are adjusted. In the AGIS report, this scenario is identified as “Scenario Two - Compliance/tuned parameters”.

The compliant parameter set is shown in table below;

Table 4: Tuned parameters for the compliant scenario

Parameter	Value
P_{ref}	0.81 pu
Q_{ref}	Q_{init}
$P_{residual}$ target	0.50 pu
P_{res1}	0.5183 pu
P_{res2}	0.5980 pu
P_{res2}	0.5200 pu
P_{Emax}	1.00 pu
f_{base}	50 Hz
K_2 Q–V droop gain	0.10
K_{pv} voltage-loop gain	0.40
K_{iv} voltage-loop gain	40
Islanding instant	5 s
Simulation stop time	60 s

The compliant scenario differs from the non-compliant scenario mainly in the active-power reference, the residual-load factors and the Q–V droop gain. The residual-load factors are tuned per Table 1 case so that the final active power settles within the $\pm 5\%$ PCNB static-value band around the 0.50 pu residual-load target. The Q–V droop gain is also reduced from 0.30 to 0.10 to improve the voltage response after islanding.

The overall compliance summary of Scenario Two indicates that all six analyses pass the final verdict. The (P_{mom}) check, residual-load check, main requirement check and final verdict are all marked as OK for voltage-source behaviour and PCNB behaviour in measurements 1.1, 1.2 and 1.3.

5.3.1 Compliant Test 1.1: (Q = 0)

Test 1.1 evaluates the tuned inverter at the neutral reactive-power operating point. The initial active power before islanding is 0.73861 pu, which satisfies the minimum required value of 0.7300 pu. The final voltage is 1.00228 pu and the final voltage deviation is -0.00210 pu, which is well within the allowed ± 0.03000 pu band.

For voltage-source behaviour, the inverter therefore maintains a stable voltage magnitude after islanding. The transient voltage reaches a maximum of 1.23014 pu immediately after islanding, but the final steady-state value returns close to the pre-islanding value. The test is therefore compliant.

Scenario Two – Voltage source behaviour – Test 1.1 plots (Appendix 11)

Scenario Two – Instantaneous phase voltages and currents – Test 1.1 plots (Appendix 12)

For PCNB behaviour, the final active power is 0.48216 pu. This lies inside the acceptable range of 0.47500 pu to 0.52500 pu around the 0.50 pu target. The final frequency is 50.86800 Hz, which is also inside the $\pm 5\%$ frequency band around 50 Hz. The active-power response also follows the correct PCNB direction. Consequently, the PCNB quantitative check is compliant.

Scenario Two – PCNB behaviour – Test 1.1 plots (Appendix 13)

5.3.2 Compliant Test 1.2: maximum inductive reactive power

Test 1.2 evaluates the tuned inverter under maximum inductive reactive-power operation. The reactive-power reference is

$$Q = -0.33 \text{ pu}$$

The initial active power before islanding is 0.73861 pu, satisfying the Table 1 (P_{mom}) condition. The final voltage is 0.96913 pu. The final voltage deviation is -0.02197 pu, which is within the allowed ± 0.03000 pu band. The voltage-source behaviour test is therefore compliant.

Scenario Two – Voltage source behaviour – Test 1.2 plots (Appendix 14)

Scenario Two – Instantaneous phase voltages and currents – Test 1.2 plot (Appendix 15)

For PCNB behaviour, the final active power is 0.51902 pu. This remains within the acceptable range of 0.47500 pu to 0.52500 pu. The final frequency is 50.74506 Hz, which

remains inside the $\pm 5\%$ frequency band. Therefore, the PCNB quantitative check is also compliant.

Scenario Two – PCNB behaviour – Test 1.2 plot (Appendix 16)

Compared with the non-compliant scenario, the tuned configuration significantly improves the inductive reactive-power case. In the baseline case, the final active power settled too low, and the final voltage deviation exceeded the $\pm 3\%$ voltage band. In the tuned case, both active-power and voltage criteria are satisfied.

5.3.3 Compliant Test 1.3: maximum capacitive reactive power

Test 1.3 evaluates the tuned inverter under maximum capacitive reactive-power operation. The reactive-power reference is

$$Q = +0.33 \text{ pu}$$

This case is important because the non-compliant scenario produced both excessive voltage deviation and excessive final active power under capacitive loading. In the tuned scenario, the AGIS compliance summary indicates that the voltage-source behaviour check, PCNB check, (P_{mom}) check and residual-load check are all satisfied.

Scenario Two – Voltage source behaviour – Test 1.3 plot (Appendix 17)

Scenario Two – Instantaneous phase voltages and currents – Test 1.3 plot (Appendix 18)

For the PCNB behaviour test, the initial active power is approximately 0.7386 pu and the final steady-state active power settles at approximately 0.50 pu. The final steady-state frequency is approximately 50.667 Hz. These values satisfy the active-power and frequency static-value checks defined by the FNN guideline.

Scenario Two – PCNB behaviour – Test 1.3 plot (Appendix 19)

The compliant result of Test 1.3 confirms that the tuned model can maintain acceptable voltage-source and PCNB behaviour not only at zero and inductive reactive power, but

also at the maximum capacitive operating point. This is important because the three measurements collectively cover the selected reactive-power range required for the pro-cured-direction virtual-island verification.

In summary, Scenario Two demonstrates that the simulator AGIS can produce a complete automated verification report for the selected FNN tests. It verifies the initial active-power condition, the residual-load condition, the voltage-source steady-state voltage criterion and the PCNB static-value criteria. All selected measurements 1.1 to 1.3 satisfy the implemented checks, and the final report-level verdict is compliant.

The comparison between Scenario One and Scenario Two shows that AGIS can distinguish between baseline non-compliant behaviour and tuned compliant behaviour. This supports the main objective of the thesis: to demonstrate how simulation-based automation can be used to generate structured, reproducible and traceable compliance evidence for grid-forming inverter models.

6 Results Interpretation

Chapter 5 presented the AGIS simulation framework and the two simulation scenarios used to evaluate the selected VDE FNN requirements. The objective of this chapter is not only to repeat the final compliant or non-compliant verdicts, but to explain how the measured quantities should be interpreted from both a guideline and a physical point of view.

The interpretation is divided into two sections. Section 6.1 analyses the voltage-source behaviour tests, while Section 6.2 analyses the PCNB behaviour tests. In both cases, the analysis follows the same logic. First, the physical requirement is recalled. Second, the EMT validation requirement is explained. Third, the measurements and deviation calculations are interpreted in order to show how the simulation results represent the physical behaviour expected from a grid-forming unit.

This distinction is important because the VDE FNN guideline separates the technical behaviour required from a grid-forming unit from the procedure used to verify that behaviour. Section 4 defines what the unit must physically do, while Section 5 defines how this behaviour must be measured, extracted and evaluated during verification. Therefore, the results presented in this chapter should be read as a bridge between the physical requirement and the EMT validation procedure.

6.1 Interpretation of voltage-source behaviour measurements

The physical requirement for voltage-source behaviour is defined in Section 4.2.1.1 of the VDE FNN guideline. From the network perspective, a grid-forming unit must behave at its terminals as a voltage source behind an effective impedance. This means that the unit must be able to establish and maintain its own voltage magnitude and phase angle, rather than simply following an externally imposed grid voltage. The guideline further explains that a voltage amplitude change at the terminals should mainly cause a reactive

current response, while a voltage angle change should mainly cause an active current response. This is the physical meaning of voltage-source behaviour.

The EMT validation requirement translates this physical behaviour into measurable quantities. Instead of directly observing an “internal voltage source”, the validation procedure observes the behaviour of the unit in the virtual island network. The virtual island test is relevant because, after disconnection from the external grid, the unit must maintain voltage and frequency without relying on an external voltage reference. In AGIS, the voltage-source behaviour test therefore records active power (P), reactive power (Q), voltage magnitude (V), and frequency (f) before islanding, during the transient response, and at the final steady state. The simulation of the voltage-source behaviour is evaluated using (P), (Q), (V), and (f), while PCNB behaviour uses only (P) and (f).

For each quantity (X), the deviation is calculated as

$$\Delta X = X - X_{init} \quad (6.1)$$

where (X_{init}) is the steady-state value before islanding. This calculation is used to quantify how much each measured quantity changes during and after the transition to islanded operation.

From the FNN guideline, section 5.5.3.6.2.2.3 requirement for voltage-source behaviour verification, the final steady-state voltage after islanding must remain within $\pm 3\%$ of the pre-islanding steady-state voltage. This is evaluated as

$$V_{init}(1 - 0.03) \leq V_{ss} \leq V_{init}(1 + 0.03) \quad (6.2)$$

where (V_{init}) is the voltage magnitude before islanding and (V_{ss}) is the final steady-state voltage after islanding. This criterion links the EMT validation result to the physical requirement of Section 4.2.1.1. Physically, if the final voltage settles close to the pre-islanding voltage, the unit has demonstrated that it can maintain its voltage-source characteristic after the external grid reference is removed. The transient maximum and minimum values show the severity of the transition, while the final value shows whether the converter re-establishes a stable voltage operating point.

6.1.1 Measurement 1.1: neutral reactive-power operation

Measurement 1.1 corresponds to the operating point where the inverter operates with approximately zero reactive power. This represents the neutral reactive-power case of the Table 1 verification procedure. The converter is initially connected to the external grid and is then separated from it at the islanding instant ($t = 5$) s. The measured quantities are shown in Table 4.

Table 5: Voltage-source behaviour measurements for Test 1.1

Quantity	Before (init)	Maximum after islanding (max)	Minimum after islanding (min)	Final (ss)
(P) [pu]	0.73861	0.74019	0.46955	0.48216
(Q) [pu]	-0.03992	-0.02047	-0.05319	-0.02112
(V) [pu]	1.00438	1.23014	0.97568	1.00228
(f) [Hz]	50.00000	50.90311	49.99976	50.86800

The deviations from the initial steady state are shown in Table 5

Table 6: Deviations for Test 1.1

Quantity	ΔX_{max}	ΔX_{min}	ΔX_{ss}
(P) [pu]	0.00158	-0.26906	-0.25645
(Q) [pu]	0.01945	-0.01327	0.01880
(V) [pu]	0.22576	-0.02870	-0.00210
(f) [Hz]	0.90311	-0.00024	0.86800

For this measurement, the voltage-source interpretation is based mainly on the steady-state voltage after islanding. The pre-islanding voltage is (1.00438) pu, and the final voltage is (1.00228) pu. The final voltage deviation is therefore

$$\Delta V_{ss} = 1.00228 - 1.00438 = -0.00210 \text{ pu} \quad (6.3)$$

The corresponding voltage band is

$$0.97438 \leq V_{ss} \leq 1.03438 \quad (6.4)$$

In this case, the voltage experiences a transient rise immediately after islanding,

reaching 1.23014 pu. However, the final voltage settles at 1.00228 pu, which is very close to the pre-islanding voltage of 1.00438 pu. From the EMT validation perspective, the final voltage therefore remains inside the $\pm 3\%$ band. From the physical perspective, this means that the converter is able to re-establish a stable voltage after the grid is disconnected. The transient voltage peak reflects the dynamic interaction between the inverter, filter, residual load and islanding event, while the final voltage value demonstrates the voltage-forming capability of the unit.

6.1.2 Measurement 1.2: maximum inductive reactive-power operation

Measurement 1.2 corresponds to the maximum inductive reactive-power operating point. In the sign convention used in this thesis, inductive operation is represented by negative reactive power. The operating point is therefore defined by

$$Q = -0.33 \text{ pu}$$

The extracted measurements are shown in Table 6.

Table 7: Voltage-source behaviour measurements for Test 1.2

Quantity	Before (init)	Maximum after islanding (max)	Minimum after islanding (min)	Final (ss)
(P) [pu]	0.73861	0.73870	0.43215	0.51902
(Q) [pu]	-0.21974	-0.01589	-0.21974	-0.01966
(V) [pu]	0.99110	1.00047	0.82821	0.96913
(f) [Hz]	50.00000	51.05357	49.98933	50.74506

The deviations from the initial steady state are shown in Table 7.

Table 8: Deviations for Test 1.2

Quantity	ΔX_{max}	ΔX_{min}	ΔX_{ss}
(P) [pu]	0.00009	-0.30646	-0.21959
(Q) [pu]	0.20385	0.00000	0.20008
(V) [pu]	0.00937	-0.16288	-0.02197
(f) [Hz]	1.05357	-0.01067	0.74506

The final voltage deviation is

$$\Delta V_{ss} = 0.96913 - 0.99110 = -0.02197 \text{ pu} \quad (6.5)$$

The corresponding voltage band is

$$0.96110 \leq V_{ss} \leq 1.02110 \quad (6.6)$$

This measurement is more demanding than Measurement 1.1 because the inverter initially operates under inductive reactive-power conditions. The voltage minimum after islanding is 0.82821 pu, showing a significant transient voltage depression. However, the final voltage settles at 0.96913 pu, which remains inside the $\pm 3\%$ band around the initial voltage. This result should be interpreted in two layers. From the EMT validation perspective, the final voltage remains within the accepted steady-state range. From the physical perspective, the converter is able to recover its voltage-source behaviour after islanding, even though the inductive operating point creates a stronger transient disturbance.

6.1.3 Measurement 1.3: maximum capacitive reactive-power operation

Measurement 1.3 corresponds to the maximum capacitive reactive-power operating point. In the sign convention used in this thesis, capacitive operation is represented by positive reactive power. The operating point is therefore defined by

$$Q = +0.33 \text{ pu}$$

The extracted measurements are shown in Table 8.

Table 9: Voltage-source behaviour measurements for Test 1.3

Quantity	Before (init)	Maximum after islanding (max)	Minimum after islanding (min)	Final (ss)
(P) [pu]	0.73861	0.97087	0.50232	0.51530
(Q) [pu]	0.15056	0.15126	-0.04282	-0.02245
(V) [pu]	1.01649	1.50594	1.01294	1.03543
(f) [Hz]	50.00000	50.79419	48.88830	50.75750

The deviation values are shown in Table 9.

Table 10: Deviations for Test 1.3

Quantity	ΔX_{max}	ΔX_{min}	ΔX_{ss}
(P) [pu]	0.23226	-0.23629	-0.22331
(Q) [pu]	0.00069	-0.19339	-0.17302
(V) [pu]	0.48945	-0.00355	0.01894
(f) [Hz]	0.79419	-1.11170	0.75750

The final voltage condition can be written as

$$0.98649 \leq V_{ss} \leq 1.04649 \quad (6.7)$$

and the final voltage deviation is

$$\Delta V_{ss} = +0.01894 \text{ pu} \quad (6.8)$$

This case differs physically from the inductive case because capacitive operation tends to support or raise the voltage. Therefore, a positive final voltage deviation is expected to be more likely than in the inductive case. The interpretation is again based on two layers. The EMT validation layer checks whether the final voltage remains inside the permitted band. The physical layer asks whether the converter still behaves as a voltage source after islanding. Since the final voltage returns to the acceptable range, the result indicates that the inverter can maintain voltage-source behaviour under capacitive loading.

6.1.4 Link between voltage-source EMT validation and physical requirement

The voltage-source tests must be interpreted as more than a pass/fail exercise. The physical requirement in Section 4.2.1.1 states that the grid-forming unit must behave like a voltage source behind an effective impedance. This means that the unit must be able to create voltage, respond to angle and voltage disturbances, and remain stable when the network condition changes. The EMT validation requirement converts this physical requirement into measurable quantities in the virtual island network.

The relationship can be summarised as follows:

Physical voltage-source requirement

⇒ ability to form voltage behind an effective impedance

EMT validation requirement

⇒ measure P , Q , V , f before, during and after islanding

Interpretation ⇒ check whether V_{ss} returns close to V_{init}

The voltage deviation calculation is therefore the numerical bridge between the physical and validation requirements. If (V_{final}) remains close to (V_{before}), the EMT model shows that the unit can re-establish a stable voltage operating point without support from the external grid. If the final voltage deviates excessively, the result suggests that the internal voltage source, effective impedance, voltage controller, passive filter or load interaction is not producing the required voltage-source behaviour.

It is also important to distinguish transient behaviour from final steady-state behaviour. The transient maximum and minimum values show how severe the islanding event is. However, the final steady-state value shows whether the grid-forming unit can settle into a new stable operating point. Therefore, a temporary voltage rise or dip does not necessarily mean that the voltage-source requirement is not physically reproduced. The decisive interpretation is whether the final voltage remains bounded and returns close to the pre-islanding value.

6.2 Interpretation of PCNB behaviour measurements

The physical requirement for PCNB is defined in Section 4.2.2.2 of the VDE FNN guideline. PCNB corresponds to a frequency-dependent active-power contribution used to support network security outside the normal frequency range. Physically, this means that the grid-forming unit must change its active power when the network frequency deviates. For the negative-inertia direction used in the thesis tests, an increase in frequency after islanding should lead to a reduction in active power. Conversely, a decrease in frequency should lead to an increase in active power.

The PCNB behaviour test evaluates the active-power and frequency response of the grid-forming inverter in the virtual island network according to Section 5.5.4.4.2.

For the PCNB verification, extracts of only two quantities are needed:

[P, f]

where (P) is the active power of the grid-forming unit and (f) is the measured frequency.

The deviations are calculated using the same method as in the voltage-source behaviour analysis:

$$\Delta P = P - P_{init} \quad (6.9)$$

$$\Delta f = f - f_{init} \quad (6.10)$$

In addition to these deviations, the guideline checks static-value requirements. The initial active power must remain close to the configured initial active-power setpoint, the final active power must remain close to the residual-load target, and the initial and final frequency must remain within the frequency static-value band. The FNN guideline states that for the PCNB model validation, the simulated static value must correspond to the value setting of the grid-forming unit with a maximum deviation of $\pm 5\%$. It also defines additional damping and settling-frequency comparison requirements when measured hardware reference data are available.

The $\pm 5\%$ active-power and frequency accepted deviation defined by the guideline can be expressed as

$$0.95P_{set} \leq P_{init/ss} \leq 1.05P_{set} \quad (6.11)$$

$$0.95f_{set} \leq f_{init/ss} \leq 1.05f_{set} \quad (6.12)$$

For the simulations considered here, the residual-load target is

$$P_{res} = 0.50 pu$$

Therefore, the final active-power band is

$$0.47500 \leq P_{ss} \leq 0.52500 \quad (6.13)$$

For the frequency setpoint

$$f_{base} = 50 Hz$$

the $\pm 5\%$ frequency band is

$$47.5 \leq f_{ss} \leq 52.5 \text{ Hz} \quad (6.15)$$

These conditions show how the EMT validation requirement is related to the physical PCNB requirement. The frequency deviation represents the disturbance in the virtual island network. The active-power deviation represents the response of the grid-forming unit to that disturbance. Therefore, PCNB can be interpreted with the relation:

$$\text{sgn}(\Delta P) = -\text{sgn}(\Delta f) \quad (6.16)$$

This means: the active-power response must move in the opposite direction to the frequency deviation, and the final active power and frequency must remain inside the static-value tolerance bands.

This distinction is essential. A simulation may show the correct physical direction of PCNB response but still fail the quantitative EMT validation check if the final active power does not settle close enough to the required target.

6.2.1 Measurement 1.1: PCNB behaviour at (Q = 0)

Measurement 1.1 evaluates PCNB behaviour at approximately zero reactive power. The extracted active-power and frequency values are shown in Table 6.6

Table 11: PCNB measurements for Test 1.1

Quantity	Before (init)	Maximum after islanding (max)	Minimum after islanding (min)	Final (ss)
(P) [pu]	0.68390	0.69065	0.45728	0.46831
(f) [Hz]	50.00000	50.76015	49.96093	50.72927

The deviations are shown in Table 11.

Table 12: PCNB deviations for Test 1.1

Quantity	ΔX_{max}	ΔX_{min}	ΔX_{ss}
(P) [pu]	0.00675	-0.22661	-0.21558
(f) [Hz]	0.76015	-0.03907	0.72927

The final active power is 0.46831 pu. Compared with the residual-load target of 0.50 pu, the final active-power error is

$$P_{error} = 0.46831 - 0.50000 = -0.03169 \text{ pu}$$

The final frequency error is

$$f_{error} = 50.72927 - 50.00000 = 0.72927 \text{ Hz}$$

The value is below the lower static-value limit of 0.47500 pu. The final frequency is From the physical PCNB perspective, the response direction is meaningful. The final frequency is higher than the pre-islanding value, and the final active power is lower than the pre-islanding active power. This indicates that the controller reduces active power when frequency increases, which is the expected direction for the negative-inertia/procured direction considered in the test. However, from the EMT validation perspective, the final active power is slightly below the lower bound of the accepted range around the residual-load target. Therefore, the result shows the difference between physical direction and quantitative validation: the response direction is correct, but the final static value is not sufficiently close to the target.

6.2.2 Measurement 1.2: PCNB behaviour at maximum inductive reactive power

Measurement 1.2 evaluates PCNB behaviour under maximum inductive reactive-power operation. The operating point is

$$Q = -0.33 \text{ pu}$$

The extracted active-power and frequency measurements are shown in Table 12.

Table 13: PCNB measurements for Test 1.2

Quantity	Before (init)	Maximum after islanding (max)	Minimum after islanding (min)	Final (ss)
(P) [pu]	0.68390	0.68414	0.26732	0.38154
(f) [Hz]	50.00000	51.43318	49.97864	51.01707

The deviations are shown in Table 13.

Table 14: PCNB deviations for Test1.2

Quantity	ΔX_{max}	ΔX_{min}	ΔX_{ss}
(P) [pu]	0.00024	-0.41658	-0.30236
(f) [Hz]	1.43318	-0.02136	1.01707

The final active-power error is

$$P_{error} = 0.38154 - 0.50000 = -0.11846 \text{ pu}$$

The final frequency error is

$$f_{error} = 51.01707 - 50.00000 = 1.01707 \text{ Hz}$$

This result clearly illustrates the two-layer interpretation. At the physical layer, the frequency increases after islanding and the active power decreases. Therefore, the sign of the response is consistent with the expected PCNB direction for negative inertia. However, at the EMT validation layer, the final active power settles far below the residual-load target band. The final power of 0.38154 pu is below the lower limit of 0.47500 pu. This means that although the controller reacts in the correct direction, the simulated model does not reach the required static operating point.

Physically, this result indicates that the active-power/frequency control is too weak or incorrectly balanced for the inductive reactive-power operating point. The inductive loading condition also affects the voltage and network operating point, which can influence the active-power response. Therefore, this case shows why PCNB interpretation must not be reduced to frequency alone. Frequency remains within the broad $\pm 5\%$ band, but the active-power response is not sufficient to reproduce the required PCNB static behaviour.

6.2.3 Measurement 1.3: PCNB behaviour at maximum capacitive reactive power

Measurement 1.3 evaluates PCNB behaviour under maximum capacitive reactive-power operation. The operating point is

$$Q = +0.33 \text{ pu}$$

The extracted measurements are shown in Table 14.

Table 15: PCNB measurements for Test 1.3

Quantity	Before (init)	Maximum after islanding (max)	Minimum after islanding (min)	Final (ss)
(P) [pu]	0.68390	1.07431	0.55092	0.56320
(f) [Hz]	50.00000	50.44646	48.44682	50.41091

The deviations are shown in Table 15.

Table 16: PCNB deviations for Test 1.3

Quantity	ΔX_{max}	ΔX_{min}	ΔX_{ss}
(P) [pu]	0.39041	-0.13298	-0.12070
(f) [Hz]	0.44646	-1.55318	0.41091

The final active-power error is

$$P_{error} = 0.56320 - 0.50000 = +0.06320 \text{ pu}$$

The final frequency error is

$$f_{error} = 50.41091 - 50.00000 = 0.41091 \text{ Hz}$$

In this case, the final frequency remains close to nominal, but the final active power is higher than the upper limit of the accepted band around the residual-load target. This means that the converter supplies more active power than expected after islanding. From the physical perspective, the active-power response shows that the controller reacts strongly to the islanding event under capacitive reactive-power conditions. From the validation perspective, the final value is outside the expected static range.

This case also shows why the maximum and minimum values are useful. The maximum active power of 1.07431 pu indicates a strong transient excursion during the islanding transition. The final value of 0.56320 pu indicates that the response does not settle to the expected residual-load target. Therefore, the transient and final values provide complementary information: the transient values describe the dynamic severity of the response, while the final value describes the steady-state validation result.

6.2.4 Link between PCNB EMT validation and physical requirement

The PCNB tests link the physical requirement of Section 4.2.2.2 to the EMT validation procedure in Section 5. The physical requirement is that the grid-forming unit must provide a frequency-dependent active-power contribution to support network security. The EMT validation requirement verifies this behaviour by recording active power and frequency during the virtual island test.

This relationship can be summarised as follows:

Physical PCNB requirement \Rightarrow *frequency-dependent active-power response*

EMT validation requirement \Rightarrow *measure $P(t)$ and $f(t)$*

Interpretation \Rightarrow *compare the sign, magnitude and final value of ΔP with Δf*

The deviation calculations are therefore not only numerical error checks. They show whether the simulated model reproduces the physical PCNB mechanism. The frequency deviation represents the disturbance. The active-power deviation represents the response of the unit. If the two quantities have the expected relationship, the physical behaviour is present. If the final value also lies within the required tolerance band, the EMT validation requirement is satisfied.

The PCNB results should therefore always be interpreted using two questions:

1. Physical response question:

Does the active power move in the correct direction when the frequency changes?

2. Validation accuracy question:

Does the final active power and final frequency settle within the required tolerance bands?

This distinction explains why a simulation can show correct physical PCNB behaviour but still fail the final validation check. For example, in Measurement 1.2, the frequency increases and active power decreases, which is the expected direction. However, the final active power settles too far below the residual-load target. The physical response direction is therefore correct, but the quantitative EMT validation requirement is not satisfied.

Consequently, Chapter 6 should not interpret the results only as compliant or non-compliant. The final verdict is already presented in Chapter 5. The purpose of this chapter is to show what the measured values mean. For voltage-source behaviour, the measured voltage response shows whether the converter can maintain its internal voltage-source characteristic after islanding. For PCNB behaviour, the measured active-power and frequency response shows whether the converter provides the expected frequency-dependent active-power contribution. In both cases, the deviation calculations provide the bridge between the physical FNN requirement and the EMT validation procedure.

7 Conclusion and Future Work

This thesis addressed the challenge of using simulation-based evidence to support grid-code certification of grid-forming inverter-based resources. As converter-based generation progressively replaces synchronous generation, power systems require new methods for verifying that inverter-based units can contribute to voltage formation, frequency stability, inertia-related behaviour and network security. The work therefore focused on the connection between technical grid-forming requirements, EMT simulation, automated test execution and compliance-oriented interpretation.

The thesis narrowed the broad European grid-code context to the VDE FNN guideline *Technical Requirements for Grid-Forming Capabilities Including Provision of Inertia*. Within this framework, the study concentrated on two requirements: voltage-source behaviour and Primary Control Based on Network Security (PCNB). These requirements were selected because they represent two essential properties of grid-forming operation. Voltage-source behaviour describes the ability of the unit to behave as a controlled voltage source behind an effective impedance, while PCNB describes the active-power response required to support frequency stability and network security.

The simulation work was carried out using the GFM model developed by Professor Lingling Fan. Since the objective of the thesis was not to design a new controller, the model was used as an EMT-based test object for certification-oriented analysis. The power architecture, passive filtering interface, transformer, residual load, grid connection and control logic were analysed in order to understand how the simulated inverter responds during virtual island network operation. Particular attention was given to the P - f droop loop, the Q - V droop loop, the outer voltage controller and the inner current controller, because these blocks determine how the inverter forms voltage and regulates active and reactive power.

A major contribution of the thesis is the development of the AGIS framework, the Automatic GFM Inverter Simulator. AGIS automates the execution of selected VDE FNN tests in MATLAB/Simulink. It allows the user to select the verification family, choose the

operating point, run the simulation, extract the required electrical quantities, calculate deviations and generate a structured validation report. The framework was implemented for Measurements 1.1, 1.2 and 1.3 of the virtual island network procedure, which correspond to operation at approximately zero reactive power, maximum inductive reactive power and maximum capacitive reactive power. The same simulation outputs were then used to assess voltage-source behaviour and PCNB behaviour.

The results showed that the automated framework can distinguish between baseline and tuned simulation scenarios. The baseline scenario was configured to reveal non-compliant behaviour, while the tuned scenario was configured to satisfy the implemented criteria. However, the thesis also showed that the final verdict does not come from the scenario label itself. It comes from the measured values, the deviation calculations and the comparison with the assessment criteria implemented in AGIS. This is important because the same scenario name may lead to different outcomes if the parameters in the MATLAB scripts are modified.

For voltage-source behaviour, the interpretation showed that the most important result is not only the transient response immediately after islanding, but the ability of the inverter to recover and maintain a stable voltage after the external grid is disconnected. The final steady-state voltage was therefore interpreted in relation to the pre-islanding steady-state voltage, with the tolerance width expressed on the nominal per-unit voltage base. This interpretation links the EMT validation procedure to the physical requirement of Section 4.2.1.1 of the VDE FNN guideline: the grid-forming unit must continue to behave as a voltage source behind an effective impedance.

For PCNB behaviour, the interpretation showed that active power and frequency must be analysed together. The frequency deviation represents the disturbance experienced by the virtual island network, while the active-power deviation represents the response of the grid-forming unit to that disturbance. The thesis therefore distinguished between two interpretation layers. The first is the physical layer, where the active-power response must move in the expected direction with respect to the frequency

deviation. The second is the validation layer, where final active power and frequency must settle within the required static-value tolerance bands. This distinction explains why a test may show the correct physical direction of response but still fail the quantitative EMT validation check if the final values do not settle sufficiently close to the required targets.

Overall, the thesis demonstrates that automated EMT-based simulation can provide structured, repeatable and traceable evidence for selected grid-forming requirements. The AGIS framework reduces manual work, limits the risk of inconsistent post-processing and creates a clearer link between the VDE FNN requirement, the simulation model, the extracted measurements and the final interpretation. In this sense, the thesis contributes not by proposing a new grid-forming controller, but by showing how an existing EMT model can be organised into a certification-oriented workflow.

The main limitation of the thesis is that the study remains simulation-based. The GFM model was used as an EMT test object, but the results were not validated against physical inverter measurements, manufacturer test data or real-time hardware experiments. Therefore, the results demonstrate the behaviour of the selected simulation model under the implemented test conditions, but they should not be interpreted as proof of compliance for a commercial physical inverter. Another limitation is that only two VDE FNN requirements were implemented: voltage-source behaviour and PCNB. Other requirements, including detailed inertia procurement tests, harmonic behaviour, damping above 10 Hz, current limitation behaviour, network-parallel operation capability and broader system-certification procedures, were outside the scope of the implemented work.

Future work should first extend AGIS to cover more VDE FNN verification requirements. This would include additional Table 1 operating points, non-procured inertia-direction cases, damping evaluations, start-up time constant verification, current limitation behaviour and supplementary tests in synchronous operation. A second direction is to improve the generality of the framework by adapting AGIS to other grid-forming models.

This would require standardising the signal names, model interface, breaker control, base values, per-unit conversions and sign conventions so that the same automation workflow can be applied to different converter models.

A third and important direction for future work is the extension toward real-time controller-hardware-in-the-loop validation. In the present thesis, C-HIL was discussed as a future validation layer, but was not implemented experimentally. A real-time C-HIL setup would allow the power circuit to be simulated on a real-time platform while the controller is executed on physical control hardware. This would strengthen the traceability between offline EMT simulation and practical controller implementation. It would also make it possible to test controller timing, signal delays, sampling effects and real-time execution constraints before moving toward laboratory or field testing.

Finally, future work should improve the link between simulation-based certification and practical grid-code evidence packages. This includes developing clearer reporting templates, better automatic traceability between guideline clauses and simulation outputs, and stronger comparison methods between EMT results, real-time simulations and measured hardware data. Such extensions would make the framework more useful not only for academic analysis, but also for future certification, pre-commissioning studies and controller development for grid-forming inverter-based resources.

In conclusion, the thesis confirms that simulation-based certification can play an important role in the validation of grid-forming technologies. As power systems become increasingly dominated by inverter-based resources, the ability to connect technical requirements, EMT models, automated testing and structured interpretation will become essential. The AGIS framework developed in this thesis represents a first step toward that objective by demonstrating how selected VDE FNN requirements can be translated into an automated MATLAB/Simulink verification workflow for grid-forming inverter models.

AI Use Declaration

I hereby declare that this thesis, entitled “**Grid Code Certification by Simulation for Grid-Forming Connected Inverters**”, submitted in partial fulfilment of the requirements for the degree of **Master of Science in Technology, Smart Energy**, at the **University of Vaasa**, is the result of my own work.

During the preparation of this thesis, artificial intelligence tools, including ChatGPT, were used as supporting tools for language improvement, text restructuring, grammar correction, formatting assistance, and clarification of technical explanations. These tools were not used to replace my own research, analysis, simulation work, interpretation of results, or academic judgment. All technical decisions, MATLAB/Simulink implementation, simulation analysis, results interpretation, and final content selection were carried out under my responsibility.

I further declare that all sources, standards, guidelines, reports, articles, models, figures, and external materials consulted during the thesis work have been appropriately cited and acknowledged in accordance with academic writing principles. The use of artificial intelligence did not remove the requirement for proper referencing, verification of technical content, or originality of the submitted work.

I accept full responsibility for the accuracy, integrity, and originality of this thesis.

Boris YONDJIN NGAMY

Vaasa, Finland

09/06/2026

References

European Commission. (2016). Commission Regulation (EU) 2016/631 of 14 April 2016 establishing a network code on requirements for grid connection of generators. Official Journal of the European Union. <https://eur-lex.europa.eu/eli/reg/2016/631/oj/eng>

ENTSO-E. (n.d.). Requirements for Generators. Retrieved May 25, 2026, from https://www.entsoe.eu/network_codes/rfg/

Fan, L. (2024). Modelling and stability analysis of inverter-based resources [Webinar slides]. IEEE Power & Energy Society.

Fan, L., & Miao, Z. (2024). Modelling and stability analysis of inverter-based resources. CRC Press. <https://doi.org/10.1201/9781003323655>

Ghimire, S., Guerreiro, G. M. G., Vatta Kkuni, K., Guest, E. D., Jensen, K. H., Yang, G., & Wang, X. (2025). Functional specifications and testing requirements for grid-forming offshore wind power plants. *Wind Energy Science*, 10, 1–15. <https://doi.org/10.5194/wes-10-1-2025>

IEEE. (2018). IEEE Std 1547-2018: IEEE Standard for Interconnection and Interoperability of Distributed Energy Resources with Associated Electric Power Systems Interfaces. IEEE Standards Association. <https://standards.ieee.org/ieee/1547/5915/>

IEEE. (2022). *IEEE Std 2800-2022: IEEE Standard for Interconnection and Interoperability of Inverter-Based Resources Interconnecting with Associated Transmission Electric Power Systems*. IEEE Standards Association. <https://standards.ieee.org/ieee/2800/10453/>

IEEE. (2026). IEEE 2800.2-2026: IEEE Approved Draft Recommended Practice for Test and Verification Procedures for Inverter-based Resources Interconnecting with Bulk Power Systems. IEEE Standards Association. <https://standards.ieee.org/ieee/2800.2/10616/>

International Renewable Energy Agency. (2022). Grid codes for renewable powered systems. IRENA. https://www.irena.org/-/media/Files/IRENA/Agency/Publication/2022/Apr/IRENA_Grid_Codes_Renewable_Systems_2022.pdf

Li, Y., Gu, Y., & Green, T. C. (2021). Revisiting grid-forming and grid-following inverters: A duality theory. *arXiv*. <https://doi.org/10.48550/arXiv.2105.13094>

North American Electric Reliability Corporation. (2023a). *White Paper: Grid Forming Functional Specifications for BPS-Connected Battery Energy Storage Systems*. NERC. https://www.nerc.com/globalassets/our-work/reports/white-papers/white_paper_gfm_functional_specification.pdf

North American Electric Reliability Corporation. (2023b). *Electromagnetic Transient Modeling for BPS-Connected Inverter-Based Resources: Recommended Model Requirements and Verification Practices*. NERC. https://www.nerc.com/globalassets/who-we-are/standing-committees/rstc/irps/reliability_guideline-emt_modeling_and_simulations.pdf

Seo, G.-S., Colombino, M., Subotić, I., Johnson, B., Groß, D., & Dörfler, F. (2018). *Dispatchable virtual oscillator control for decentralized inverter-dominated power systems: Analysis and experiments*. *arXiv*. <https://doi.org/10.48550/arXiv.1811.08842>

SFS-EN 50549-2. (2019). Requirements for generating plants to be connected in parallel with distribution networks — Part 2: Connection to a MV distribution network — Generating plants up to and including Type B. Finnish Standards Association SFS.

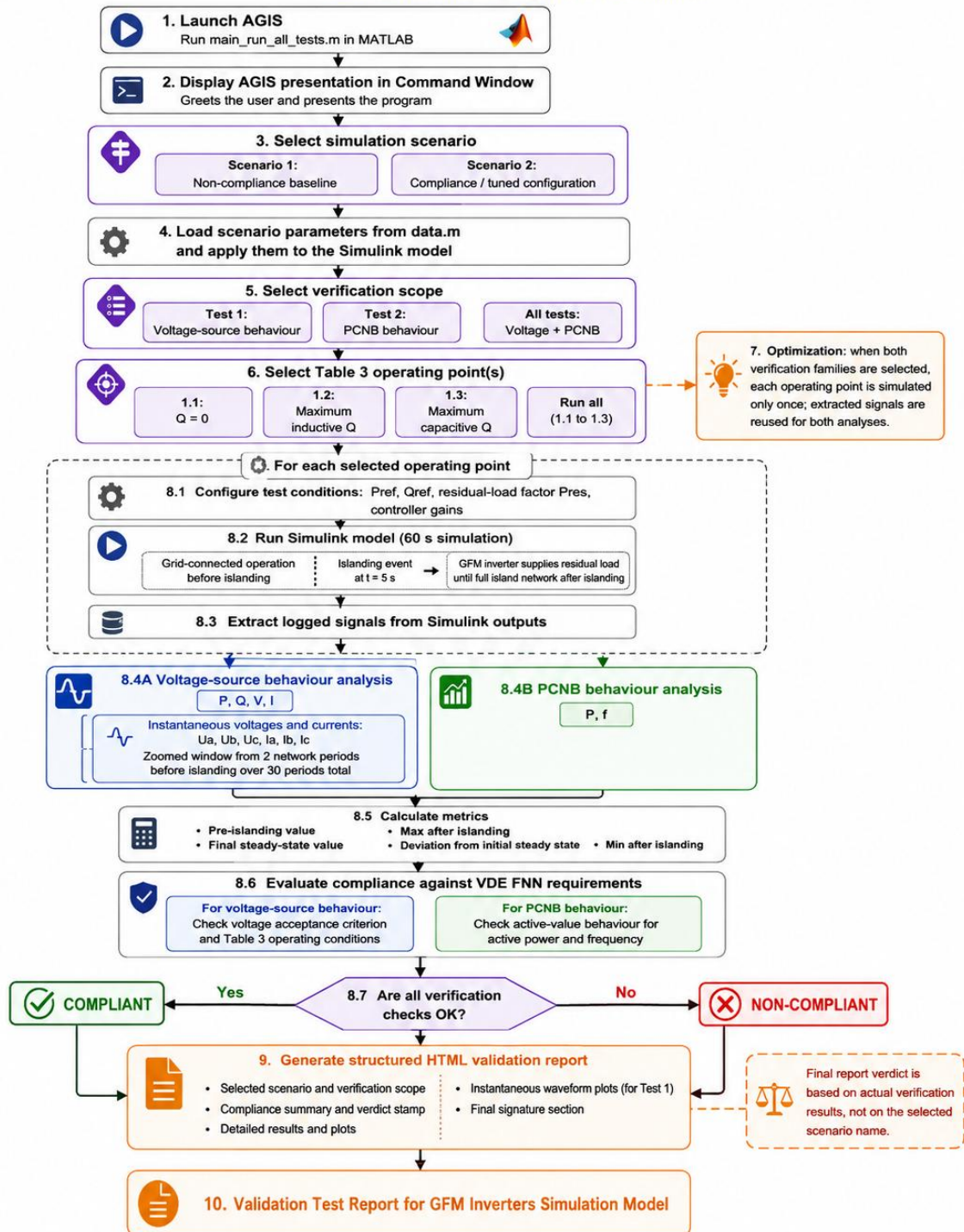
VDE FNN. (2025). Technical requirements for grid-forming capabilities including provision of inertia: Requirements and verifications for grid-forming units (Version 2.0). Forum Network Technology/Network Operation in the VDE.

Appendices

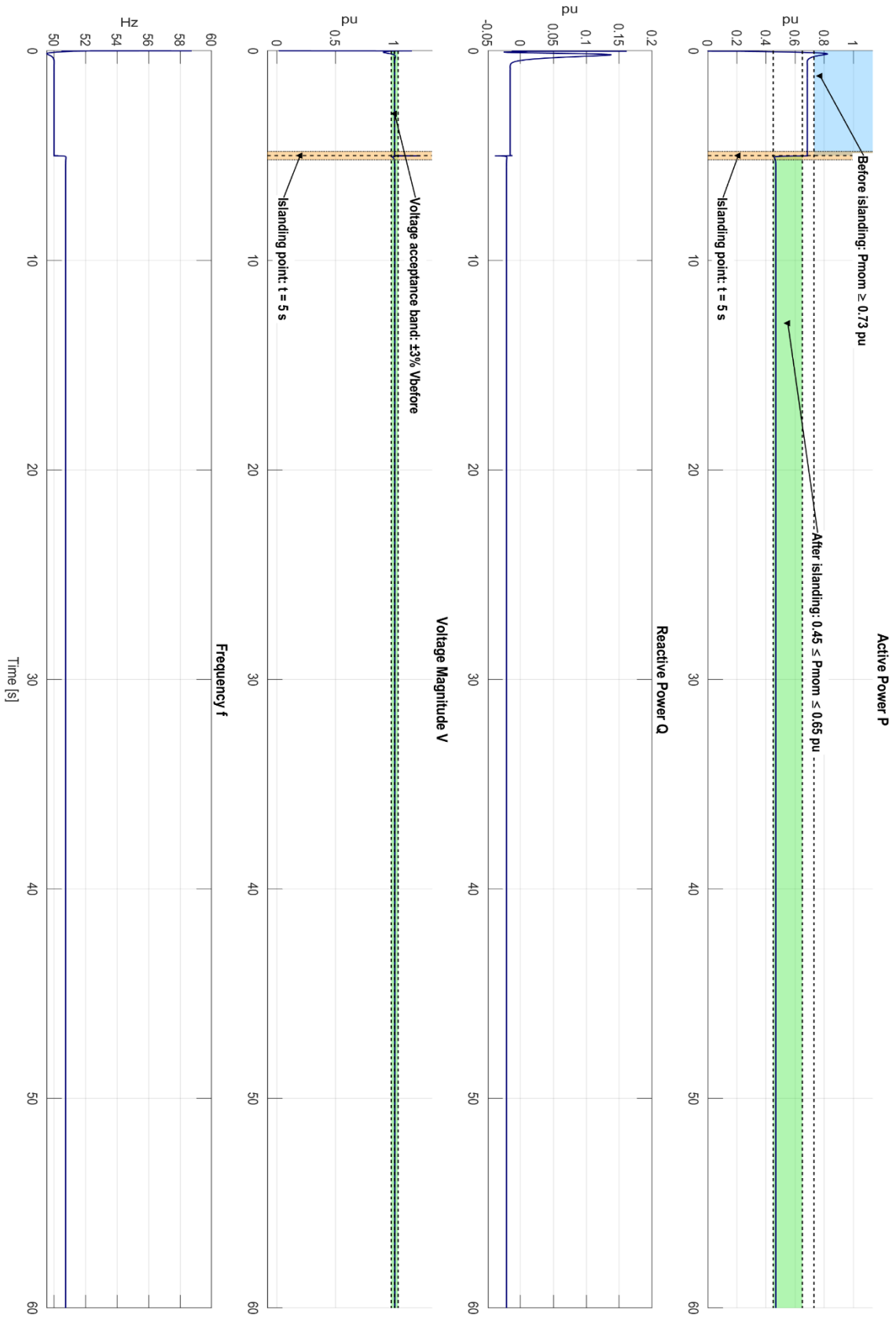
Appendix 1. General workflow of the AGIS automation framework

General Workflow of the AGIS Automation Framework

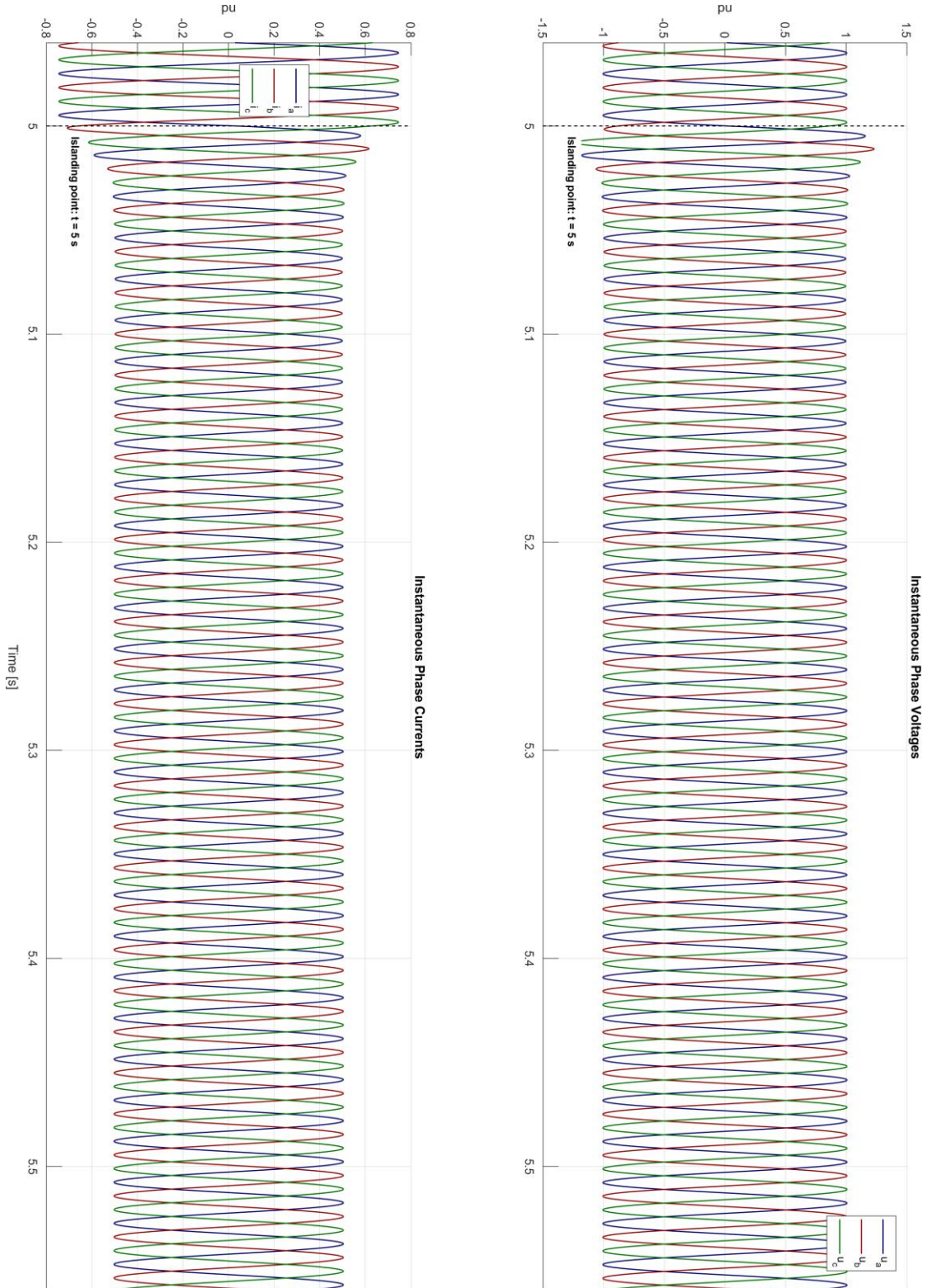
AGIS = Automatic GFM Inverter Simulator



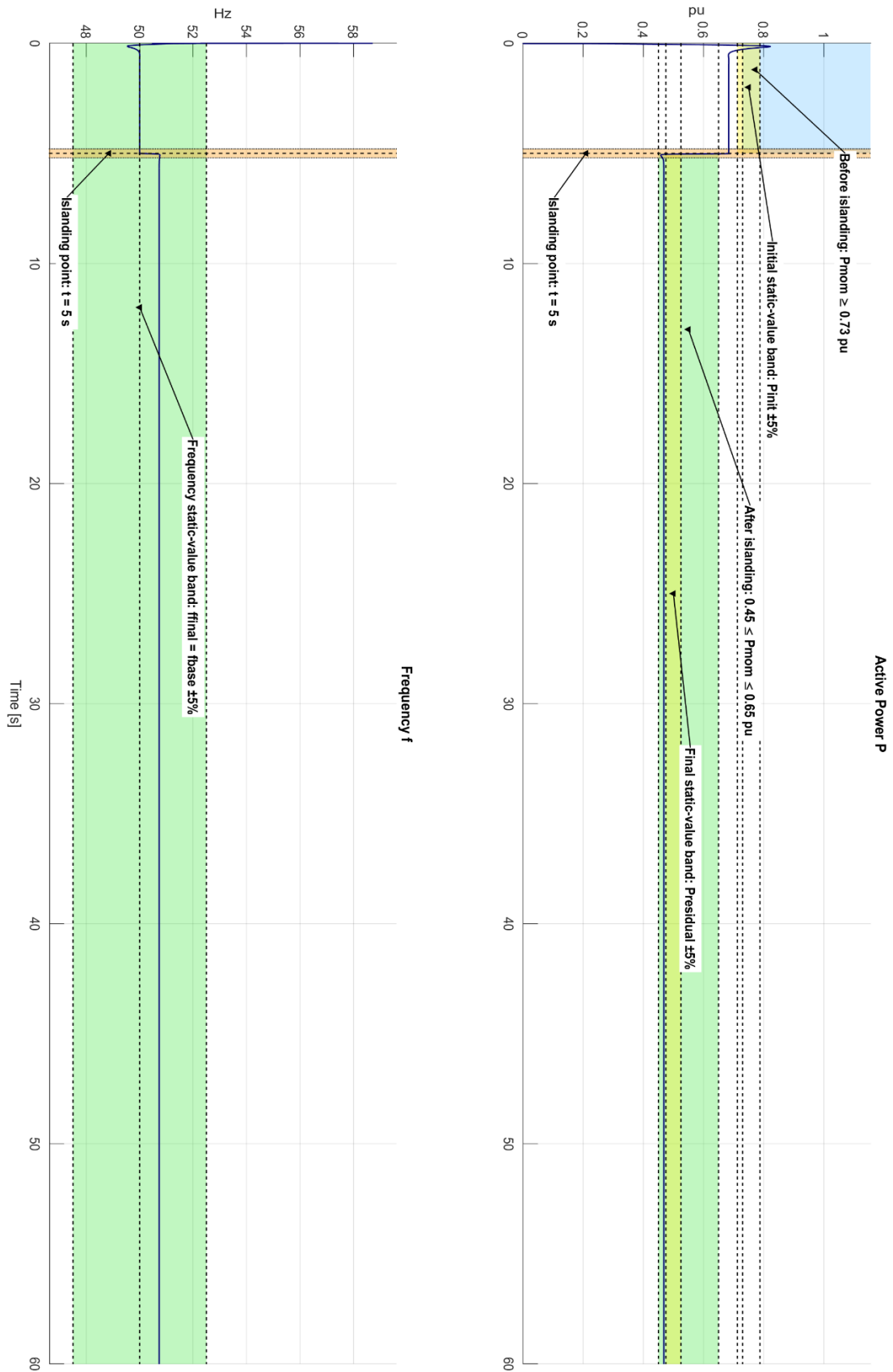
Appendix 2. Scenario One - Voltage source behaviour - Test 1.1 plots



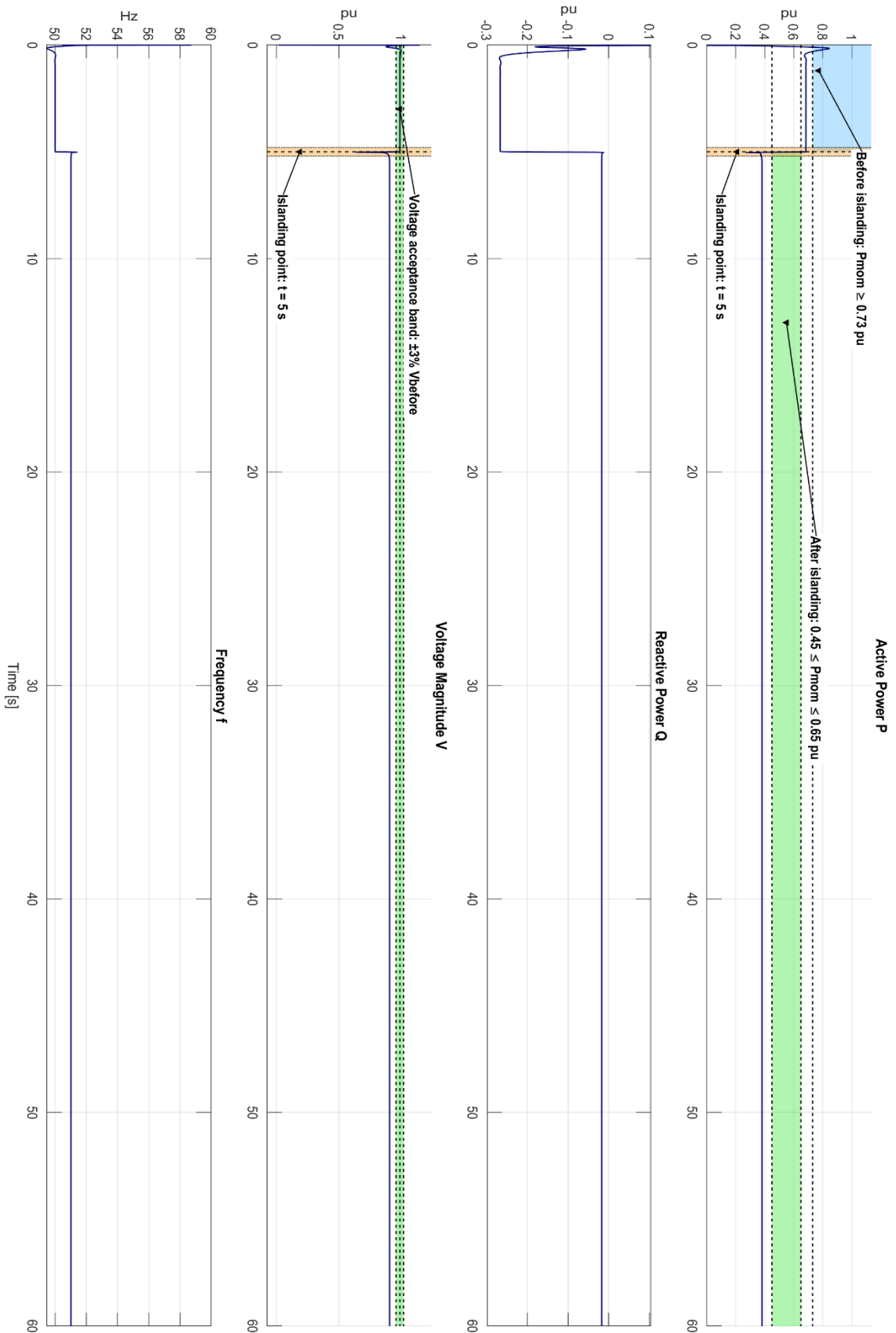
Appendix 3. Scenario One - Instantaneous phase voltages and currents - Test 1.1 plot



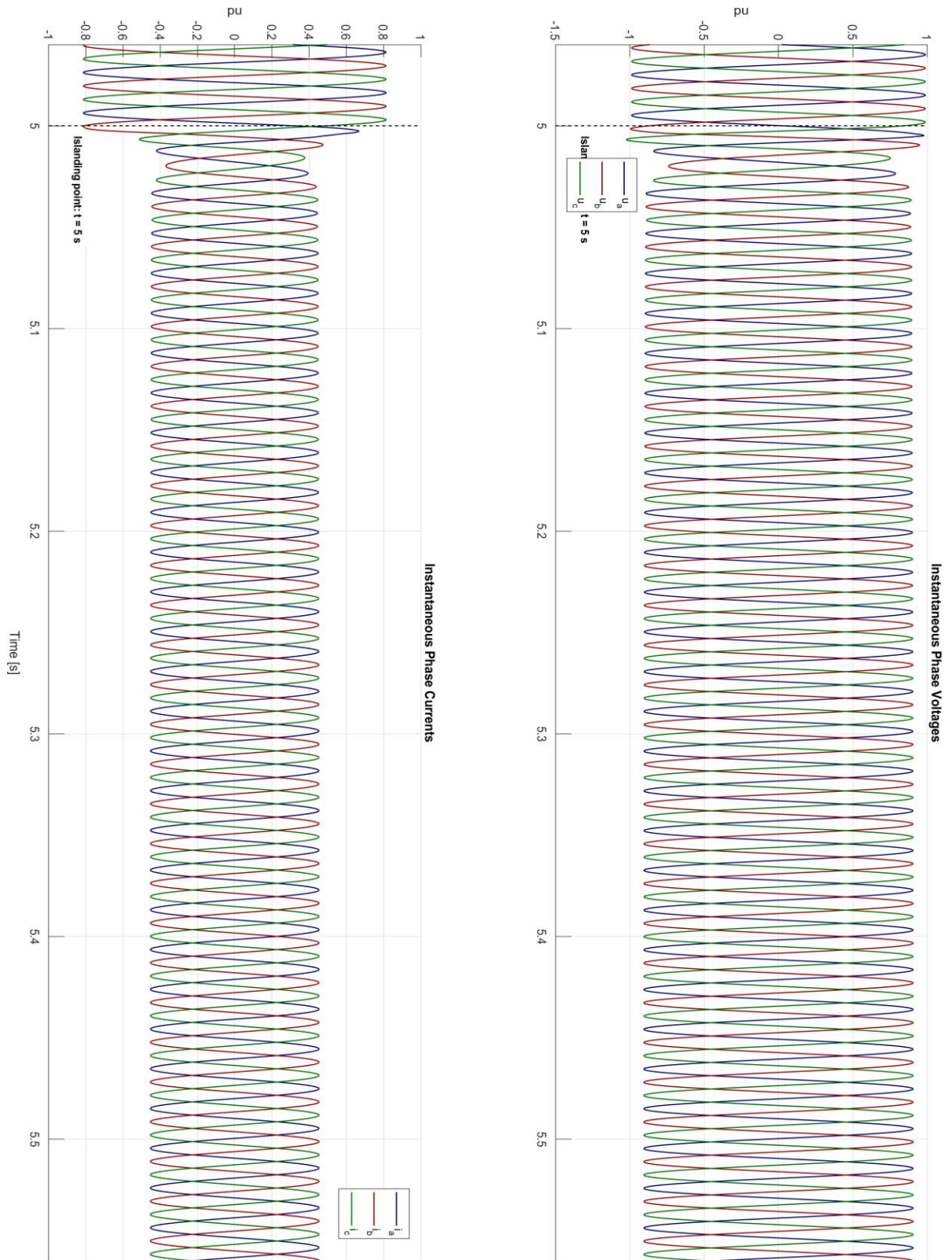
Appendix 4. Scenario One - PCNB behaviour - Test 1.1 plot



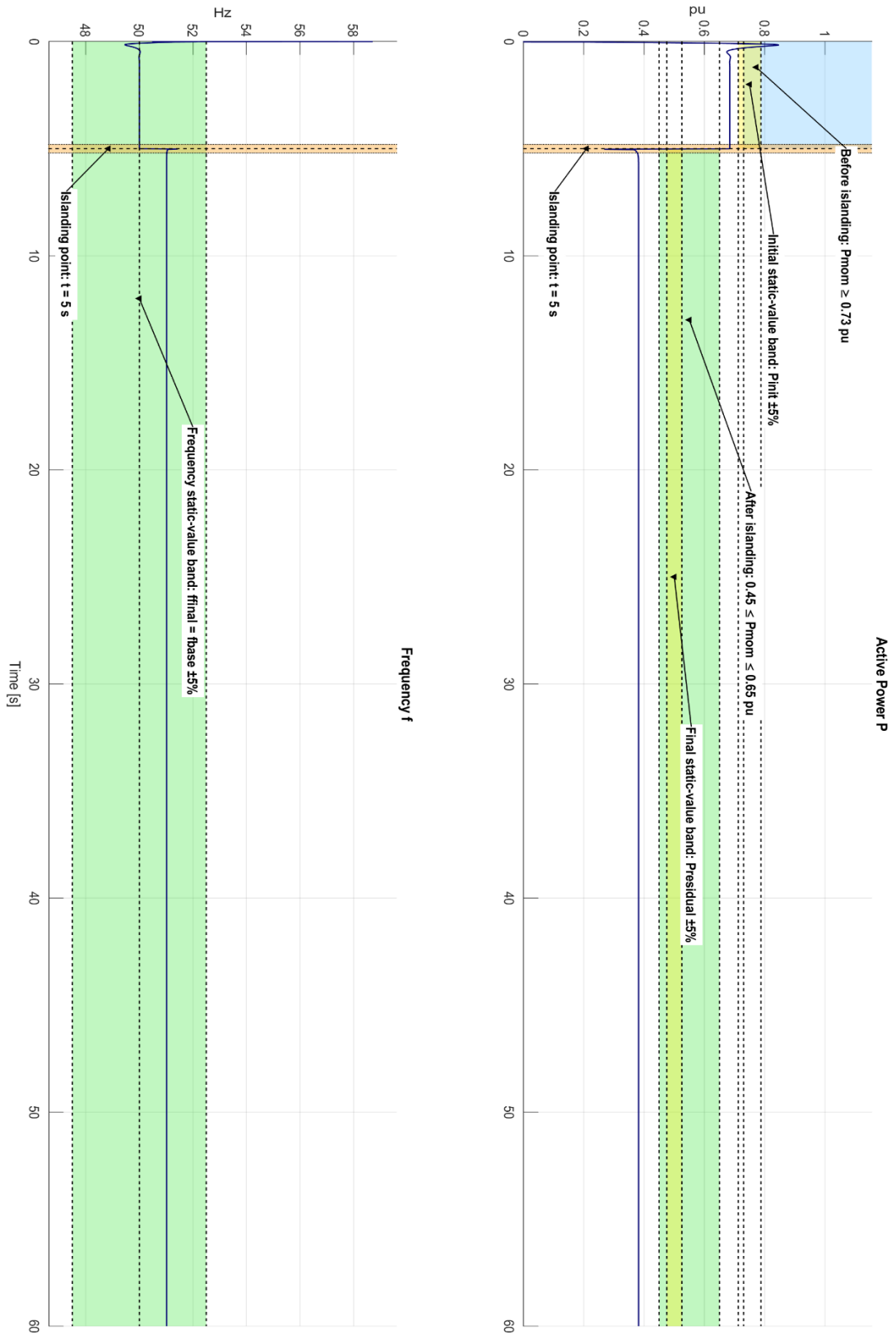
Appendix 5. Scenario One - Voltage source behaviour - Test 1.2 plot



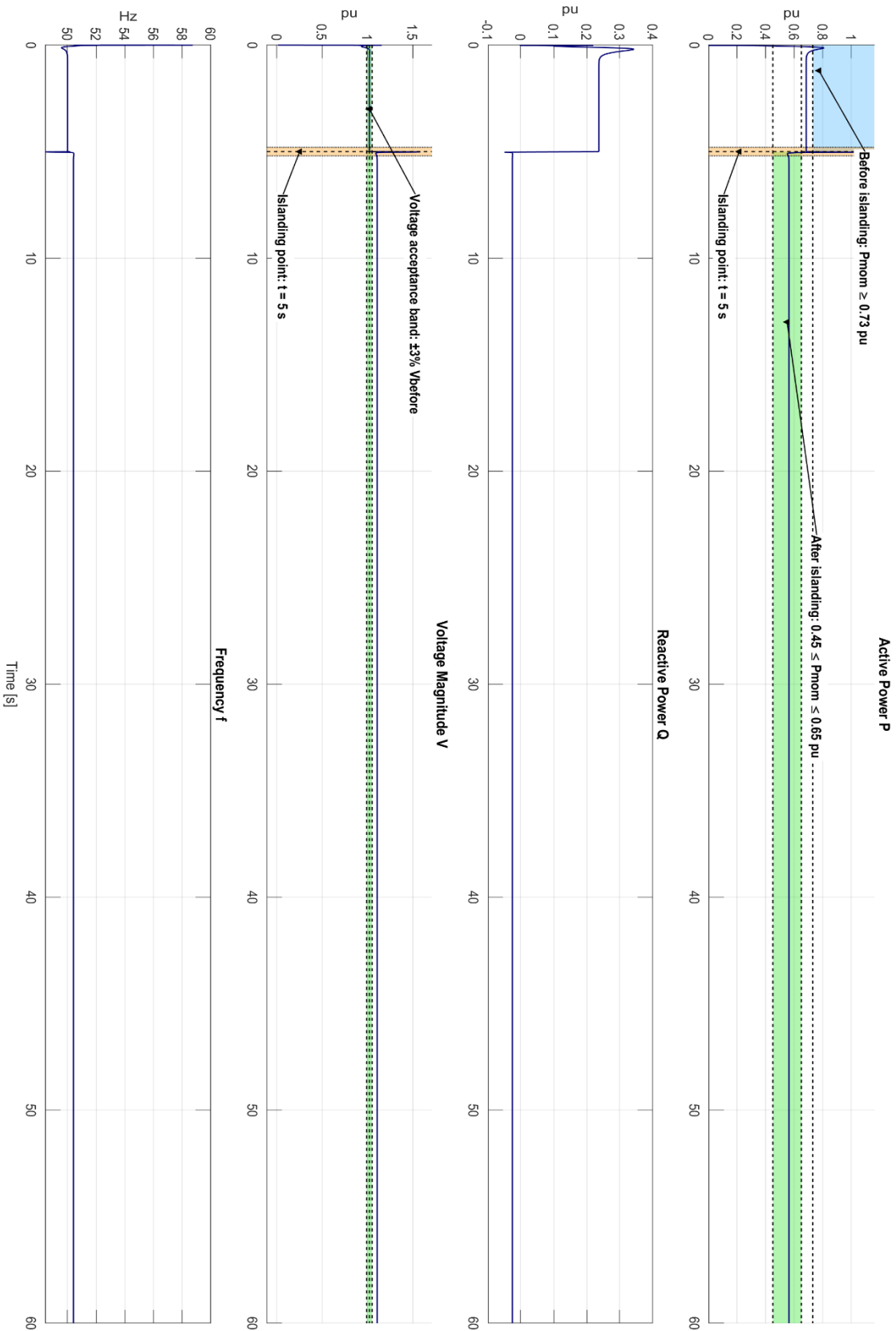
**Appendix 6. Scenario One - Instantaneous phase voltages and currents -
Test 1.2 plot**



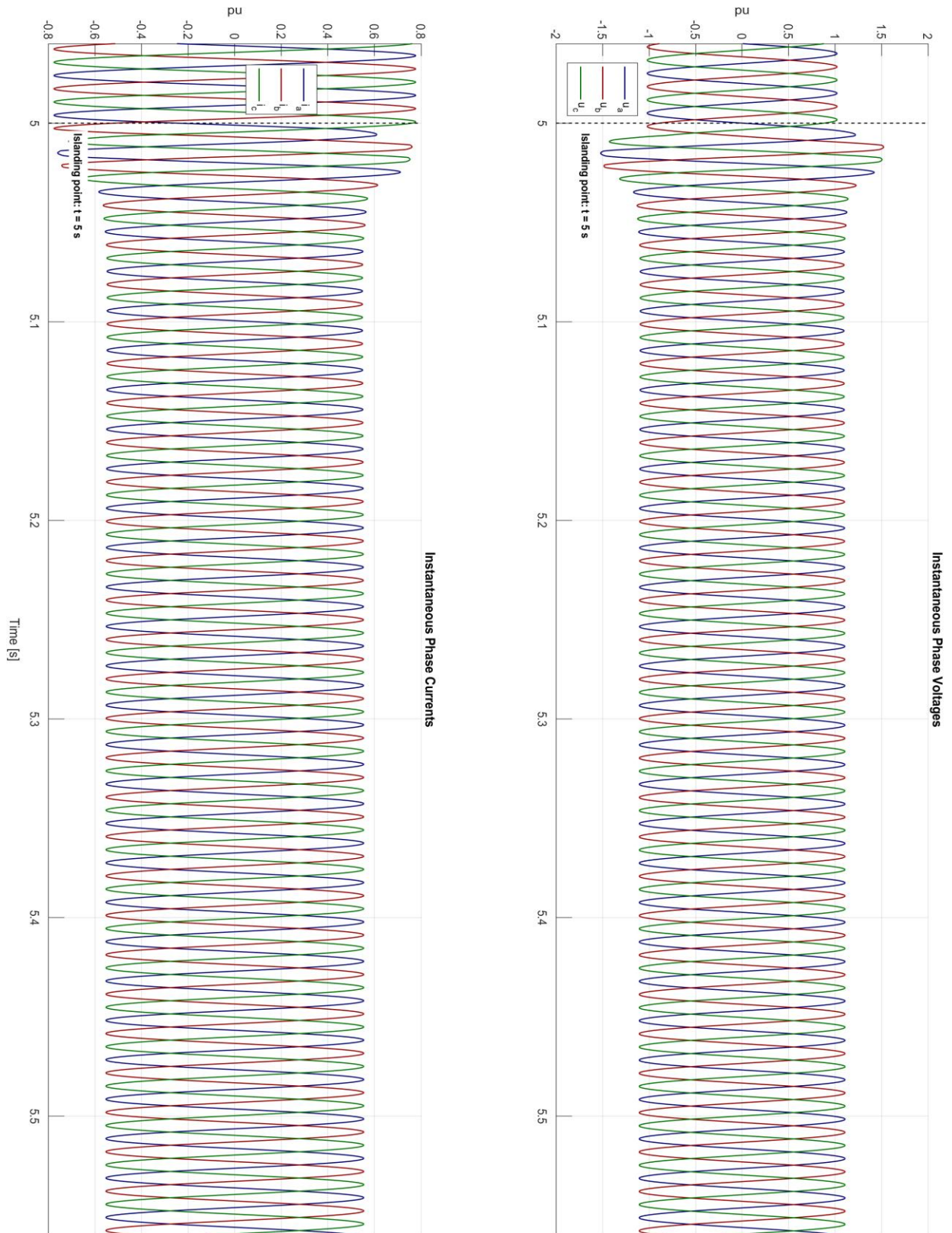
Appendix 7. Scenario One - PCNB behaviour - Test 1.2 - active power and frequency plot



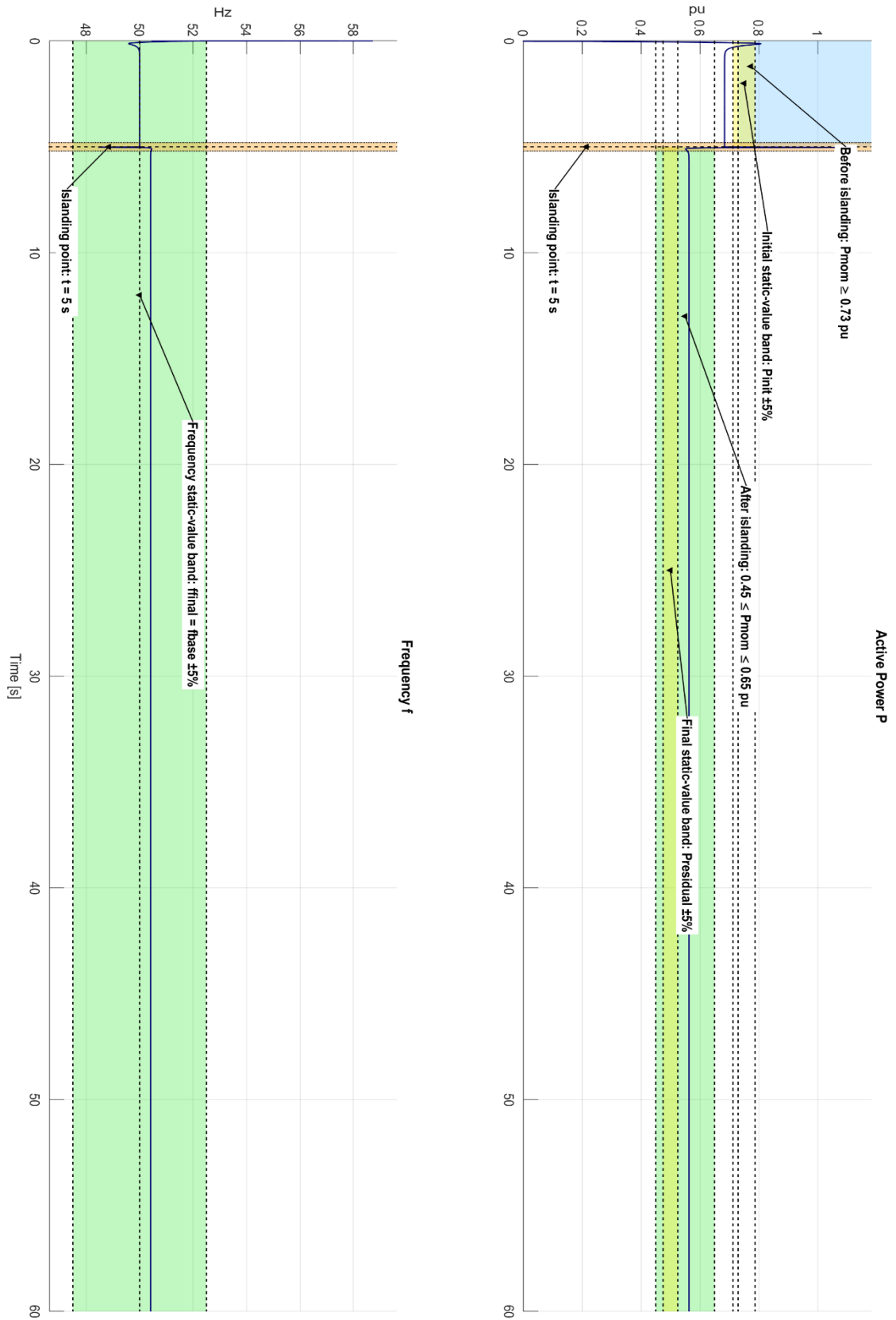
Appendix 8. Scenario One - Voltage source behaviour - Test 1.3 plot



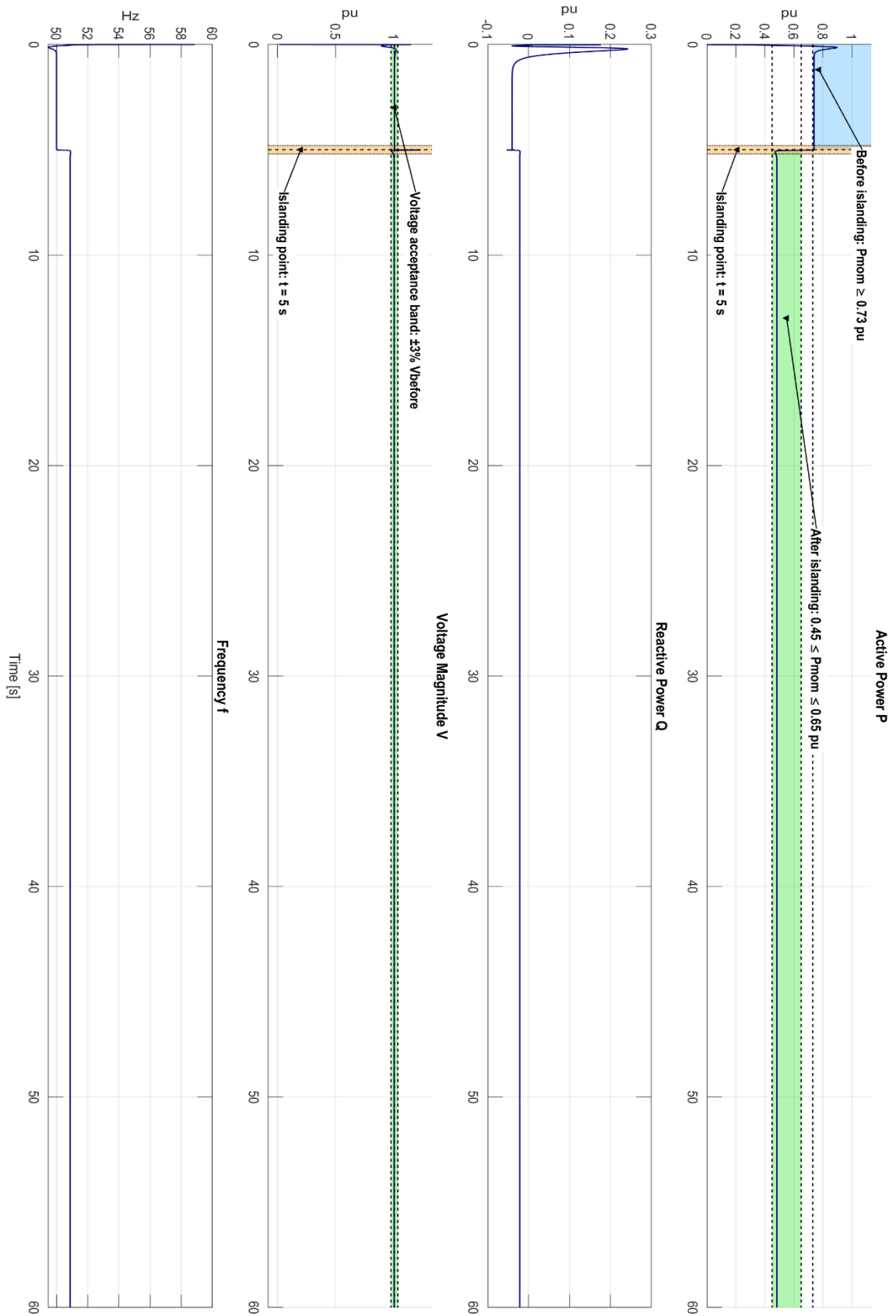
Appendix 9. Scenario One - Instantaneous phase voltages and currents - Test 1.3 plot



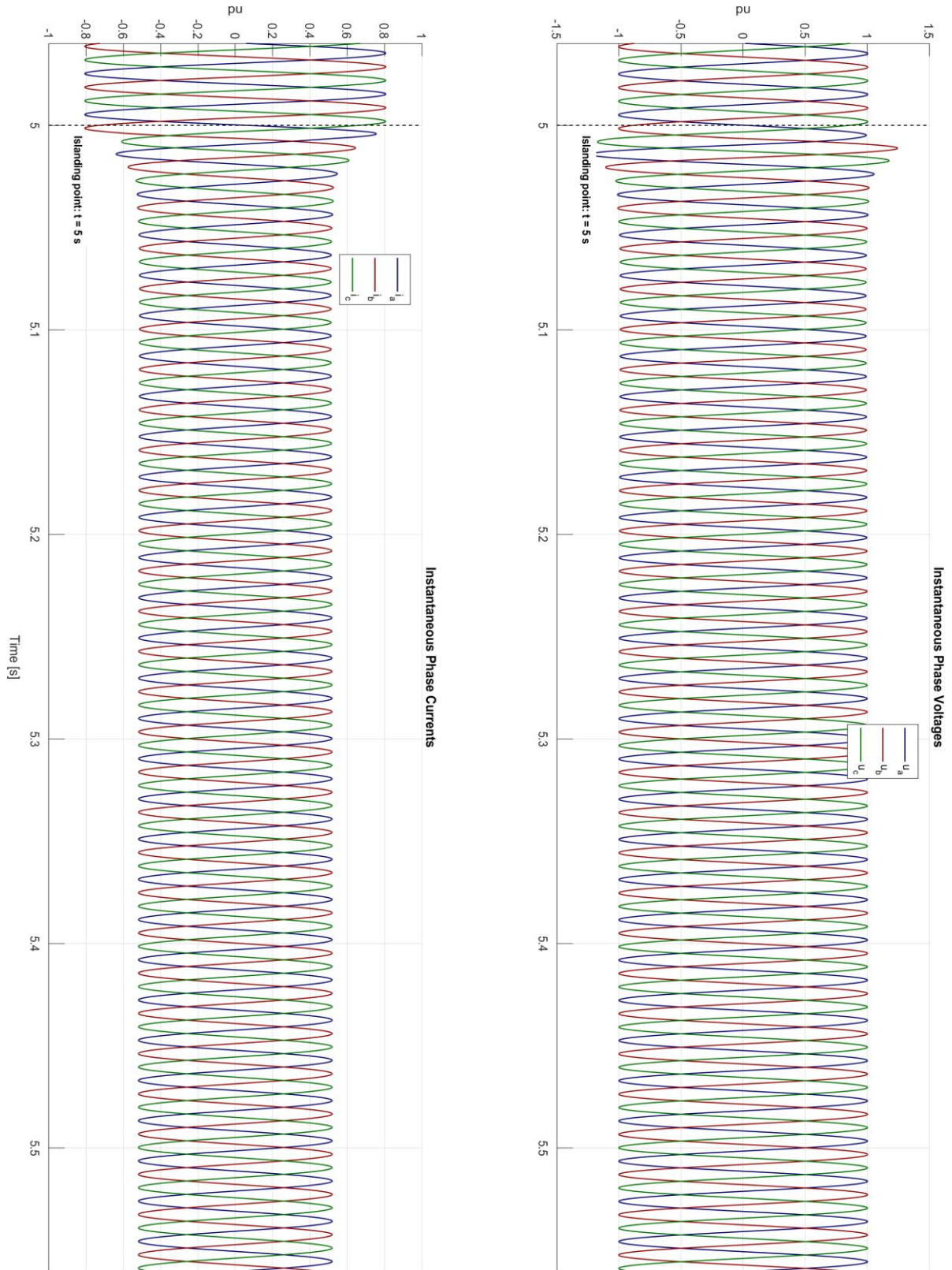
Appendix 10. Scenario One - PCNB behaviour - Test 1.3 plot



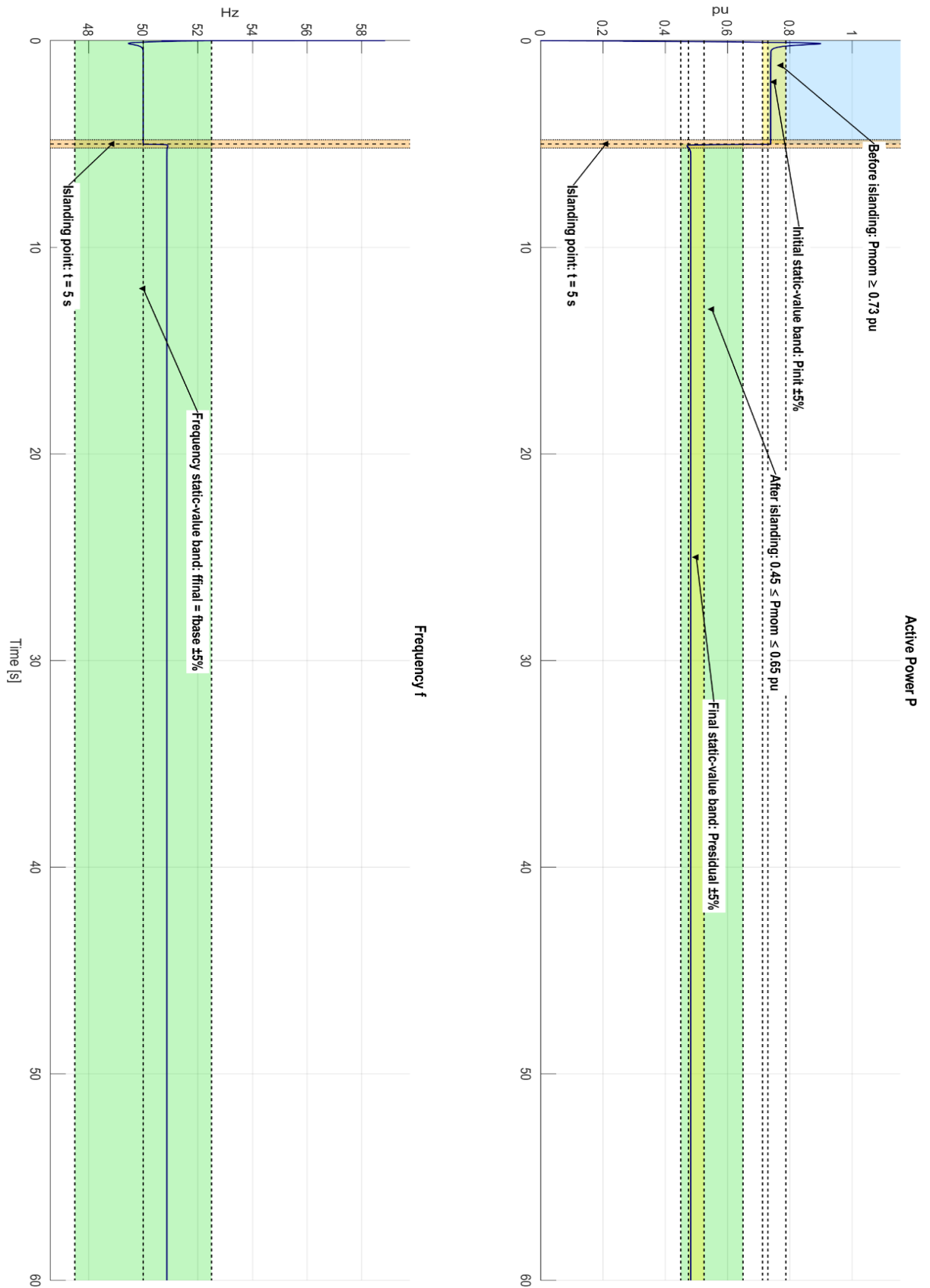
Appendix 11. Scenario Two - Voltage source behaviour - Test 1.1 plots



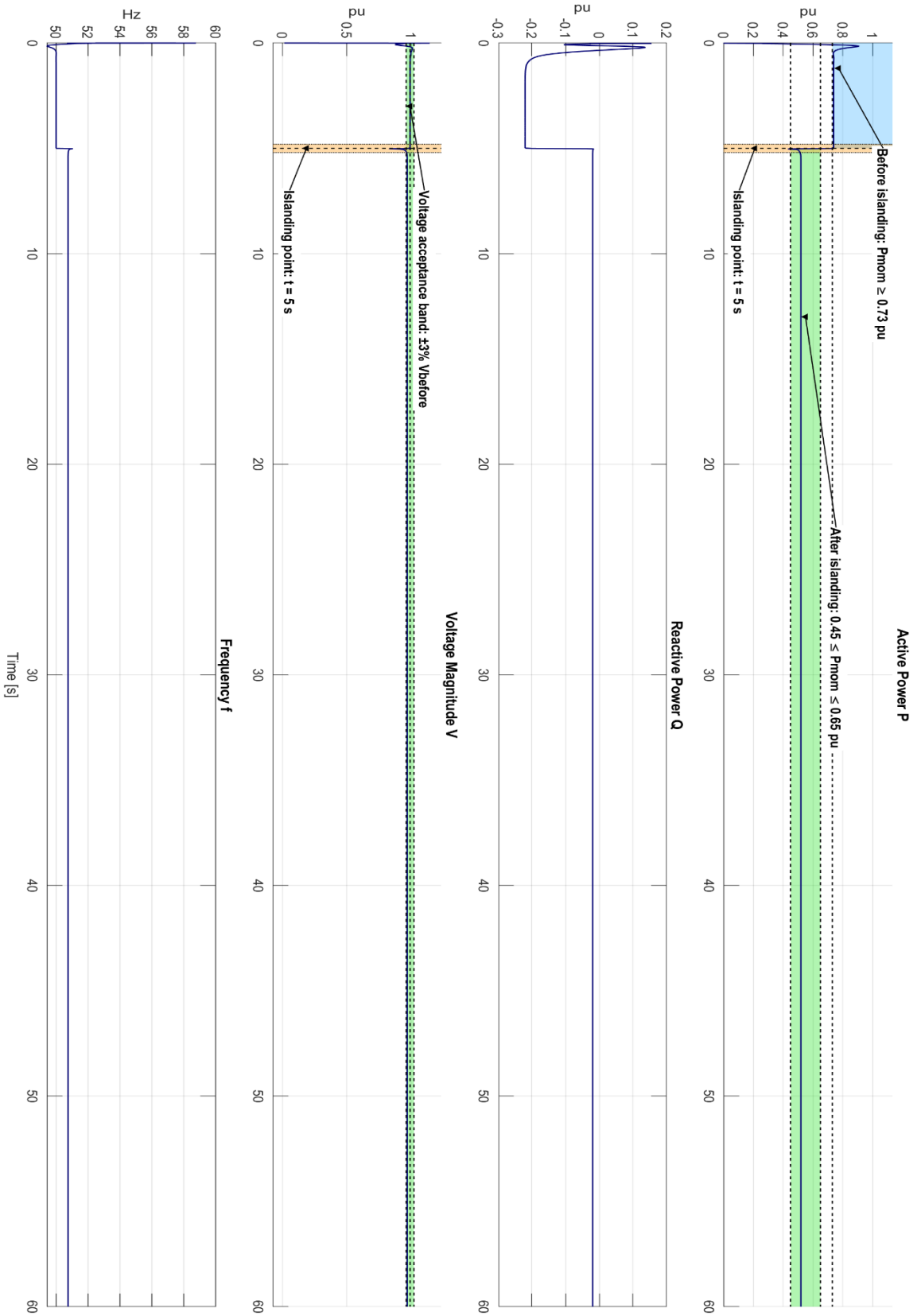
**Appendix 12. Scenario Two - Instantaneous phase voltages and currents -
Test 1.1 plot**



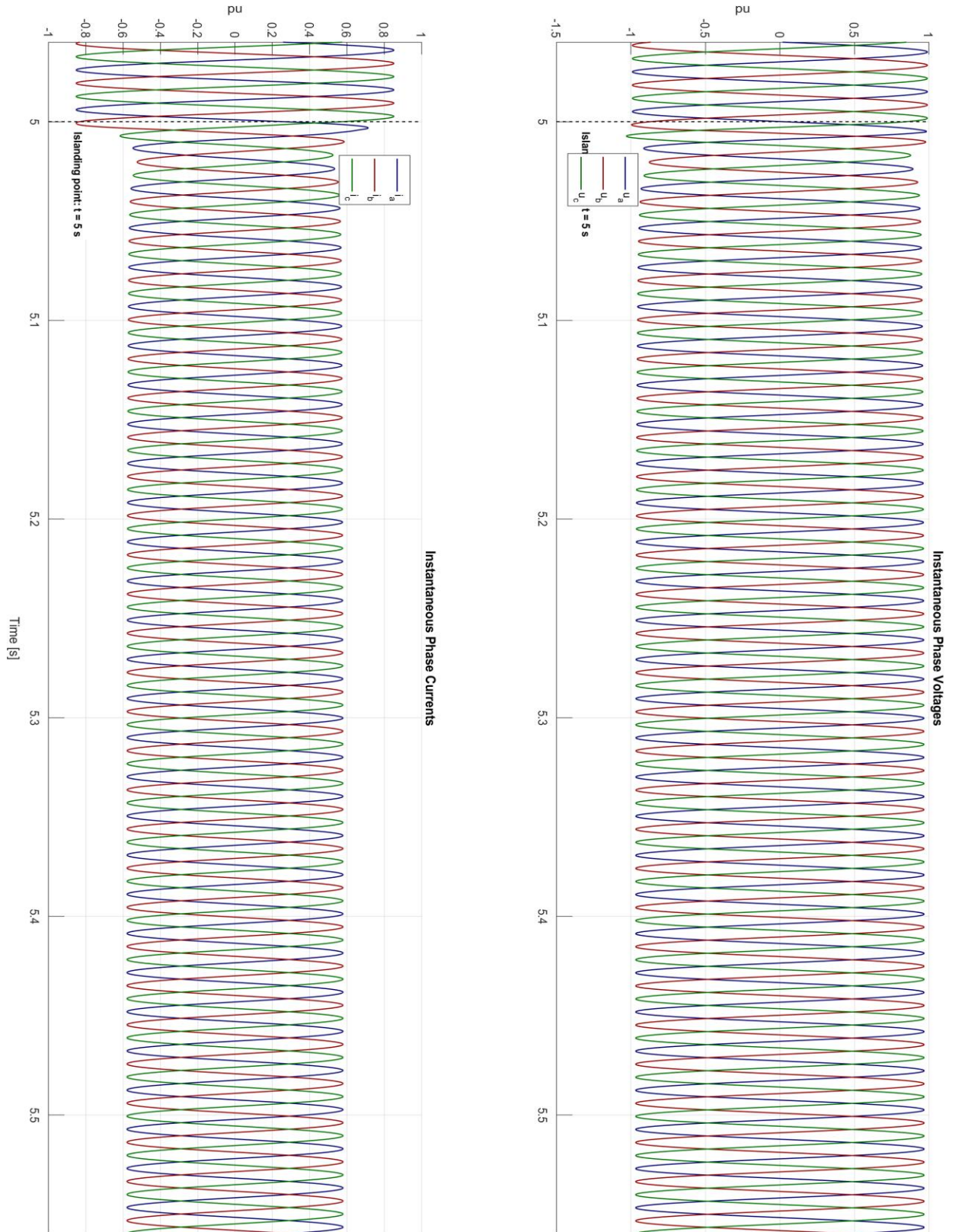
Appendix 13. Scenario Two - PCNB behaviour - Test 1.1 plot



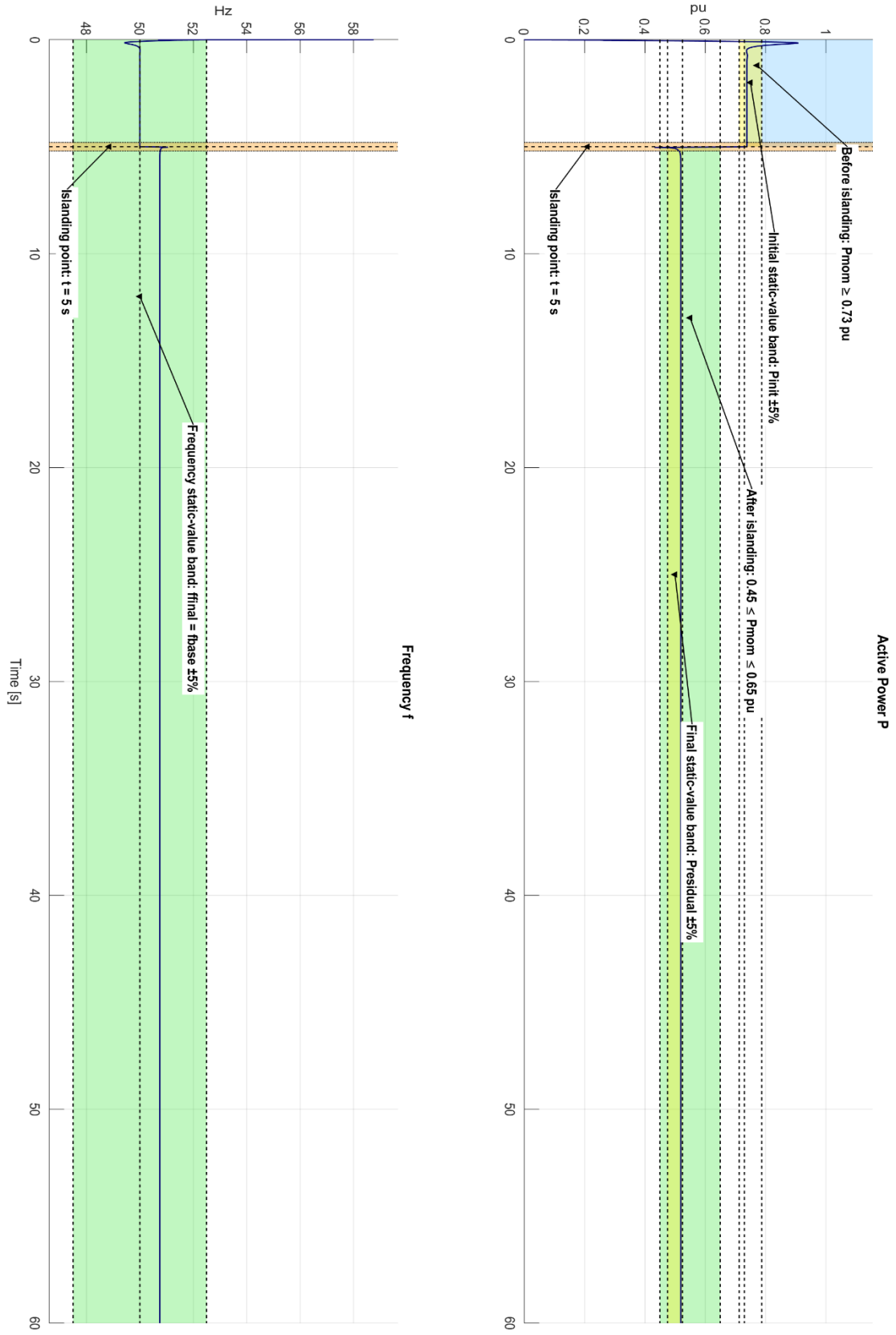
Appendix 14. Scenario Two - Voltage source behaviour - Test 1.2 plot



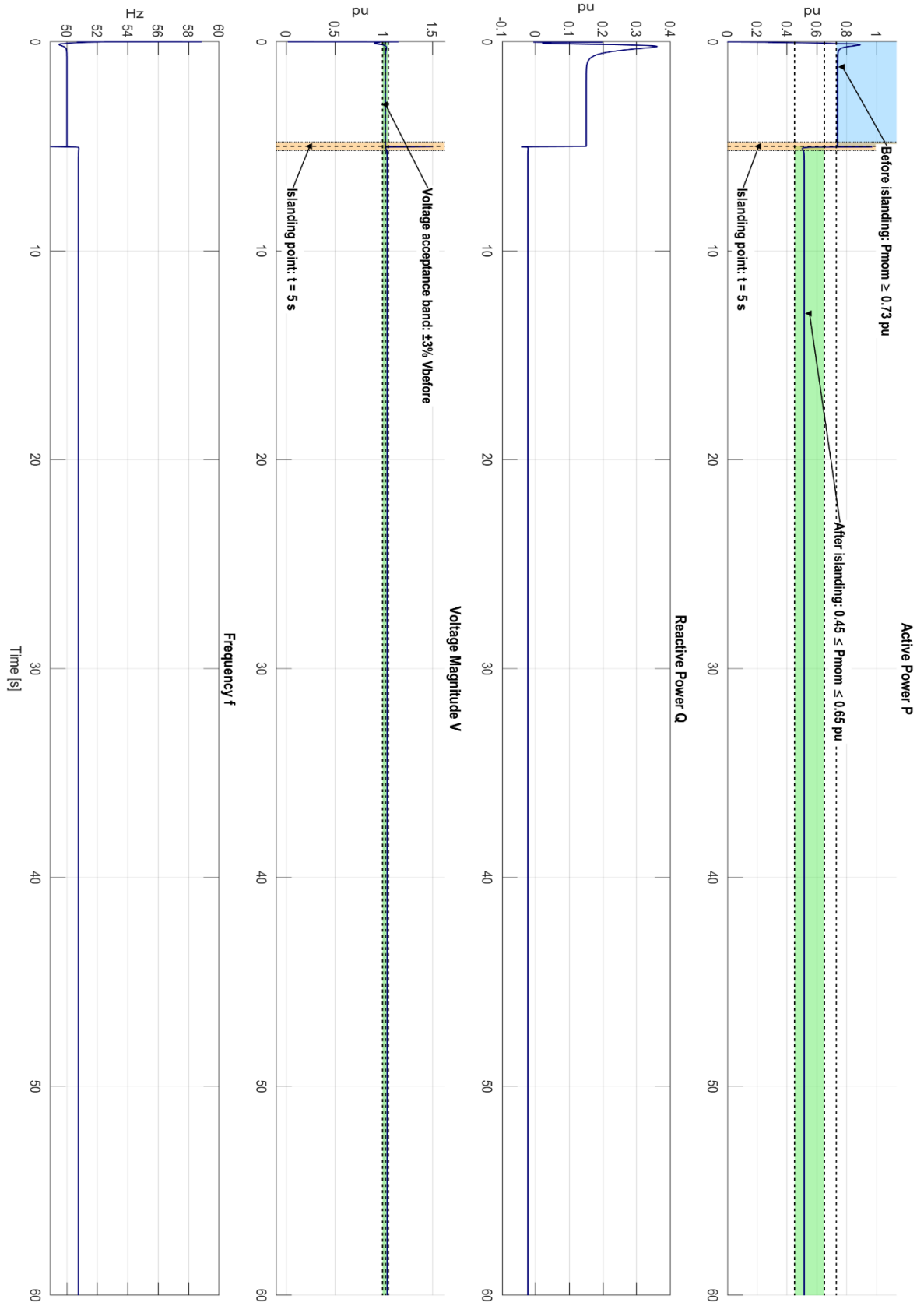
Appendix 15. Scenario Two - Instantaneous phase voltages and currents - Test 1.2 plot



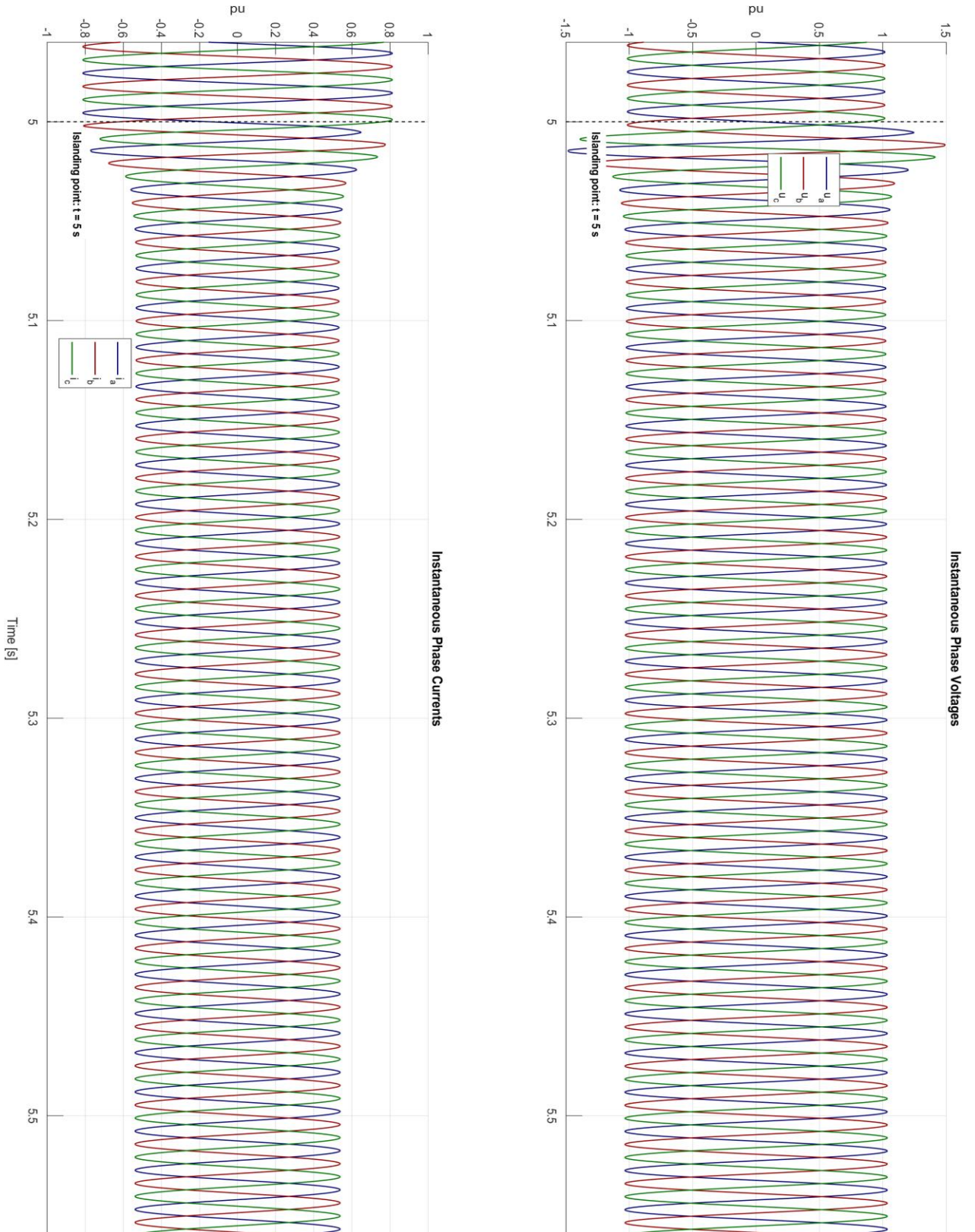
Appendix 16. Scenario Two - PCNB behaviour - Test 1.2 - active power and frequency plot



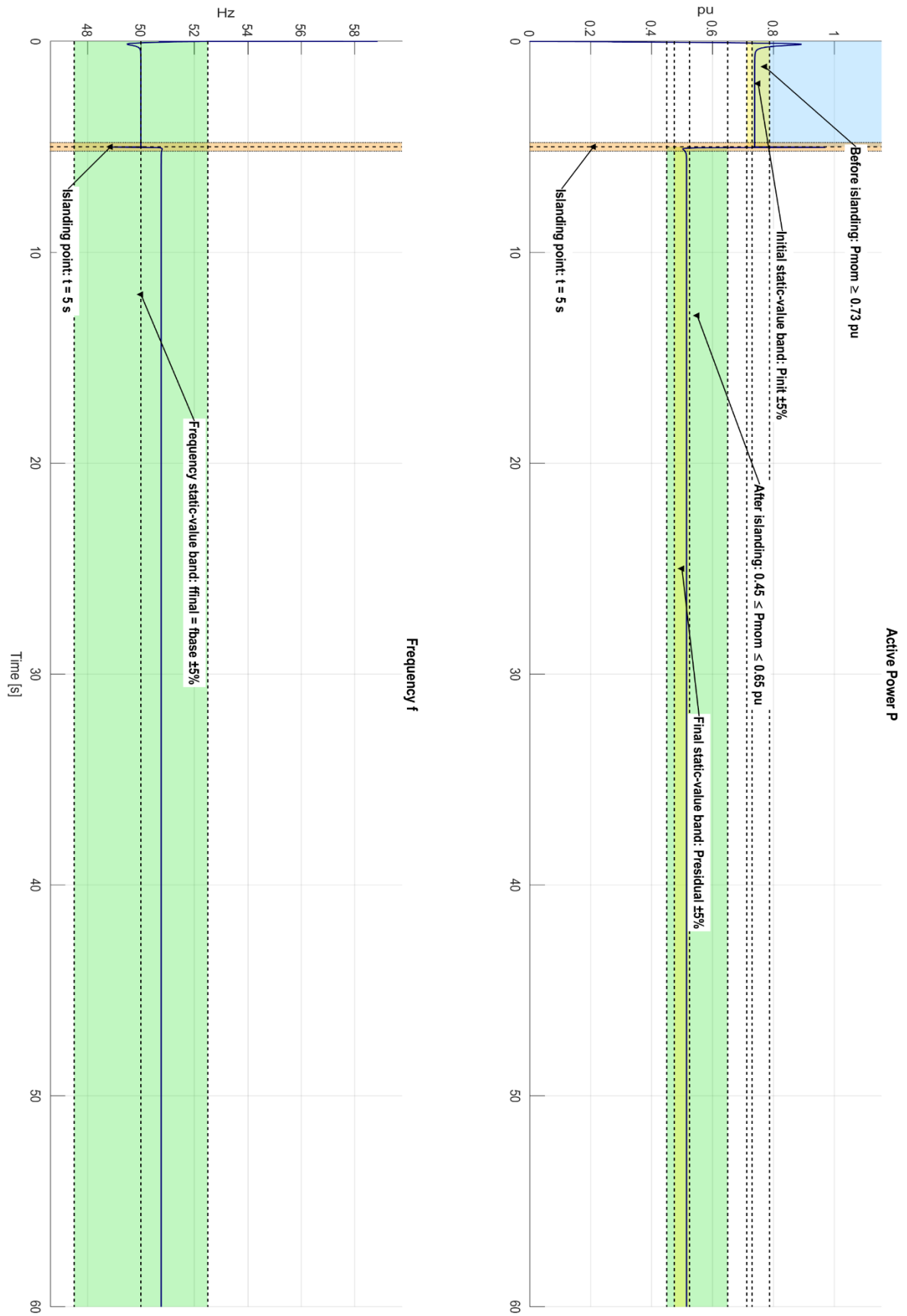
Appendix 17. Scenario Two - Voltage source behaviour - Test 1.3 plot



Appendix 18. Scenario Two - Instantaneous phase voltages and currents - Test 1.3 plot



Appendix 19. Scenario Two - PCNB behaviour - Test 1.3 plot



Appendix 20. main_run_all_tests

```

clear; clc; close all;

modelName = "testbed_overall";
addpath(genpath(pwd));

if ~exist("results", "dir"), mkdir("results"); end
if ~exist("reports", "dir"), mkdir("reports"); end
if ~exist("figures", "dir"), mkdir("figures"); end

run("config/define_FNN_tests.m");
load_system(modelName);

fprintf("\n=====
=====\\n");
fprintf("          AGIS - Automatic GFM Inverter Simulator\\n");
fprintf("=====
=====\\n");
fprintf("Hello, welcome to AGIS.\\n\\n");
fprintf("AGIS is an automated MATLAB/Simulink verification
program\\n");
fprintf("developed for the thesis project:\\n");
fprintf("  Grid Code Certification by Simulation for Grid-
Forming Connected Inverters\\n\\n");
fprintf("Student researcher: Boris YONDJIN NGAMY\\n");
fprintf("Supervisor: Assistant Professor Mustafa Alrayah
Hassan Ibraheem\\n");
fprintf("Institution: University of Vaasa\\n");
fprintf("-----
-----\\n");
fprintf("This program runs selected FNN validation simula-
tions, extracts\\n");

```

```

fprintf("the required measurements, evaluates compliance,
and generates\n");
fprintf("an HTML validation report with plots and quantita-
tive verdicts.\n");
fprintf("=====\n\n");

fprintf("Available verification modes:\n");
fprintf("1 Voltage source behaviour test (P, Q, V, f)\n");
fprintf("2 PCNB behaviour test (P, f)\n");
fprintf("3 All tests (Voltage +
PCNB)\n");

fprintf("\nSelect the simulation scenario:\n");
fprintf("1 Scenario One - Non-compliance baseline parame-
ters\n");
fprintf("2 Scenario Two - Compliance/tuned parame-
ters\n\n");
scenarioChoice = input("Which scenario do you want to simu-
late? Enter 1 or 2: ", "s");
scenarioChoice = strtrim(scenarioChoice);

if scenarioChoice == "1"
    FNN_scenario = "noncompliance";
    scenarioText = "Scenario One - Non-compliance baseline";
elseif scenarioChoice == "2"
    FNN_scenario = "compliance";
    scenarioText = "Scenario Two - Compliance/tuned config-
uration";
else
    error("Invalid scenario selection. Please enter 1 or
2.");
end

```

```

assignin('base','FNN_scenario',FNN_scenario);

fprintf("\nSelected scenario: %s\n", scenarioText);

familyChoice = input("Which verification do you want to run?
Enter 1, 2, or 3: ", "s");
familyChoice = strtrim(familyChoice);

if familyChoice == "1"
    selectedTestTypes = "voltage";
    measurementChoice = ask_measurement_choice();
    selectedTestIdx = measurement_choice_to_indices(meas-
urementChoice, length(tests));
elseif familyChoice == "2"
    selectedTestTypes = "pcnb";
    measurementChoice = ask_measurement_choice();
    selectedTestIdx = measurement_choice_to_indices(meas-
urementChoice, length(tests));
elseif familyChoice == "3"
    selectedTestTypes = ["voltage", "pcnb"];
    selectedTestIdx = 1:length(tests);
    measurementChoice = "4";
else
    error("Invalid selection. Please enter 1, 2, or 3.");
end

% IMPORTANT OPTIMISATION:
% Each Table 3 operating point is simulated only once.
% The same extracted signals are then reused to generate the
voltage-source
% and/or PCNB analyses.
allResults = struct([]);
r = 0;

```

```

fprintf("\n=====
=====\\n");
fprintf("Running selected simulations\\n");
fprintf("=====
=====\\n");

for idx = selectedTestIdx
    fprintf("\\nRunning simulation for %s: %s\\n",
tests(idx).id, tests(idx).name);

    testCase = tests(idx);
    [simOut, testCase] = run_single_test(modelName, test-
Case);

    Ppcc = simOut.get('Ppcc1');
    fdroop = simOut.get('fdroop');
    t = Ppcc.Time;
    P = Ppcc.Data;
    f = fdroop.Data;

    Q = [];
    V = [];
    Ua = []; Ub = []; Uc = [];
    Ia = []; Ib = []; Ic = [];
    t_abc = [];

    needQV = any(selectedTestTypes == "voltage");
    if needQV
        Qpcc = simOut.get('Qpcc1');
        vd1 = simOut.get('vd1');
        Q = Qpcc.Data;
        V = vd1.Data;

```

```

    % Optional instantaneous phase quantities required
    for the detailed

```

```

    % voltage-source measurement report. These To Work-
    space blocks should

```

```

    % be named Ua, Ub, Uc, Ia, Ib and Ic in the Simulink
    model.

```

```

    [Ua, t_abc] = try_get_timeseries(simOut, 'Ua');
    [Ub, ~]     = try_get_timeseries(simOut, 'Ub');
    [Uc, ~]     = try_get_timeseries(simOut, 'Uc');
    [Ia, ~]     = try_get_timeseries(simOut, 'Ia');
    [Ib, ~]     = try_get_timeseries(simOut, 'Ib');
    [Ic, ~]     = try_get_timeseries(simOut, 'Ic');

```

```

end

```

```

for testType = selectedTestTypes

```

```

    if testType == "voltage"

```

```

        metrics = extract_metrics(t, P, Q, V, f, test-
        Case.t_island, "voltage");

```

```

    else

```

```

        metrics = extract_metrics(t, P, [], [], f, test-
        Case.t_island, "pcnb");

```

```

    end

```

```

    verdict = fnn_evaluate_compliance(metrics, testCase,
    testType);

```

```

    r = r + 1;

```

```

    allResults(r).testType = testType;

```

```

    allResults(r).scenarioChoice = scenarioChoice;

```

```

    allResults(r).scenario = FNN_scenario;

```

```

    allResults(r).scenarioText = scenarioText;

```

```

    allResults(r).test = testCase;

```

```
allResults(r).metrics = metrics;
allResults(r).verdict = verdict;
allResults(r).t = t;
allResults(r).P = P;
allResults(r).Q = Q;
allResults(r).V = V;
allResults(r).f = f;
allResults(r).t_abc = t_abc;
allResults(r).Ua = Ua;
allResults(r).Ub = Ub;
allResults(r).Uc = Uc;
allResults(r).Ia = Ia;
allResults(r).Ib = Ib;
allResults(r).Ic = Ic;

fprintf("Analysis %-7s for %s: ", upper(testType),
testCase.id);
if verdict.overall
    fprintf("COMPLIANT\n");
else
    fprintf("NON-COMPLIANT\n");
end
end
end

save("results/all_FNN_results.mat", "allResults");

reportFile = generate_fnn_report(allResults, familyChoice,
measurementChoice, scenarioChoice);
fprintf("\nSelected FNN verification completed.\n");
fprintf("Report generated: %s\n", reportFile);

function choice = ask_measurement_choice()
```

```

fprintf("\nSelect the Table 3 measurement case:\n");
fprintf("1  Measurement 1.1 - Q = 0\n");
fprintf("2  Measurement 1.2 - Maximum inductive Q\n");
fprintf("3  Measurement 1.3 - Maximum capacitive Q\n");
fprintf("4  All measurements 1.1, 1.2 and 1.3\n\n");
choice = input("Which measurement case do you want to
run? Enter 1, 2, 3, or 4: ", "s");
choice = strtrim(choice);
end

```

```

function idx = measurement_choice_to_indices(choice, nTests)
    switch choice
        case "1"
            idx = 1;
        case "2"
            idx = 2;
        case "3"
            idx = 3;
        case "4"
            idx = 1:nTests;
        otherwise
            error("Invalid measurement selection. Please en-
ter 1, 2, 3, or 4.");
    end
end

```

```

function [data, time] = try_get_timeseries(simOut, varName)
%TRY_GET_TIMESERIES Safely read optional To Workspace out-
puts.
% The report can still be generated if the optional abc phase
signals are
% not present in the model.

```

```

data = [];
time = [];
try
    sig = simOut.get(varName);
    data = sig.Data;
    time = sig.Time;
catch
    warning("Optional signal '%s' was not found in si-
mOut. The instantaneous abc plot will be skipped.", varName);
end
end
end

```

Appendix 21. data

```

%% AGIS data file with two simulation scenarios
% Scenario 1: Non-compliance baseline
% Scenario 2: Compliance/tuned configuration
%
% The scenario is selected in main_run_all_tests.m and passed
through the
% base-workspace variable FNN_scenario. If the file is exe-
cuted manually
% without a scenario selection, the tuned compliance scenario
is used by default.

if ~exist('FNN_scenario','var')
    FNN_scenario = "compliance";
end

switch lower(string(FNN_scenario))
    case "noncompliance"
        % Scenario One: initial/non-compliant configuration
        P_ref = Pinit;

```

```

    Q_ref = Qinit;
    Pres  = 0.5;
    Pres1 = 0.5;
    Pres2 = 0.5;
    Pres3 = 0.5;

    case "compliance"
        % Scenario Two: tuned/compliant configuration veri-
fied by the user
        P_ref = 0.81;
        Q_ref = Qinit;
        Pres1 = 0.5183;
        Pres2 = 0.598;
        Pres3 = 0.52;

    otherwise
        error("Unknown FNN_scenario: %s. Use 'noncompliance'
or 'compliance'.", string(FNN_scenario));
    end

f = fbase;
Sb = 1e6; % base power
Vb_S = 13.2e3*sqrt(2)/sqrt(3); % secondary side base voltage
phase to ground
Ib_S = Sb/Vb_S; % secondary side base current
Vb_P = 400*sqrt(2)/sqrt(3); % primary side base V
Ib_P = Sb/Vb_P; % primary side base I
Zb = ((400)^2)/Sb; % primary side base impedance
Zs = ((13.2e3)^2)/Sb; % secondary side base impedance
Zt = 0.02+1i*0.0721; % transformer impedance
Vg = 1;
P = Pinit;
Q = Qinit;

```

```

S = P+1i*Q;
I3 = conj(S/Vg);
V3 = Vg+I3*Zt; % pcc voltage in S side
% Vpcc = V3*Vb_S/Vb_P; % P side
Vpcc = V3;
R1 = 0.001/Zb;
L1 = (1i*120*pi*46e-6)/Zb; % impedacne ZL1
C1 = -(1i/(120*pi*3*444e-6))/Zb; %impedance ZC1
I2 = Vpcc/C1; % curreent going through the Capcitor
I1 = I2+I3;
V1 = Vpcc+I1*(R1+L1);
V = V1*Vb_P;

%%%

Ts = 50e-6; s = tf('s');

%%%

f = fbase; w0 = 2*pi*f;vdc = 1000;
sb = 1e6;vn1 = 400;vn2 = 13.2e3;
vb1 = vn1*sqrt(2/3);
zb1 = vn1^2/sb;
zb2 = vn2^2/sb;
%%% passive
rfpu = 0.034;
rf = rfpu*zb1;

xfpu = 2*pi*50*(46e-6)/0.16; %0.1084;
lf = xfpu*zb1/w0;
cf = 444e-6*3;
%bc = 0.102; xcpcu = 1/bc;
%cf = 1/xcpcu/zb1/w0;
bc = w0*cf*zb1;

```

```

% grid
xgpu = 0.35;
lg = xgpu*zb2/w0;
rgpu = xgpu/10;
rg = rgpu*zb2;

%% grid impedance
xgrid_pu = 0.8; %0.2 pu is working 0.19 is not working
lg_real = xgrid_pu*zb2/w0;

rgrid_pu = xgrid_pu/10;
rg_real = rgrid_pu*zb2;

%%% controller
Pdroop1 = 0.02*w0;
Pdroop2 = 0.05*w0;

% Scenario-dependent voltage-control gains
switch lower(string(FNN_scenario))
    case "noncompliance"
        Kp_v = 0.4; Ki_v = 40; % GFL
        kpv = 0.4; kiv = 40; % GFM voltage loop
        K2 = 0.3; % Q-V droop gain
    case "compliance"
        Kp_v = 0.4; Ki_v = 40; % GFL
        kpv = 0.4; kiv = 40; % GFM voltage loop
        K2 = 0.10; % tuned Q-V droop gain
end

Kp_vq = 1; Ki_vq = 10; %GFM 3
Kp_P = 0.25; Ki_P = 25;
%Kp_P = 0.1; Ki_P = 10;

```

```

%kpvd = 3; kivd = 300;
k = 0.1;
%kpvd = 1*k; kivd = 100*k;
kpvd = 0.4; kivd = 40;
kpq = 0.2; kiq = 20;
% kpv = 0.25; kiv = 25;
% kpv = 1; kiv = 100;

ang_0 = 22*pi/180;

% Yazdani's GFM
%kp_v = 1; kiv = 100;
%Kp_v=1; Ki_v = 100;

%%%
%kpi = 0.4758;
%kii = 3.2655; % current control
kpi = 0.4758; kii = 3.2655; % current control

OL = (kpi+kii/s)/(rfpu+xfpu*s);
bw_in = bandwidth(feedback(OL, 1))/2/pi;

%%%
kp_PLL = 60; ki_PLL = 1400;
%kp_PLL = 30; ki_PLL = 600;

Gs_PLL = (kp_PLL/s+ki_PLL/s/s)/(1+kp_PLL/s+ki_PLL/s/s);
bw_PLL = bandwidth(Gs_PLL)/2/pi;

%%%%
Tc=3e-3;
Td=25e-6;

```

```
wn=2*pi*15;
f1=1;f2=30;fc=sqrt(f1*f2);
Q=fc/(f2-f1);
zeta=1/2/Q;
%% GFM claculation
SL = P+(Q)*1i;
Vpcc_gfm = 1;
I3_gfm = conj(SL/Vpcc_gfm);
Zb = 400^2/1e6;
XC1 = -(1i/(120*pi*3*444e-6))/Zb; %impedance ZC1
I2_gfm = Vpcc_gfm/XC1;
I1_gfm = I2_gfm + I3_gfm;
Spcc = Vpcc_gfm*conj(I1_gfm);
real(Spcc);
1-real(Spcc);

R = 0.05;

Tc=1e-3;
Td=25e-6;
K1 = 1/0.05;
% K2 is scenario-dependent and is defined above.
```

Appendix 22. define_FNN_test

```
%% Definition of FNN automated test cases: Table 3, Measure-
ments 1.1 to 1.3
```

```
common.Presidual = 0.50;
common.PEmax = 1.0;
common.fbase = 50;
common.t_island = 5;
common.Vnom = 1.0;
% For voltage-source behaviour (Section 5.5.3.6.2.2.3),
% the steady-state voltage after islanding is checked within
+/-3%
% relative to the pre-islanding steady-state voltage, using
Vnom as base.
common.VfinalMin = 0.90; % kept only for backward compati-
bility; not used for voltage-source verdict
common.VfinalMax = 1.10; % kept only for backward compati-
bility; not used for voltage-source verdict
common.maxFinalFreqDeviationHz = 2.0;

tests(1).id = "FNN_1_1";
tests(1).name = "Test 1.1 - Q = 0";
tests(1).Pinit = 0.75;
tests(1).Qinit = 0;
tests(1).PresVar = "Pres1"; % Simulink residual-load tuning
value from config/data.m

tests(2).id = "FNN_1_2";
tests(2).name = "Test 1.2 - Maximum inductive Q";
tests(2).Pinit = 0.75;
tests(2).Qinit = -0.33;
```

```
tests(2).PresVar = "Pres2"; % Simulink residual-load tuning
value from config/data.m
```

```
tests(3).id = "FNN_1_3";
tests(3).name = "Test 1.3 - Maximum capacitive Q";
tests(3).Pinit = 0.75;
tests(3).Qinit = 0.33;
tests(3).PresVar = "Pres3"; % Simulink residual-load tuning
value from config/data.m
```

```
for k = 1:length(tests)
    tests(k).Presidual = common.Presidual;
    tests(k).PEmax = common.PEmax;
    tests(k).fbase = common.fbase;
    tests(k).t_island = common.t_island;
    tests(k).Vnom = common.Vnom;
    tests(k).VfinalMin = common.VfinalMin;
    tests(k).VfinalMax = common.VfinalMax;
    tests(k).maxFinalFreqDeviationHz = common.maxFinal-
FreqDeviationHz;

    % Default Simulink load factor. The final value is re-
solved in
    % run_single_test.m from Pres1, Pres2 or Pres3 defined
in config/data.m.
    % The compliance target remains test.Presidual = 0.50
pu.
    tests(k).Pres = common.Presidual;
end
```

Appendix 23. run_single_test

```

function [simOut, test] = run_single_test(modelName, test)
%RUN_SINGLE_TEST Configure one Table 3 operating point and
run the Simulink model.
%
% The FNN compliance target for the residual load remains
test.Presidual
% (typically 0.50 pu). However, the actual Simulink load
block may use a
% tuned factor Pres so that the final active-power settling
point is within
% the +/-5% PCNB static-value band. The 500 kW residual-load
block should be
% parametrised as: Pres*Sb.
%
% For Table 3 cases, Pres is resolved from config/data.m as:
%   FNN_1_1 -> Pres1
%   FNN_1_2 -> Pres2
%   FNN_1_3 -> Pres3

Pinit      = test.Pinit;
Qinit      = test.Qinit;
Presidual  = test.Presidual;
PEmax      = test.PEmax;
fbase      = test.fbase;
w0         = 2*pi*fbase;

assignin('base','Pinit',Pinit);
assignin('base','Qinit',Qinit);
assignin('base','Presidual',Presidual);
assignin('base','PEmax',PEmax);
assignin('base','fbase',fbase);

```

```

assignin('base','w0',w0);

% Load model parameters for the selected scenario. The
scenario is
% controlled by the base-workspace variable FNN_scenario,
set in
% main_run_all_tests.m. The data file then defines Pres1,
Pres2 and Pres3.
if ~evalin('base','exist(''FNN_scenario'', 'var''))
    assignin('base','FNN_scenario',"compliance");
end
evalin('base','run("config/data.m")');
scenarioUsed = evalin('base','FNN_scenario');
test.scenario = scenarioUsed;

% Store the effective scenario-dependent parameters in
the test structure
% so that the report can clearly distinguish between
P_ref and Pinit, and
% show the tuning used for the selected scenario.
if evalin('base','exist(''P_ref'', 'var''))
    test.Pref = evalin('base','P_ref');
end
if evalin('base','exist(''Q_ref'', 'var''))
    test.Qref = evalin('base','Q_ref');
end
if evalin('base','exist(''K2'', 'var''))
    test.K2 = evalin('base','K2');
end
if evalin('base','exist(''kp_v'', 'var''))
    test.kp_v = evalin('base','kp_v');
end
if evalin('base','exist(''kiv'', 'var''))

```

```

        test.kiv = evalin('base','kiv');
    end

    % Resolve the Simulink residual-load factor for the se-
    lected Table 3 case.
    % This is the value used by the block parameter Pres*Sb.
    Pres = Presidual;
    if      isfield(test,      'PresVar')      &&
    strlength(string(test.PresVar)) > 0
        presVarName = char(test.PresVar);
        if evalin('base', sprintf('exist('%s', 'var'),'
presVarName))
            Pres = evalin('base', presVarName);
        else
            warning('Residual-load tuning variable %s was
not found in config/data.m. Using Presidual = %.4f pu in-
stead.', presVarName, Presidual);
        end
    elseif isfield(test, 'Pres')
        Pres = test.Pres;
    end

    assignin('base','Pres',Pres);
    test.Pres = Pres;

    fprintf(' Scenario = %s\n', char(string(scenarioUsed)));
    fprintf(' Compliance residual target Presidual = %.5f
pu\n', Presidual);
    fprintf(' Simulink residual-load factor Pres = %.5f pu,
used in load block as Pres*Sb\n', Pres);

    t_stop = 60;

```

```
simOut = sim(modelName, ...
    'StopTime', num2str(t_stop), ...
    'ReturnWorkspaceOutputs', 'on');
end
```

Appendix 24. extract_metrics

```
function metrics = extract_metrics(t, P, Q, V, f, t_island,
testType)
%EXTRACT_METRICS Extract FNN report values for voltage or
PCNB tests.
% Voltage-source behaviour uses P, Q, V and f.
% PCNB behaviour uses only P and f.

    if nargin < 7
        testType = "voltage";
    end

    t = t(:); P = P(:); f = f(:);
    if ~isempty(Q), Q = Q(:); end
    if ~isempty(V), V = V(:); end
```

```

preWindow    = t > (t_island - 1.0) & t < (t_island -
0.1);
postWindow   = t > t_island;
finalWindow  = t > (max(t) - 5.0);

if ~any(preWindow),    error("Pre-islanding window is
empty. Check t_island or simulation time."); end
if ~any(postWindow),  error("Post-islanding window is
empty. Check t_island or simulation time."); end
if ~any(finalWindow), error("Final steady-state window
is empty. Check simulation stop time."); end

metrics.testType = testType;

metrics.P_before = mean(P(preWindow), 'omitnan');
metrics.P_max    = max(P(postWindow), [], 'omitnan');
metrics.P_min    = min(P(postWindow), [], 'omitnan');
metrics.P_final  = mean(P(finalWindow), 'omitnan');

metrics.f_before = mean(f(preWindow), 'omitnan');
metrics.f_max    = max(f(postWindow), [], 'omitnan');
metrics.f_min    = min(f(postWindow), [], 'omitnan');
metrics.f_final  = mean(f(finalWindow), 'omitnan');

metrics.dP_max   = metrics.P_max   - metrics.P_before;
metrics.dP_min   = metrics.P_min   - metrics.P_before;
metrics.dP_final = metrics.P_final - metrics.P_before;

metrics.df_max   = metrics.f_max   - metrics.f_before;
metrics.df_min   = metrics.f_min   - metrics.f_before;
metrics.df_final = metrics.f_final - metrics.f_before;

if strcmpi(testType, "voltage")

```

```

if isempty(Q) || isempty(V)
    error("Voltage behaviour test requires Q and V
signals.");
end

metrics.Q_before = mean(Q(preWindow), 'omitnan');
metrics.Q_max    = max(Q(postWindow), [], 'omitnan');
metrics.Q_min    = min(Q(postWindow), [], 'omitnan');
metrics.Q_final  = mean(Q(finalWindow), 'omitnan');

metrics.V_before = mean(V(preWindow), 'omitnan');
metrics.V_max    = max(V(postWindow), [], 'omitnan');
metrics.V_min    = min(V(postWindow), [], 'omitnan');
metrics.V_final  = mean(V(finalWindow), 'omitnan');

metrics.dQ_max   = metrics.Q_max   - metrics.Q_be-
fore;
metrics.dQ_min   = metrics.Q_min   - metrics.Q_be-
fore;
metrics.dQ_final = metrics.Q_final - metrics.Q_be-
fore;

metrics.dV_max   = metrics.V_max   - metrics.V_be-
fore;
metrics.dV_min   = metrics.V_min   - metrics.V_be-
fore;
metrics.dV_final = metrics.V_final - metrics.V_be-
fore;
end
end

```

Appendix 25. fnn_evaluate_compliance

```

function verdict = fnn_evaluate_compliance(metrics, testCase,
testType)
%FNN_EVALUATE_COMPLIANCE Quantitative checks for FNN Table
3 tests.
%
% Important distinction used in this version:
% - Table 3 entry conditions are checked for illustration
and traceability
% (Pmom before islanding and residual-load range).
% - For voltage-source behaviour according to Section
5.5.3.6.2.2.3,
% the main quantitative requirement is the steady-state
voltage after
% transition to island operation: V_final must remain
within +/-3% of the
% pre-islanding steady-state voltage, using nominal volt-
age as base.
% - For PCNB according to Section 5.5.3.6.2.2.5, the static
% value check is applied to both active power and frequency.
Active power
% is compared with the Presidual target, and frequency is
compared with
% the configured frequency setpoint fbase, both with +/-
5% tolerance.

    if nargin < 3
        testType = "voltage";
    end

    tol5 = 0.05;
    tol3V = 0.03;

```

```

verdict.testType = testType;

if isfield(testCase, "Vnom")
    Vnom = testCase.Vnom;
else
    Vnom = 1.0;
end
verdict.Vnom = Vnom;

%% Table 3 entry conditions
verdict.Pmom_required = testCase.Presidual + 0.23*test-
Case.PEmax;
verdict.Pmom_ok = metrics.P_before >= verdict.Pmom_re-
quired;

verdict.residual_load_lower = 0.45*testCase.PEmax;
verdict.residual_load_upper = 0.65*testCase.PEmax;
verdict.residual_load_ok = testCase.Presidual >= ver-
dict.residual_load_lower && ...
                                testCase.Presidual <= ver-
dict.residual_load_upper;

verdict.frequency_finite_ok = isfinite(metrics.f_before)
&& isfinite(metrics.f_final) && ...
                                isfinite(metrics.f_min)
&& isfinite(metrics.f_max);
verdict.power_finite_ok = isfinite(metrics.P_before) &&
isfinite(metrics.P_final) && ...
                                isfinite(metrics.P_min) &&
isfinite(metrics.P_max);

if strcmpi(testType, "voltage")
    %% Section 5.5.3.6.2.2.3: voltage-source behaviour

```

```

    % The automated report does NOT use a +/-5% active-
power final-value
    % check for voltage-source behaviour. P is still
plotted/measured, but
    % the main quantitative voltage-source requirement
is the +/-3% final
    % steady-state voltage band.
    verdict.reactive_finite_ok = isfinite(metrics.Q_be-
fore) && isfinite(metrics.Q_final) && ...
                                isfinite(metrics.Q_min)
&& isfinite(metrics.Q_max);
    verdict.voltage_finite_ok = isfinite(metrics.V_be-
fore) && isfinite(metrics.V_final) && ...
                                isfinite(metrics.V_min)
&& isfinite(metrics.V_max);

    verdict.voltage_tolerance = tol3V*Vnom;
    verdict.voltage_lower = metrics.V_before - ver-
dict.voltage_tolerance;
    verdict.voltage_upper = metrics.V_before + ver-
dict.voltage_tolerance;
    verdict.final_V_error = metrics.V_final - met-
rics.V_before;
    verdict.final_V_ok = metrics.V_final >= ver-
dict.voltage_lower && ...
                                metrics.V_final <= ver-
dict.voltage_upper;

    verdict.req_5_5_3_6_2_2_3_ok = verdict.final_V_ok
&& ...
                                verdict.voltage_fi-
nite_ok && ...

```

```

verdict.reac-
tive_finite_ok;

    % Final verdict: Table 3 entry conditions + voltage-
    source main requirement.
    verdict.overall = verdict.Pmom_ok && verdict.resid-
    ual_load_ok && ...
                                verdict.req_5_5_3_6_2_2_3_ok;
else
    %% Section 5.5.3.6.2.2.5: PCNB behaviour
    verdict.final_P_tolerance = tol5*max(abs(test-
    Case.Presidual), eps);
    verdict.final_P_error = metrics.P_final - test-
    Case.Presidual;
    verdict.final_P_lower = testCase.Presidual - ver-
    dict.final_P_tolerance;
    verdict.final_P_upper = testCase.Presidual + ver-
    dict.final_P_tolerance;
    verdict.final_P_ok = abs(verdict.final_P_error) <=
    verdict.final_P_tolerance;

    verdict.final_f_tolerance = tol5*max(abs(test-
    Case.fbase), eps);
    verdict.final_f_error = metrics.f_final - test-
    Case.fbase;
    verdict.final_f_lower = testCase.fbase - verdict.fi-
    nal_f_tolerance;
    verdict.final_f_upper = testCase.fbase + verdict.fi-
    nal_f_tolerance;
    verdict.final_f_ok = abs(verdict.final_f_error) <=
    verdict.final_f_tolerance;

```

```

        verdict.initial_P_tolerance = tol5*max(abs(test-
Case.Pinit), eps);
        verdict.initial_P_error = metrics.P_before - test-
Case.Pinit;
        verdict.initial_P_ok = abs(verdict.initial_P_error)
<= verdict.initial_P_tolerance;

        verdict.initial_f_tolerance = tol5*max(abs(test-
Case.fbase), eps);
        verdict.initial_f_error = metrics.f_before - test-
Case.fbase;
        verdict.initial_f_ok = abs(verdict.initial_f_error)
<= verdict.initial_f_tolerance;

        verdict.stable_ok = verdict.frequency_finite_ok &&
verdict.power_finite_ok && ...
                                abs(metrics.f_final - test-
Case.fbase) < testCase.maxFinalFreqDeviationHz;

        verdict.droop_static_ok = verdict.final_P_ok && ver-
dict.final_f_ok;

        if metrics.f_final > metrics.f_before
            verdict.pcnb_direction_ok = metrics.P_final <
metrics.P_before;
        elseif metrics.f_final < metrics.f_before
            verdict.pcnb_direction_ok = metrics.P_final >
metrics.P_before;
        else
            verdict.pcnb_direction_ok = abs(metrics.P_final
- metrics.P_before) < verdict.final_P_tolerance;
        end

```

```
        verdict.req_5_5_3_6_2_2_5_ok = verdict.initial_P_ok
&& verdict.initial_f_ok && verdict.droop_static_ok && ...
                                verdict.pcnb_direc-
tion_ok && verdict.stable_ok;

        verdict.overall = verdict.Pmom_ok && verdict.resid-
ual_load_ok && ...
                                verdict.req_5_5_3_6_2_2_5_ok;
    end
end
```

Appendix 26. generate_report

```
function generate_report(test, testType, metrics, verdict,
t, P, Q, V, f)
%GENERATE_REPORT Legacy compatibility wrapper.
% The updated workflow uses generate_fnn_report.m to create
one combined
% report. This wrapper is kept only in case an older script
still calls it.

    if nargin < 9, f = []; end
    if nargin < 8, V = []; end
    if nargin < 7, Q = []; end

    R.test = test;
    R.testType = testType;
    R.metrics = metrics;
    R.verdict = verdict;
    R.t = t;
    R.P = P;
    R.Q = Q;
    R.V = V;
    R.f = f;

    generate_fnn_report(R, "", "");
end
```

Appendix 27. generate_fnn_report

```

function reportFile = generate_fnn_report(allResults, fami-
lyChoice, measurementChoice, scenarioChoice)
%GENERATE_FNN_REPORT Generate one structured HTML report for
the selected analyses.
% This function intentionally creates a single report, even
when several
% Table 3 measurements and/or both verification families are
selected.

    if nargin < 2, familyChoice = ""; end
    if nargin < 3, measurementChoice = ""; end
    if nargin < 4, scenarioChoice = ""; end

    timestamp = datestr(now, 'yyyymmdd_HHMMSS');
    reportTitle = "Validation Test Report for GFM Inverters
Simulation Model";

    if string(familyChoice) == "1"
        reportBase = "voltage_source_behaviour";
    elseif string(familyChoice) == "2"
        reportBase = "pcnb_behaviour";
    elseif string(familyChoice) == "3"
        reportBase = "complete_fnn_verification";
    else
        reportBase = "fnn_verification";
    end

    reportFile = fullfile("reports", reportBase + "_" +
timestamp + ".html");
    fid = fopen(reportFile, 'w');
    if fid < 0

```

```

        error("Could not create report file: %s", report-
File);
    end

```

```

    guidelineLink          =          'https://www.vde.com/re-
source/blob/2405504/cd87a82107a12d014626e497e4d77a1d/fnn-
guideline---technical-requirements-for-grid-forming-cap-
abilities--october-2025--data.pdf';

```

```

    fprintf(fid, '<html><head><meta charset="UTF-8"><ti-
tle>%s</title>', reportTitle);

```

```

    fprintf(fid, ['<style>' ...

```

```

        'body{font-family:Arial,Helvetica,sans-serif;mar-
gin:35px;line-height:1.45;color:#222;}' ...

```

```

        'h1,h2,h3{color:#222;} h1{font-size:30px;} h2{mar-
gin-top:28px;border-bottom:2px solid #444;padding-bot-
tom:5px;}' ...

```

```

        'table{border-collapse:collapse;margin:12px 0 20px
0;} th,td{border:1px solid #777;padding:6px 10px;text-
align:right;}' ...

```

```

        'th:first-child,td:first-child{text-align:left;}
th{background:#eee;} .ok{color:green;font-
weight:bold;} .fail{color:red;font-weight:bold;}' ...

```

```

        '.note{background:#f6f6f6;padding:12px;border-
left:4px solid #777;margin:14px 0;}' ...

```

```

        '.case{border-top:3px solid #444;margin-
top:32px;padding-top:12px;}' ...

```

```

        '.stamp{display:inline-block;padding:16px 28px;mar-
gin:12px 0 20px 0;border:4px solid;font-weight:bold;font-
size:22px;letter-spacing:1px;transform:rotate(-3deg);}' ...

```

```

        '.stamp.okstamp{color:green;border-
color:green;background:
ground:#f2fff2;}.stamp.failstamp{color:red;border-
color:red;background:#fff2f2;}' ...

        '.signature{margin-top:40px;border-top:3px    solid
#444;padding-top:15px;font-size:13px;back-
ground:#f8f8f8;padding:15px;}' ...

        'a{color:#005bb5;text-decoration:none;}
a:hover{text-decoration:underline;} ul{margin-top:6px;}' ...

        '</style>']]);
fprintf(fid, '</head><body>');

%% Title and programme presentation
fprintf(fid, '<h1>%s</h1>', reportTitle);
fprintf(fid, ['<p class="note">This report is an auto-
matically generated output of <b>AGIS</b> ' ...

        '(Automatic GFM Inverter Simulator</i>), a
MATLAB/Simulink-based verification programme developed dur-
ing the thesis research project ' ...

        '<b>"Grid Code Certification by Simulation for Grid-
Forming Connected Inverters"</b> at the University of Vaasa.
' ...

        'The work was conducted by <b>Boris YONDJIN
NGAMY</b>, an Erasmus student in the SMACCs programme, under
the supervision of ' ...

        'Assistant Professor <b>Mustafa Alrayah Hassan Ib-
raheem</b>. The simulation tests documented in this report
follow the verification logic of the ' ...

        '<a href="%s#page=57">VDE FNN Guideline, Section
5.5.3.6.2</a>, which defines validation requirements for EMT
simulation models of grid-forming units.</p>'], guide-
lineLink);

```

```
fprintf(fid, '<p class="note"><b>Simulation optimisa-
tion:</b> each selected Table 3 operating point is simulated
only once. The extracted signals are then reused for the
selected analyses. For voltage-source behaviour, P, Q, V and
f are evaluated. For PCNB behaviour, only P and f are eval-
uated.</p>');
```

```
%% Summary of scope
```

```
fprintf(fid, '<h2>1. Summary of Selected Verification
Scope</h2>');
```

```
fprintf(fid, '
                                <table><tr><th>Item</th><th>Value</th></tr>');
```

```
fprintf(fid, '
                                <tr><td>Simulation          sce-
nario</td><td>%s</td></tr>', scenario_text(scenarioChoice));
```

```
fprintf(fid, '
                                <tr><td>Main              selec-
tion</td><td>%s</td></tr>', selection_text(familyChoice));
```

```
fprintf(fid, '
                                <tr><td>Measurement        selec-
tion</td><td>%s</td></tr>', measurement_text(measure-
mentChoice));
```

```
fprintf(fid, '
                                <tr><td>Number of analyses in this re-
port</td><td>%d</td></tr>', length(allResults));
```

```
fprintf(fid, '</table>');
```

```
write_scope_introduction(fid, familyChoice, scenario-
Choice, guidelineLink);
```

```
%% Compliance summary and global verdict stamp
```

```
fprintf(fid, '<h2>2. Overall Compliance Summary</h2>');
```

```
fprintf(fid, '
                                <table><tr><th>Verification</th><th>Meas-
urement</th><th>Pmom          check</th><th>Residual
load</th><th>Main          requirement</th><th>Final          ver-
dict</th></tr>');
```

```
globalOk = true;
```

```

for k = 1:length(allResults)
    R = allResults(k);
    fprintf(fid, '<tr>');
    fprintf(fid, '    <td>%s</td>', test_type_title(R.testType));
    fprintf(fid, '    <td>%s</td>', R.test.id);
    fprintf(fid, '    <td>%s</td>', ok_text(R.verdict.Pmom_ok));
    fprintf(fid, '    <td>%s</td>', ok_text(R.verdict.residual_load_ok));
    if string(R.testType) == "voltage"
        mainOk = R.verdict.req_5_5_3_6_2_2_3_ok;
    else
        mainOk = R.verdict.req_5_5_3_6_2_2_5_ok;
    end
    fprintf(fid, '    <td>%s</td>', ok_text(mainOk));
    fprintf(fid, '    <td>%s</td>', ok_text(R.verdict.overall));
    fprintf(fid, '</tr>');
    globalOk = globalOk && R.verdict.Pmom_ok && R.verdict.residual_load_ok && mainOk && R.verdict.overall;
end
fprintf(fid, '</table>');
if globalOk
    fprintf(fid, '    <div class="stamp okstamp">COMPLIANT</div>');
else
    fprintf(fid, '    <div class="stamp failstamp">NON-COMPLIANT</div>');
end
fprintf(fid, '    <p>The stamp above is calculated from the verification results in the summary table. It is not determined by the selected scenario name; therefore, if any check

```

returns **FAIL**, the report-level verdict becomes **NON-COMPLIANT**.</p>');</div>

```
%% Detailed results
```

```
fprintf(fid, '<h2>3. Detailed Results</h2>');
```

```
if string(measurementChoice) == "4"
```

```
    fprintf(fid, ['<p class="note">This report includes
measurements 1.1, 1.2 and 1.3 from ' ...
```

```
        '<a href="%s#page=73">Table 3 of the VDE FNN
Guideline</a>. Measurement 1.4 and measurement 2.1 are not
executed in this automation framework. ' ...
```

```
        'Measurement 1.4 is mainly relevant to active-
power reversal conditions, typically applicable to units
that can operate both as generation and load, such as storage
systems. ' ...
```

```
        'Measurement 2.1 concerns the small-signal be-
haviour in the non-procured direction of inertia. The pre-
sent Simulink testbed and thesis scope focus on the procured-
direction virtual-island tests 1.1 to 1.3.</p>'], guide-
lineLink);
```

```
    end
```

```
    fprintf(fid, ['<p>The simulation stop time is set to
<b>60 s</b>. Since islanding is applied at <b>t = 5 s</b>,
this duration provides sufficient time to observe the pre-
islanding steady state, ' ...
```

```
        'the transient response immediately after islanding,
and the final steady-state values computed over the last
part of the simulation window.</p>']);
```

```
for k = 1:length(allResults)
```

```
    R = allResults(k);
```

```
    fprintf(fid, '<div class="case">');
```

```

        fprintf(fid, '<h3>%s - %s</h3>', test_type_title(R.testType), R.test.name);
        write_case_explanation(fid, R, guidelineLink);

        write_configuration(fid, R.test);

        if string(R.testType) == "voltage"
            fprintf(fid, '<h4>Extracted measurements: P, Q, V and f</h4>');
            write_measurement_table(fid, ["P" "Q" "V" "f"], R.metrics);
            fprintf(fid, '<h4>Deviations from the initial steady state</h4>');
            write_deviation_table(fid, ["P" "Q" "V" "f"], R.metrics);
            write_voltage_analysis(fid, R.metrics, R.verdict, guidelineLink);
        else
            fprintf(fid, '<h4>Extracted measurements: P and f only</h4>');
            write_measurement_table(fid, ["P" "f"], R.metrics);
            fprintf(fid, '<h4>Deviations from the initial steady state</h4>');
            write_deviation_table(fid, ["P" "f"], R.metrics);
            write_pcnb_analysis(fid, R.metrics, R.verdict, guidelineLink);
        end

        fprintf(fid, '<h4>Final verdict</h4>');
        if R.verdict.overall
            fprintf(fid, '<p class="ok">COMPLIANT</p>');

```

```

else
    fprintf(fid, '<p class="fail">NON-COMPLI-
ANT</p>');
end

plotFile = save_result_plot(R);
fprintf(fid, '<h4>Plot</h4>');
fprintf(fid, '', strrep(plotFile, '\\',
'/'));

if string(R.testType) == "voltage" && has_instanta-
neous_phase_signals(R)
    instPlotFile = save_instantaneous_phase_plot(R);
    fprintf(fid, '<h4>Instantaneous phase quanti-
ties</h4>');
    fprintf(fid, ['<p>In accordance with <a
href="%s#page=76">Section 5.5.4.5.1</a>, the instantaneous
phase voltages ' ...
        'u<sub>a</sub>, u<sub>b</sub>, u<sub>c</sub>
and phase currents i<sub>a</sub>, i<sub>b</sub>,
i<sub>c</sub> are displayed over a zoomed window around the
islanding instant. ' ...
        'For a 50 Hz network, one period is 0.02 s;
therefore, the plot starts two network periods before is-
landing and covers 30 network periods in total.</p>'], guide-
lineLink);
    fprintf(fid, '',
strrep(instPlotFile, '\\', '/'));
elseif string(R.testType) == "voltage"

```

```

        fprintf(fid, ['<p class="note"><b>Instantaneous
phase quantities not plotted:</b> the optional To Workspace
outputs ' ...

```

```

                '<code>Ua</code>',          <code>Ub</code>,
<code>Uc</code>',    <code>Ia</code>',    <code>Ib</code>' and
<code>Ic</code>' were not all available in the simulation
output.</p>']]);

```

```

        end

```

```

        fprintf(fid, '</div>');

```

```

    end

```

```

    write_signature(fid);

```

```

    fprintf(fid, '</body></html>');

```

```

    fclose(fid);

```

```

end

```

```

function write_scope_introduction(fid, familyChoice, sce-
narioChoice, guidelineLink)

```

```

    fprintf(fid, '<h3>Introduction to the selected scenario
and verification scope</h3>');

```

```

    if string(scenarioChoice) == "1"

```

```

        fprintf(fid, ['<p><b>Scenario One</b> represents the
baseline non-compliance scenario. It uses the initial/de-
fault control configuration of the model: ' ...

```

```

                '<code>P_ref = 0</code>', <code>Q_ref = 0</code>,
<code>Pres = Pres1 = Pres2 = Pres3 = 0.5 pu</code>', <code>K2
= 0.3</code>', <code>kpv = 0.4</code>', and <code>kiv =
40</code>.' ...

```

```

                'This scenario is intended to illustrate how the
model behaves before the tuning required to satisfy the ver-
ification criteria.</p>']]);

```

```

elseif string(scenarioChoice) == "2"
    fprintf(fid, ['<p><b>Scenario Two</b> represents the
tuned compliance scenario. Compared with the baseline, the
model uses the verified tuning values ' ...
        '<code>P_ref = 0.81</code>, <code>Q_ref =
Qinit</code>, <code>Pres1 = 0.5183</code>, <code>Pres2 =
0.598</code>, <code>Pres3 = 0.52</code>, and <code>K2 =
0.10</code>.' ...
        'The voltage and current control gains are kept
consistent with the validated configuration used in the sim-
ulation campaign, including <code>kpv = 0.4</code> and
<code>kiv = 40</code>.</p>']);
    else
        fprintf(fid, '<p>The scenario was not specified ex-
plicitly. The report uses the parameters active in the MATLAB
base workspace during execution.</p>');
    end

if string(familyChoice) == "1"
    fprintf(fid, ['<p>The selected verification family
is the <b>voltage-source behaviour test</b>. According to
' ...
        '<a href="%s#page=63">Section 5.5.3.6.2.2.3</a>
and the virtual-island test defined in Section 5.5.4, the
model is evaluated by checking whether the final steady-
state voltage remains within the allowed band after island-
ing.</p>'], guidelineLink);
    elseif string(familyChoice) == "2"
        fprintf(fid, ['<p>The selected verification family
is the <b>PCNB behaviour test</b>. According to ' ...
            '<a href="%s#page=63">Section 5.5.3.6.2.2.5</a>,
the initial and final steady states are used to verify the
PCNB droop/static-value behaviour, including the active-

```

```
power and frequency response after islanding.</p>'], guidelineLink);
```

```
    else
```

```
        fprintf(fid, ['<p>The report combines both verification families: <b>voltage-source behaviour</b> according to ' ...
```

```
            '<a href="%s#page=63">Section 5.5.3.6.2.2.3</a> and <b>PCNB behaviour</b> according to ' ...
```

```
            '<a href="%s#page=63">Section 5.5.3.6.2.2.5</a>. The same simulation data are reused for both analyses whenever the same Table 3 operating point is selected.</p>'], guidelineLink, guidelineLink);
```

```
    end
```

```
        fprintf(fid, ['<p>The measurement cases follow the operating points of ' ...
```

```
            '<a href="%s#page=73">Section 5.5.4.3 / Table 3</a>. The values presented in the report follow the recording logic of Section 5.5.4.4: values are extracted before islanding, after islanding during the transient, and at the final steady state.</p>'], guidelineLink);
```

```
        fprintf(fid, ['<ul><li><b>Pmom</b>: active power of the grid-forming unit immediately before the islanding event, used to verify the Table 3 initial active-power condition.</li>' ...
```

```
            '<li><b>PEmax</b>: maximum active-power capability of the unit, used as the per-unit reference for the Table 3 limits.</li>' ...
```

```
            '<li><b>Presidual</b>: target residual active load in the virtual island network, here used as the PCNB final active-power compliance target.</li>' ...
```

'Pres: Simulink residual-load factor applied to the load block as `Pres × Sb</code>. In the tuned scenario, it may differ from Presidual to make the simulated final active power settle within the compliance band.' ...`

'Pinit / Qinit: initial active- and reactive-power operating points of the grid-forming unit before the islanding event.' ...

'fbase: nominal frequency of the model, used as the frequency setpoint for the steady-state checks.' ...

'Islanding instant: the time at which the external grid is disconnected from the virtual island network; in this automation, it is set to 5 s.']);
end

```
function write_case_explanation(fid, R, guidelineLink)
    if string(R.testType) == "voltage"
        fprintf(fid, ['<p>This case evaluates the voltage-
source behaviour of the GFM inverter in virtual island op-
eration. The model is first brought to the selected initial
active- and reactive-power operating point, then the grid is
disconnected at the islanding instant. ' ...
        'The expected final condition is a stable volt-
age magnitude close to the pre-islanding steady-state volt-
age. In accordance with ' ...
        '<a href="%s#page=74">Section 5.5.4.4.1</a>,
the report records P, Q, V and f before islanding, the max-
imum and minimum values after islanding, and the final
steady-state values.</p>'], guidelineLink);
    else
        fprintf(fid, ['<p>This case evaluates the behaviour
of the PCNB in the virtual island network. The initial
```

active-power operating point is established before islanding, and after separation the model must settle to a final active-power and frequency response compatible with the configured droop/static-value requirements. ' ...

'In accordance with [Section 5.5.4.4.2](%s#page=75), the PCNB report focuses on the measured P and f quantities.</p>'], guidelineLink);

end

if abs(R.test.Qinit + 0.33) < 1e-6

fprintf(fid, ['<p>Reactive-power operating point: this is the maximum inductive reactive-power case. The value Q = -0.33 pu is used to represent the default capability of absorbing reactive power up to 33% of rated active power. In this model sign convention, inductive operation is represented by negative reactive power.</p>']);

elseif abs(R.test.Qinit - 0.33) < 1e-6

fprintf(fid, ['<p>Reactive-power operating point: this is the maximum capacitive reactive-power case. The value Q = +0.33 pu is used to represent reactive-power injection at 33% of rated active power. In this model sign convention, capacitive operation is represented by positive reactive power.</p>']);

elseif abs(R.test.Qinit) < 1e-9

fprintf(fid, '<p>Reactive-power operating point: this case is performed at Q = 0 pu, which represents the neutral reactive-power condition of Table 3.</p>');

end

end

function write_configuration(fid, test)

fprintf(fid, '<h4>Test configuration</h4>');

```

        fprintf(fid,                                '<table><tr><th>Parame-
ter</th><th>Value</th></tr>');
        if isfield(test, 'Pref')
            fprintf(fid,                                '<tr><td>P_ref</td><td>%.4f
pu</td></tr>', test.Pref);
        end
        fprintf(fid, '<tr><td>Pinit</td><td>%.4f pu</td></tr>',
test.Pinit);
        if isfield(test, 'Qref')
            fprintf(fid,                                '<tr><td>Q_ref</td><td>%.4f
pu</td></tr>', test.Qref);
        end
        fprintf(fid, '<tr><td>Qinit</td><td>%.4f pu</td></tr>',
test.Qinit);
        fprintf(fid,      '<tr><td>Residual      compliance      tar-
get</td><td>%.4f pu</td></tr>', test.Presidual);
        if isfield(test, 'Pres')
            fprintf(fid,      '<tr><td>Simulink      load      factor
Pres</td><td>%.5f pu</td></tr>', test.Pres);
            fprintf(fid,      '<tr><td>Residual      load      block
P</td><td>Pres × Sb = %.5f × Sb</td></tr>', test.Pres);
        end
        fprintf(fid, '<tr><td>PEmax</td><td>%.4f pu</td></tr>',
test.PEmax);
        fprintf(fid, '<tr><td>fbase</td><td>%.4f Hz</td></tr>',
test.fbase);
        if isfield(test, 'K2')
            fprintf(fid,      '<tr><td>K2          Q-V          droop
gain</td><td>%.4f</td></tr>', test.K2);
        end
        if isfield(test, 'kpV')
            fprintf(fid,      '<tr><td>kpV          voltage-loop
gain</td><td>%.4f</td></tr>', test.kpV);

```

```

end
if isfield(test, 'kiv')
    fprintf(fid,          '<tr><td>kiv          voltage-loop
gain</td><td>%.4f</td></tr>', test.kiv);
end
if isfield(test, 'scenario')
    fprintf(fid,          '<tr><td>Simulation          sce-
nario</td><td>%s</td></tr>', string(test.scenario));
end
fprintf(fid,  '<tr><td>Islanding  instant</td><td>%.4f
s</td></tr>', test.t_island);
fprintf(fid, '</table>');
end

```

```

function write_measurement_table(fid, vars, metrics)
    fprintf(fid,          '<table><tr><th>Quantity</th><th>Be-
fore</th><th>Max after islanding</th><th>Min after island-
ing</th><th>Final</th></tr>');
    for v = vars
        before = metrics.(v + "_before");
        vmax   = metrics.(v + "_max");
        vmin   = metrics.(v + "_min");
        final  = metrics.(v + "_final");
        fprintf(fid,
'<tr><td>%s</td><td>%.5f</td><td>%.5f</td><td>%.5f</td><td>
%.5f</td></tr>', v, before, vmax, vmin, final);
    end
    fprintf(fid, '</table>');
end

```

```

function write_deviation_table(fid, vars, metrics)
    fprintf(fid, '<p>For each quantity X, deviations are
calculated as  $\Delta X = X - X_{\text{before}}$ .</p>');

```

```

        fprintf(fid,                                '<table><tr><th>Quan-
tity</th><th> $\Delta$ max</th><th> $\Delta$ min</th><th> $\Delta$ final</th></tr>');
    for v = vars
        dmax    = metrics.("d" + v + "_max");
        dmin    = metrics.("d" + v + "_min");
        dfinal  = metrics.("d" + v + "_final");
        fprintf(fid,
'<tr><td>%s</td><td>%.5f</td><td>%.5f</td><td>%.5f</td></tr>
>', v, dmax, dmin, dfinal);
    end
    fprintf(fid, '</table>');
end

```

```

function write_voltage_analysis(fid, metrics, verdict,
guidelineLink)
    fprintf(fid, '<h4>Quantitative voltage-source behaviour
analysis</h4>');
    fprintf(fid, '<p>For the voltage-source behaviour veri-
fication, P, Q, V and f are extracted and shown. However,
the main quantitative criterion from <a
href="%s#page=63">Section 5.5.3.6.2.2.3</a> is applied to
the steady-state voltage after islanding: V<sub>final</sub>
must remain within  $\pm 3\%$  of the pre-islanding steady-state
voltage, using nominal voltage as base. The active-power and
residual-load checks are kept as Table 3 entry-condition
checks, not as the main voltage-source compliance crite-
rion.</p>', guidelineLink);
    fprintf(fid, '<ul>');
    fprintf(fid, '<li>Table 3 Pmom entry condition: Pmom
= %.4f pu; required minimum = %.4f pu: %s</li>', met-
rics.P_before, verdict.Pmom_required, ok_text(ver-
dict.Pmom_ok));

```

```

    fprintf(fid, '<li>Table 3 residual load condition: Pre-
residual inside 0.45-0.65 PEmax: %s</li>', ok_text(verdict.re-
sidual_load_ok));
    fprintf(fid, '<li>Voltage band for Section
5.5.3.6.2.2.3: %.5f pu ≤ Vfinal ≤ %.5f pu</li>', ver-
dict.voltage_lower, verdict.voltage_upper);
    fprintf(fid, '<li>Final voltage deviation: ΔVfinal
= %.5f pu, allowed = ±%.5f pu: %s</li>', verdict.final_V_er-
ror, verdict.voltage_tolerance, ok_text(verdict.fi-
nal_V_ok));
    fprintf(fid, '<li>Requirement 5.5.3.6.2.2.3 voltage
check: %s</li>', ok_text(verdict.req_5_5_3_6_2_2_3_ok));
    fprintf(fid, '</ul>');
end

```

```

function write_pcnb_analysis(fid, metrics, verdict, guide-
lineLink)

```

```

    fprintf(fid, '<h4>Quantitative PCNB behaviour analy-
sis</h4>');

```

```

    fprintf(fid, '<p>For the PCNB verification, P and f are
evaluated. In this implementation of <a
href="%s#page=63">Section 5.5.3.6.2.2.5</a>, the static-
value requirement is checked for both active power and fre-
quency: P<sub>before</sub> must remain within ±5%% of the
configured Pinit, P<sub>final</sub> must remain within ±5%%
of the Presidual target, and f<sub>before</sub>/f<sub>fi-
nal</sub> must remain within ±5%% of the configured frequency
setpoint fbase.</p>', guidelineLink);

```

```

    fprintf(fid, '<ul>');

```

```

    fprintf(fid, '<li>Pmom = %.4f pu; required minimum = %.4f
pu: %s</li>', metrics.P_before, verdict.Pmom_required,
ok_text(verdict.Pmom_ok));

```

```

    fprintf(fid, '<li>Residual load target inside 0.45-0.65
PEmax: %s</li>', ok_text(verdict.residual_load_ok));
    fprintf(fid, '<li>Initial P within ±5%% of configured
Pinit: %s</li>', ok_text(verdict.initial_P_ok));
    fprintf(fid, '<li>Initial f within ±5%% of fbase: error
= %.5f Hz, tolerance = %.5f Hz: %s</li>', verdict.ini-
tial_f_error, verdict.initial_f_tolerance, ok_text(ver-
dict.initial_f_ok));
    fprintf(fid, '<li>Final P within ±5%% of Presidual tar-
get: %.5f pu ≤ Pfinal ≤ %.5f pu; error = %.5f pu: %s</li>',
verdict.final_P_lower, verdict.final_P_upper, verdict.fi-
nal_P_error, ok_text(verdict.final_P_ok));
    fprintf(fid, '<li>Final f within ±5%% of fbase: %.5f Hz
≤ ffinal ≤ %.5f Hz; error = %.5f Hz: %s</li>', verdict.fi-
nal_f_lower, verdict.final_f_upper, verdict.final_f_error,
ok_text(verdict.final_f_ok));
    fprintf(fid, '<li>Correct PCNB direction: %s</li>',
ok_text(verdict.pcnb_direction_ok));
    fprintf(fid, '<li>Requirement 5.5.3.6.2.2.5 quantita-
tive check: %s</li>', ok_text(ver-
dict.req_5_5_3_6_2_2_5_ok));
    fprintf(fid, '</ul>');
    fprintf(fid, '<p class="note">The Simulink residual-load
factor Pres may be tuned per Table 3 case to make the simu-
lated final active power settle inside the ±5%% PCNB static-
value band around the Presidual target. The active-power
plot also shows the initial Pinit ±5%% band before islanding,
and the frequency static-value band is shown in the frequency
plot. A detailed damping and transient-frequency comparison
against measured hardware data can be added when reference
measurements are available.</p>');
end

```

```

function write_signature(fid)
    fprintf(fid, '<div class="signature">');
    fprintf(fid, '<h3>Report signature</h3>');
    fprintf(fid, '<p><b>Programme:</b> AGIS – Automatic GFM
Inverter Simulator</p>');
    fprintf(fid, '<p><b>Research thesis:</b> Grid Code Cer-
tification by Simulation for Grid-Forming Connected Invert-
ers</p>');
    fprintf(fid, '<p><b>Student researcher:</b> Boris
YONDJIN NGAMY</p>');
    fprintf(fid, '<p><b>Personal email:</b> nga-
myboris@gmail.com<br><b>Student email:</b> x0327345@stu-
dent.uwasa.fi<br><b>Tel:</b> +34 641 809 367</p>');
    fprintf(fid, '<p><b>Institution:</b> University of
Vaasa</p>');
    fprintf(fid, '</div>');
end

function plotFile = save_result_plot(R)
    plotFile = fullfile("figures", string(R.testType) + "_"
+ R.test.id + "_plot.png");

    % Larger figure to prevent axis boundary values and an-
notations from overlapping
    fig = figure('visible','off', 'Units','pixels', 'Posi-
tion',[100 100 1600 1450]);

    darkBlue = [0.00 0.00 0.45]; % darker blue, same
thin line style as original
    lineWidthMain = 1.0;
    fontSizeAxes = 10;
    fontSizeText = 10;

```

```

if string(R.testType) == "voltage"
    triggerWidth = 0.20;
    t1          =          tiledlayout(fig,4,1,'TileSpacing',
'loose','Padding','compact');

    %% Active power plot with Table 3 shaded regions and
black dashed boundaries
    axP = nexttile(t1,1);
    hold(axP,'on'); grid(axP,'on');
    title(axP,'Active Power P'); ylabel(axP,'pu');
    xlim(axP,[min(R.t) max(R.t)]);
    set(axP,'FontSize',fontSizeAxes);

    pBeforeLower = R.verdict.Pmom_required;
    pAfterLower  = R.verdict.residual_load_lower;
    pAfterUpper  = R.verdict.residual_load_upper;
    yMaxP = max([max(R.P), pBeforeLower, pAfterUpper,
1.05]);
    yMinP = min([min(R.P), 0]);
    pMargin = 0.08*(yMaxP-yMinP);
    ylim(axP,[yMinP yMaxP+pMargin]);

    add_rect_patch(axP,    min(R.t),    R.test.t_island,
pBeforeLower, yMaxP+pMargin, [0.25 0.70 1.00], 0.35);
    add_rect_patch(axP,    R.test.t_island,    max(R.t),
pAfterLower, pAfterUpper, [0.20 0.90 0.20], 0.38);
    add_rect_patch(axP,    R.test.t_island-triggerWidth,
R.test.t_island+triggerWidth, yMinP, yMaxP+pMargin, [1.00
0.62 0.10], 0.38);

    plot(axP, R.t, R.P, 'Color', darkBlue, 'LineWidth',
lineWidthMain);
    add_boundary_yline(axP, pBeforeLower);

```

```

add_boundary_yline(axP, pAfterLower);
add_boundary_yline(axP, pAfterUpper);
add_trigger_xlines(axP, R.test.t_island, triggerWidth);

add_arrow_label(axP, min(R.t)+5, yMaxP+0.02*(yMaxP-yMinP), min(R.t)+1.2, pBeforeLower+0.04*(yMaxP-yMinP), ...
    sprintf('Before islanding: Pmom ≥ %.2f pu', pBeforeLower), fontSizeText);
add_arrow_label(axP, R.test.t_island+18, pAfterUpper+0.10*(yMaxP-yMinP), R.test.t_island+8, mean([pAfterLower pAfterUpper]), ...
    sprintf('After islanding: %.2f ≤ Pmom ≤ %.2f pu', pAfterLower, pAfterUpper), fontSizeText);
add_arrow_label(axP, R.test.t_island+2, yMinP+0.10*(yMaxP-yMinP), R.test.t_island, yMinP+0.20*(yMaxP-yMinP), ...
    'Islanding point: t = 5 s', fontSizeText);
hold(axP, 'off');

%% Reactive power plot
axQ = nexttile(tl,2);
plot(axQ, R.t, R.Q, 'Color', darkBlue, 'LineWidth', lineWidthMain);
title(axQ, 'Reactive Power Q'); grid(axQ, 'on'); ylabel(axQ, 'pu');
xlim(axQ, [min(R.t) max(R.t)]);
set(axQ, 'FontSize', fontSizeAxes);

%% Voltage plot with zoomed +/-3% band and black dashed boundaries
axV = nexttile(tl,3);
hold(axV, 'on'); grid(axV, 'on');

```

```

title(axV, 'Voltage Magnitude V'); ylabel(axV, 'pu');
xlim(axV, [min(R.t) max(R.t)]);
set(axV, 'FontSize', fontSizeAxes);

vLower = R.verdict.voltage_lower;
vUpper = R.verdict.voltage_upper;
vCenter = R.metrics.V_before;
yMinV_data = min([min(R.V), vLower]);
yMaxV_data = max([max(R.V), vUpper]);
vMargin = max(0.015, 0.08*(yMaxV_data - yMinV_data));
yMinV = yMinV_data - vMargin;
yMaxV = yMaxV_data + vMargin;
ylim(axV, [yMinV yMaxV]);

add_rect_patch(axV, min(R.t), max(R.t), vLower, vUpper,
[0.20 0.90 0.20], 0.38);
add_rect_patch(axV, R.test.t_island-triggerWidth,
R.test.t_island+triggerWidth, yMinV, yMaxV, [1.00 0.62 0.10],
0.38);
plot(axV, R.t, R.V, 'Color', darkBlue, 'LineWidth',
lineWidthMain);

add_boundary_yline(axV, vLower);
add_boundary_yline(axV, vUpper);
add_boundary_yline(axV, vCenter);
add_trigger_xlines(axV, R.test.t_island, triggerWidth);

add_arrow_label(axV, min(R.t)+7, yMaxV-0.10*(yMaxV-
yMinV), min(R.t)+3, mean([vLower vUpper]), ...
sprintf('Voltage acceptance band: ±3%% Vbefore'),
fontSizeText);

```

```

        add_arrow_label(axV, R.test.t_island+2,
yMinV+0.10*(yMaxV-yMinV), R.test.t_island,
yMinV+0.20*(yMaxV-yMinV), ...
        'Islanding point: t = 5 s', fontSizeText);
hold(axV,'off');

%% Frequency plot
axF = nexttile(tl,4);
plot(axF, R.t, R.f, 'Color', darkBlue, 'LineWidth',
lineWidthMain);
title(axF,'Frequency f'); grid(axF,'on'); yla-
bel(axF,'Hz'); xlabel(axF,'Time [s]');
xlim(axF,[min(R.t) max(R.t)]);
set(axF,'FontSize',fontSizeAxes);
else
    triggerWidth = 0.20;
    tl = tiledlayout(fig,2,1,'TileSpac-
ing','loose','Padding','compact');

    %% Active power plot with Table 3 and +/-5% PCNB
static-value shaded regions
    axP = nexttile(tl,1);
    hold(axP,'on'); grid(axP,'on');
    title(axP,'Active Power P'); ylabel(axP,'pu');
    xlim(axP,[min(R.t) max(R.t)]); set(axP,'Font-
Size',fontSizeAxes);

    pBeforeLower = R.verdict.Pmom_required;
    pAfterLower = R.verdict.residual_load_lower;
    pAfterUpper = R.verdict.residual_load_upper;
    p5Lower = R.verdict.final_P_lower;
    p5Upper = R.verdict.final_P_upper;

```

```

    pInitLower = R.test.Pinit - R.verdict.initial_P_tol-
erance;
    pInitUpper = R.test.Pinit + R.verdict.initial_P_tol-
erance;
    yMaxP = max([max(R.P), pBeforeLower, pAfterUpper,
p5Upper, pInitUpper, 1.05]);
    yMinP = min([min(R.P), pAfterLower, p5Lower, pIn-
itLower, 0]);
    pMargin = 0.10*(yMaxP-yMinP);
    ylim(axP,[yMinP yMaxP+pMargin]);

    add_rect_patch(axP, min(R.t), R.test.t_island,
pBeforeLower, yMaxP+pMargin, [0.25 0.70 1.00], 0.26);
    add_rect_patch(axP, min(R.t), R.test.t_island, pIn-
itLower, pInitUpper, [1.00 0.95 0.10], 0.36);
    add_rect_patch(axP, R.test.t_island, max(R.t),
pAfterLower, pAfterUpper, [0.20 0.90 0.20], 0.30);
    add_rect_patch(axP, R.test.t_island, max(R.t),
p5Lower, p5Upper, [1.00 0.95 0.10], 0.34);
    add_rect_patch(axP, R.test.t_island-triggerWidth,
R.test.t_island+triggerWidth, yMinP, yMaxP+pMargin, [1.00
0.62 0.10], 0.38);
    plot(axP, R.t, R.P, 'Color', darkBlue, 'LineWidth',
lineWidthMain);

    add_boundary_yline(axP, pBeforeLower);
    add_boundary_yline(axP, pInitLower);
    add_boundary_yline(axP, pInitUpper);
    add_boundary_yline(axP, pAfterLower);
    add_boundary_yline(axP, pAfterUpper);
    add_boundary_yline(axP, p5Lower);
    add_boundary_yline(axP, p5Upper);

```

```

    add_trigger_xlines(axP, R.test.t_island, triggerWidth);

    add_arrow_label(axP, min(R.t)+5, yMaxP+0.02*(yMaxP-yMinP), min(R.t)+1.2, pBeforeLower+0.04*(yMaxP-yMinP), ...
        sprintf('Before islanding: Pmom ≥ %.2f pu', pBeforeLower), fontSizeText);
    add_arrow_label(axP, min(R.t)+9, pInitUpper+0.04*(yMaxP-yMinP), min(R.t)+2.0, mean([pInitLower pInitUpper]), ...
        sprintf('Initial static-value band: Pinit ±5%%'),
        fontSizeText);
    add_arrow_label(axP, R.test.t_island+16, pAfterUpper+0.10*(yMaxP-yMinP), R.test.t_island+8, mean([pAfterLower pAfterUpper]), ...
        sprintf('After islanding: %.2f ≤ Pmom ≤ %.2f pu', pAfterLower, pAfterUpper), fontSizeText);
    add_arrow_label(axP, R.test.t_island+27, p5Upper+0.03*(yMaxP-yMinP), R.test.t_island+20, mean([p5Lower p5Upper]), ...
        sprintf('Final static-value band: Presidual ±5%%'),
        fontSizeText);
    add_arrow_label(axP, R.test.t_island+2, yMinP+0.10*(yMaxP-yMinP), R.test.t_island, yMinP+0.20*(yMaxP-yMinP), ...
        'Islanding point: t = 5 s', fontSizeText);
    hold(axP, 'off');

    %% Frequency plot with +/-5% static-value shaded region and islanding marker
    axF = nexttile(tl,2);
    hold(axF, 'on'); grid(axF, 'on');

```

```

        title(axF, 'Frequency f'); ylabel(axF, 'Hz'); xlabel(axF, 'Time [s]');
        xlim(axF, [min(R.t) max(R.t)]); set(axF, 'FontSize', fontSizeAxes);

        f5Lower = R.verdict.final_f_lower;
        f5Upper = R.verdict.final_f_upper;
        yMinF = min([min(R.f), f5Lower]);
        yMaxF = max([max(R.f), f5Upper]);
        fMargin = max(0.2, 0.08*(yMaxF-yMinF));
        ylim(axF, [yMinF-fMargin yMaxF+fMargin]);

        add_rect_patch(axF, min(R.t), max(R.t), f5Lower,
f5Upper, [0.20 0.90 0.20], 0.30);
        add_rect_patch(axF, R.test.t_island-triggerWidth,
R.test.t_island+triggerWidth, yMinF-fMargin, yMaxF+fMargin,
[1.00 0.62 0.10], 0.38);
        plot(axF, R.t, R.f, 'Color', darkBlue, 'LineWidth',
lineWidthMain);

        add_boundary_yline(axF, f5Lower);
        add_boundary_yline(axF, f5Upper);
        add_boundary_yline(axF, R.test.fbase);
        add_trigger_xlines(axF, R.test.t_island, triggerWidth);

        add_arrow_label(axF, min(R.t)+18, f5Upper-
0.10*(f5Upper-f5Lower), min(R.t)+12, mean([f5Lower f5Upper]), ...
        sprintf('Frequency static-value band: ffinal =
fbase ±5%'), fontSizeText);

```

```

        add_arrow_label(axF, R.test.t_island+2, yMinF-
0.02*(yMaxF-yMinF), R.test.t_island, yMinF+0.12*(yMaxF-
yMinF), ...
            'Islanding point: t = 5 s', fontSizeText);
        hold(axF,'off');
    end

    try
        exportgraphics(fig, plotFile, 'Resolution', 220);
    catch
        saveas(fig, plotFile);
    end
    close(fig);
end

function add_rect_patch(ax, x1, x2, y1, y2, color, al-
phaValue)
    axes(ax);
    patch([x1 x2 x2 x1], [y1 y1 y2 y2], color, 'FaceAlpha',
alphaValue, 'EdgeColor', 'none');
end

function add_boundary_yline(ax, yValue)
    axes(ax);
    x1 = xlim(ax);
    plot(x1, [yValue yValue], 'k--', 'LineWidth', 0.90);
end

function add_trigger_xlines(ax, tIsland, triggerWidth)
    axes(ax);
    y1 = ylim(ax);
    plot([tIsland tIsland], y1, 'k--', 'LineWidth', 0.85);
end

```

```

        plot([tIsland-triggerWidth tIsland-triggerWidth], y1,
'k:', 'LineWidth', 0.75);
        plot([tIsland+triggerWidth tIsland+triggerWidth], y1,
'k:', 'LineWidth', 0.75);
end

```

```

function add_arrow_label(ax, textX, textY, targetX, targetY,
labelText, fontSizeText)

```

```

    axes(ax);
    text(ax, textX, textY, labelText, 'FontSize', font-
SizeText, 'FontWeight','bold', 'Color','k', 'BackgroundCol-
or','w', 'Margin',2, 'Clipping','off');
    plot(ax, [textX targetX], [textY targetY], 'k-', 'Lin-
eWidth', 0.80, 'Clipping','off');
    plot(ax, targetX, targetY, 'kv', 'MarkerFaceColor','k',
'MarkerSize',4, 'Clipping','off');
end

```

```

function tf = has_instantaneous_phase_signals(R)

```

```

    tf = isfield(R,'t_abc') && ~isempty(R.t_abc) && ...
        isfield(R,'Ua') && ~isempty(R.Ua) && ...
        isfield(R,'Ub') && ~isempty(R.Ub) && ...
        isfield(R,'Uc') && ~isempty(R.Uc) && ...
        isfield(R,'Ia') && ~isempty(R.Ia) && ...
        isfield(R,'Ib') && ~isempty(R.Ib) && ...
        isfield(R,'Ic') && ~isempty(R.Ic);
end

```

```

function plotFile = save_instantaneous_phase_plot(R)

```

```

    plotFile = fullfile("figures", "instantaneous_abc_" +
R.test.id + "_plot.png");

```

```

fig = figure('visible','off', 'Units','pixels', 'Position',[100 100 1600 1050]);
darkBlue = [0.00 0.00 0.45];
redLine = [0.60 0.00 0.00];
greenLine = [0.00 0.45 0.00];
lineWidthMain = 1.0;
fontSizeAxes = 10;

fbase = R.test.fbase;
Tnet = 1/fbase;
tStart = R.test.t_island - 2*Tnet;
tEnd = tStart + 30*Tnet;
idx = R.t_abc >= tStart & R.t_abc <= tEnd;

t1 = tiledlayout(fig,2,1,'TileSpacing','loose','Padding','compact');

axU = nexttile(t1,1);
hold(axU,'on'); grid(axU,'on');
title(axU,'Instantaneous Phase Voltages');
ylabel(axU,'pu');
plot(axU, R.t_abc(idx), R.Ua(idx), 'Color', darkBlue,
'LineWidth', lineWidthMain);
plot(axU, R.t_abc(idx), R.Ub(idx), 'Color', redLine,
'LineWidth', lineWidthMain);
plot(axU, R.t_abc(idx), R.Uc(idx), 'Color', greenLine,
'LineWidth', lineWidthMain);
xlim(axU,[tStart tEnd]);
add_instantaneous_islanding_marker(axU, R.test.t_island);
legend(axU, {'u_a','u_b','u_c'}, 'Location','best');
set(axU,'FontSize',fontSizeAxes);

```

```

axI = nexttile(tl,2);
hold(axI,'on'); grid(axI,'on');
title(axI,'Instantaneous Phase Currents');
ylabel(axI,'pu'); xlabel(axI,'Time [s]');
plot(axI, R.t_abc(idx), R.Ia(idx), 'Color', darkBlue,
'LineWidth', lineWidthMain);
plot(axI, R.t_abc(idx), R.Ib(idx), 'Color', redLine,
'LineWidth', lineWidthMain);
plot(axI, R.t_abc(idx), R.Ic(idx), 'Color', greenLine,
'LineWidth', lineWidthMain);
xlim(axI,[tStart tEnd]);
add_instantaneous_islanding_marker(axI, R.test.t_is-
land);
legend(axI, {'i_a','i_b','i_c'}, 'Location','best');
set(axI,'FontSize',fontSizeAxes);

try
    exportgraphics(fig, plotFile, 'Resolution', 220);
catch
    saveas(fig, plotFile);
end
close(fig);
end

function add_instantaneous_islanding_marker(ax, tIsland)
    yl = ylim(ax);
    plot(ax, [tIsland tIsland], yl, 'k--', 'LineWidth',
0.90);
    yText = yl(1) + 0.08*(yl(2)-yl(1));
    text(ax, tIsland + 0.005, yText, 'Islanding point: t =
5 s', ...
        'FontWeight','bold', 'FontSize',9, 'BackgroundCol-
or','w', 'Margin',2);

```

end

```
function txt = ok_text(value)
    if value
        txt = '<span class="ok">OK</span>';
    else
        txt = '<span class="fail">FAIL</span>';
    end
end
```

end

```
function txt = test_type_title(testType)
    if string(testType) == "voltage"
        txt = "Voltage source behaviour";
    else
        txt = "PCNB behaviour";
    end
end
```

end

```
function txt = scenario_text(choice)
    if string(choice) == "1"
        txt = "Scenario One - Non-compliance baseline param-
eters";
    elseif string(choice) == "2"
        txt = "Scenario Two - Compliance/tuned parameters";
    else
        txt = "Not specified";
    end
end
```

end

```
function txt = selection_text(choice)
    if string(choice) == "1"
        txt = "1 - Voltage source behaviour";
    elseif string(choice) == "2"
```

```
        txt = "2 - PCNB behaviour";
elseif string(choice) == "3"
    txt = "3 - All tests: voltage source behaviour and
PCNB";
else
    txt = "Not specified";
end
end
end
```

```
function txt = measurement_text(choice)
    if string(choice) == "1"
        txt = "Measurement 1.1 only";
    elseif string(choice) == "2"
        txt = "Measurement 1.2 only";
    elseif string(choice) == "3"
        txt = "Measurement 1.3 only";
    elseif string(choice) == "4"
        txt = "All measurements 1.1, 1.2 and 1.3";
    else
        txt = "All selected measurements";
    end
end
end
```

